Multiple Roles of Noggin, a BMP Antagonist, in Development of Craniofacial Skeletal Elements and Neural Tube

by

Maiko Matsui

Department of Cell Biology
Duke University

Date:_____

Approved:

_____
John Klingensmith, Advisor

_____
Fan Wang, Supervisor

_____
Blanche Capel

_____
David McClay

_____
Kathleen Smith

Dissertation submitted in partial fulfillment of
the requirements for the degree of Doctor
of Philosophy in the Department of
Cell Biology in the Graduate School
of Duke University

2014

ABSTRACT

Multiple Roles of Noggin, a BMP Antagonist, in Development of Craniofacial Skeletal Elements and Neural Tube

by

Maiko Matsui

Department of Cell Biology
Duke University

Date:_____

Approved:

_____
John Klingensmith, Advisor

_____
Fan Wang, Supervisor

_____
Blanche Capel

_____
David McClay

_____
Kathleen Smith

An abstract of a dissertation submitted in partial fulfillment of the requirements for the degree of Doctor of Philosophy in the Department of Cell Biology in the Graduate School of Duke University

2014

Abstract

Proper morphogenesis is essential for both form and function of mammalian craniofacial and neural tube development. Craniofacial deformities and neural tube defects are highly prevalent human birth defects. Although studies concerning craniofacial and neural tube development have revealed important genetic and/or environmental factors, understanding the mechanisms underlying proper development and the defects remain incomplete.

Among many genes that were cloned as the gastrula organizer genes in 1990s, *Noggin* (*Nog*), a secreted BMP antagonist, is expressed in the relevant domains during craniofacial and neural tube development. Previous studies show that *Nog* null embryos exhibit fully penetrant spina bifida (open spine) and to the lesser extent exencephaly (open brain). Moreover, *Nog* null mice display deformities in skeletal structures including defects in craniofacial skeleton. As such, *Nog* is essential for proper neural tube and craniofacial development. However, it is still not clear that which domain(s) of *Nog* are responsible for proper craniofacial development or neural tube closure. In addition, it is also an important question when, and in what capacity *Nog* is necessary during development of craniofacial and neural tube.

Here, we used mouse genetic approach to assess tissue-specific roles of *Nog* in NCCs and axial midline for craniofacial skeletogenesis, and in the roof palate and axial midline for neural tube closure.

Our mouse genetic approach showed that ablating *Nog* from the axial midline on *Chordin* (another BMP antagonist) null background caused rostral truncation, namely micrognathia which is similar to the phenotype seen in compound knock-out mutant of *Chordin* and *Nog* (*Chrd*$^{-/-}$;*Nog*$^{+/-}$). However, neither defects in neural tube closure nor thickened mandibular structure that were found in the compound mutant or *Nog* null were present in this class of mutant embryos. Importantly, neural tube defects were not found when *Nog* was ablated in the roof plate either. Instead, enlarged Meckel's cartilage resulted from increased cell proliferation was present when *Nog* is absent in NCCs. Additionally, absence of *Nog* in NCCs also caused secondary cleft palate due to the insufficient palatal shelf elevation caused by enlarged pterygoid bone invasion into the developing posterior palatal shelves. Thus, we found a novel mechanism of secondary cleft palate. These studies demonstrate that two distinct domains of *Nog* are required in different stages of craniofacial development, although these two domains of *Nog* are not responsible for neural tube closure.

Dedication

This dissertation is dedicated to my parents, Umpei and Ayako Matsui, who gave constant support and encouragement, and to Anoop Sadanandan, for being there.

Contents

List of Tables

List of Figures

1. Introduction

This chapter includes modified "Development of the Craniofacial Skeleton" originally published in Primer on the Metabolic Bone Diseases and Disorders of Mineral Metabolism. John Wiley & Sons, Inc., 2013 Aug; pp. 893-903.

1.1 Developmental Biology and Human Congenital Malformations

Developmental biology is the study of the processes through which organisms change shapes and establish a complete living system. Studying developmental biology help us understand the normal development as well as mechanisms underlying the congenital deformities.

Congenital malformations are structural and/or functional defects of organs or body parts present at birth. Among the congenital deformities found in human newborns, craniofacial defects such as cleft palate, cleft lip, and micrognathia - mandibular hypoplasia occur highest only after the congenital heart deformities. The severities of the deformities vary case by case. The congenital craniofacial anomalies frequently occur as part of genetic syndromes such as DiGeorge and Treacher Collins syndromes. They also appear sporadically as isolated forms. In some cases, environmental factors such as teratogenic chemicals and maternal smoking/alcohol intake are responsible for the causes.

Another common human birth defect is the neural tube defects (NTDs). They are mainly divided into two major groups - open NTDs and closed NTDs (Fig. 1.1). Among the open NTDs, one that occurs at the spine is called spina bifida and one that occurs in the brain is called exencephaly in which the brain is exposed without any protections such as skull bone or skin. When the exencephaly progresses the exposed brain degenerates and anencephaly (no brain) results. Those individuals may be born but do not survive after birth. Some but not all of the NTDs can be prevented by supplementing folic acid because pathways and mechanisms causing NTDs are not always same.

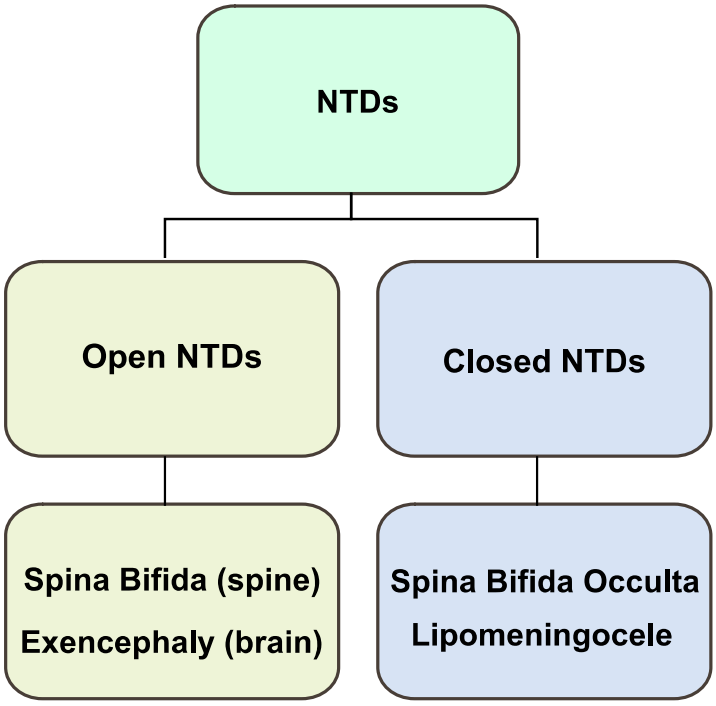

Figure 1.1: Types of NTDs

NTDs are divided into two categories; open NTDs and closed NTDs. The category of open NTDs includes NTDs such as spina bifida and exencephaly. Spina bifida occulta, which is most common form of NTDs, and lipomeningocele are included in closed NTDs.

1.2 Craniofacial Development and Malformations

Craniofacial skeletal elements are the most developmentally complex skeletal structures in mammals. We humans have distinct, identifying facial features, the result of small variations in craniofacial development. Such differences are usually benign and result in features that make us distinct individuals. However, variable effects of gene expression or environmental factors can lead to cosmetic and functional abnormalities.

Among the congenital deformities found in newborns, craniofacial defects such as orofacial clefts, micrognathia and craniosynostosis occur at a frequency second only to the congenital heart defects. The severity of craniofacial deformities varies case by case. The deformities frequently occur as part of genetic syndromes. They also appear sporadically as isolated forms. In some cases, teratogenic chemicals are responsible. Such craniofacial deformities may be fatal, but more often impact on quality of life because they affect normal breathing and feeding. Unfortunately, there are often negative social responses to the deformities, which take a psychological toll on the effected person. The etiology of most congenital craniofacial anomalies has just begun to be understood. It is essential to clarify the normal and pathological development of craniofacial skeletal elements and the underlying molecular and cellular mechanisms. This knowledge will enhance our ability to design strategies for future treatment and prevention of craniofacial birth defects.

1.2.1 Origin of craniofacial skeletal elements and neural crest cells

Mammalian craniofacial skeletal elements consist of more than twenty small bones and cartilages that are formed precisely during development to create functional structures - the face and the head. Most facial skeletal elements, collectively the viscerocranium, are derived from cranial neural crest cells (NCCs). These pluripotent cells are collectively sometimes called "the fourth germ layer" because of the diversity of tissues they form. In early craniofacial development, presumptive cranial NCCs arise in dorsal midline ectoderm of the midbrain and the hindbrain rhombomeres, undergo an epithelial-to-mesenchymal transition, delaminate, then migrate ventrolaterally between the ectoderm and endoderm (Fig 1.2A, 1.3). While the rostral cranial NCCs develop the frontonasal skeleton and the skull vault, NCCs from each rhombomere faithfully take distinct pathways to populate different pharyngeal arches (PA), numbered rostrocaudally from 1 to 6. NCCs from rhombomeres 1 and 2 migrate into PA1 and the frontonasal process. PA1 gives rise to the incus and malleus of the ears, the mandible, and the maxilla. The frontonasal process gives rise to tissues in the upper half of the face, including the forehead, nose, eyes, and philtrum (the vertical groove between the nose and the upper lip). NCCs from rhombomeres 3 and 4 migrate into PA2, which gives rise to the stapes bone of the middle ear, the styloid process of temporal bone, and a part of the hyoid bone (Fig. 1.2A).

The rest of the mammalian craniofacial skeletal elements that enclose and support the brain and cranial sense organs are called the neurocranium. They compose the skull vault and base. While the ventral craniofacial bones and anterior skull base are derived from cranial NCCs, most of the bones at the back of the head, including the parietal bones and occipital bone, and the posterior part of the skull base are derived from both NCCs and paraxial mesoderm (Jeong et al., 2004; McBratney-Owen et al., 2008) (Fig. 1.2B). The skull vault is formed through intramembranous ossification and the cranial base is formed through endochondral ossification (Sahar et al., 2005).

A.

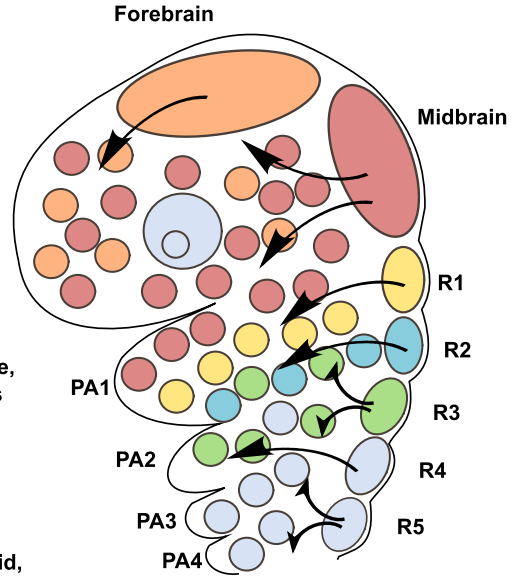

Fore/midbrain: frontal membranous bones of skull vault

PA1: maxilla, Meckel's cartilage, mandible, incus, malleus, palate, zgoma, squamous

PA2: styloid process, stapes, temporal, hyoid

PA3: hyoid

PA4: thyroid, cricoid, epiglotis

B.

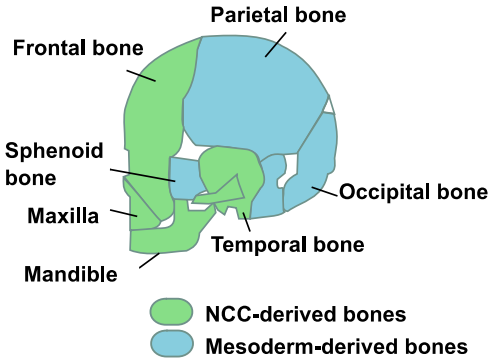

Figure 1.2: Origin of craniofacial skeletal elements

(A) NCCs go through epithelial-mesenchymal transition and migrate ventrolaterally from rhombomeres (R) to populate in pharyngeal arches (PA). NCCs in R3 and R5 merge with streams of NCCs from neighboring rhombomeres. Bones and cartilages derived from each PA are listed. (B) Facial and frontal bones are derived from NCCs. Posterior skull base and vault are mostly derived from somitic mesoderm.

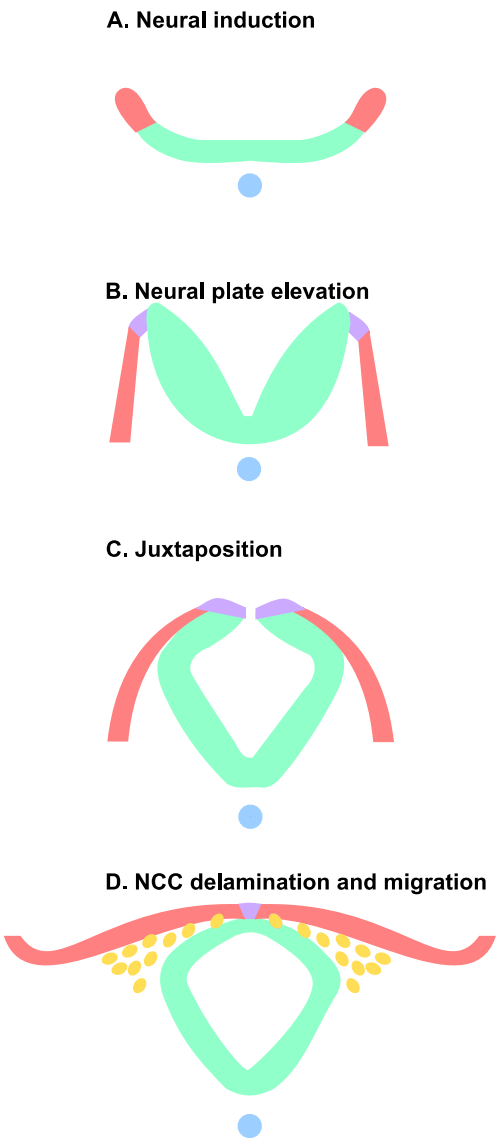

Figure 1.3: NCC formation and migration

(A) Neural induction begins in the flat neural plate (pink and green). (B) Both edges of the neural plate elevate dorsally. (C) Neural folds (purple) are apposed. (D) Around closing neural folds, NCCs (yellow) delaminate and migrate ventrally.

1.2.2 Palatal development

Palatogenesis is a dynamic process, with each step crucial for proper development of the palate. The palate is divided into two main parts, the primary and secondary palate. Both are mostly derived from NCCs of PA1. The primary palate develops from the intermaxillary segment, where the medial nasal processes fuse with the maxillary process, to form the most anterior part of the definitive hard palate (Figs. 1.4A and B). Development of the secondary palate begins with downward protrusion of the two palatal shelves of the maxillary prominences on either side of the tongue, at the fifth week in humans and between embryonic day (E) 11.5 and E12.5 in mice (Figs. 1.4B and 1.5A). Interaction between epithelial and mesenchymal cells influences the survival and continued proliferation of NCCs necessary for morphogenesis of palatal shelves (Rice et al., 2004).

The downward protrusions of the palatal shelves turn medially and elevate horizontally to meet and fuse at the midline, at about the eighth week in humans and E14.5 in mice. The tongue meanwhile moves downward to give enough space for the palatal shelves to elevate. The primary and secondary palates also fuse together to form the complete palate, compartmentalizing the oral and nasal cavities. Fusion of palatal shelves involves loss of medial edge epithelium (MEE; Fig. 1.5A), and the cellular

processes of apoptosis, epithelial migration, and epithelial-to-mesenchymal transition (Jin and Ding, 2006).

The ventral two thirds of the secondary palate becomes the hard palate, containing bone, and the rest becomes the muscular soft palate. Postnatal development of the palate may be influenced by osteogenic responses to retain functional integrity against mechanical stress, for example, elevated masticatory load increased the bone density of secondary hard palate in growing rabbits (Menegaz et al., 2009).

In addition to environmental risk factors, several genes and signaling pathways important for palatogenesis have been identified (Fig. 1.5B). One key pathway involved in palatogenesis is BMP signaling. In early embryogenesis, BMPs influence cell migration, differentiation, proliferation, apoptosis, and condensation. Later, among other roles, BMP signaling promotes osteogenesis and chondrogenesis in skeletal formation throughout the body. For example, BMP signaling is important for mesenchymal condensation in progenitors of palatal bone (Baek et al., 2011). Altering BMP signaling in NCCs or in the oral epithelium results in CP (He et al., 2010; Li et al., 2011).

Table 1.1: Genes important for palatal development.

Stage	Mesenchyme	Epithelium
E12-E13 Palatal shelf growth	Fgf10, Fgf7, Msx1	Fgfr2b, Shh
E13-E14 Palatal shelf elevation	Fgf10, Fgfr1b, Fgf2b, Msx1, TGFβ1, TGFβ2	Fgfr1, Fgfr2b, Shh, Wnt11
E14-E15 Palatal fusion	Bmp2, Bmp3, Bmp4, Fgf10, Msx1	Bmp3, Fgfr2, Shh, TGFβ3

BMP2 and BMP7 expression in palatal mesenchyme is regulated by the Msx1 homeobox gene (Fig. 1.5B), which plays an important role in epithelial-mesenchymal interaction throughout embryogenesis. Msx1 null mice display multiple deformities in craniofacial skeletal elements, including secondary CP and abnormal tooth and mandible development (Satokata and Maas, 1994). Msx1 is also required for expression of Shh in the MEE, the site of palatal shelf fusion (Zhang et al., 2002). Expression of Shh and BMP2, as well as CP, in Msx1 mutant mice is rescued by transgenic expression of Bmp4, suggesting a gene network of BMP and Shh signaling pathways in development of palatal shelves (Zhang et al., 2002).

The Hedgehog signaling pathway also interacts with Fgf signaling in palatogenesis. Fgf10 is expressed in mesenchyme, while its receptor, Fgfr2b is expressed in epithelium. Fgf10 is required for Shh expression in epithelium. Loss of either can cause CP due to insufficient survival or proliferation of NCCs (Rice et al., 2004).

Current models suggest that apoptosis is the major cellular mechanism for palatal fusion (Kaartinen et al., 1995; Proetzel et al., 1995; Taya et al., 1999b). Tgfβ3 promotes apoptosis in juxtaposed MEE to form a single layered medial edge seam (MES; Fig. 1.5B and Table 1.1). Tgfβ3 expression in MEE is regulated by Wnt/β-catenin signaling (He et al., 2011).

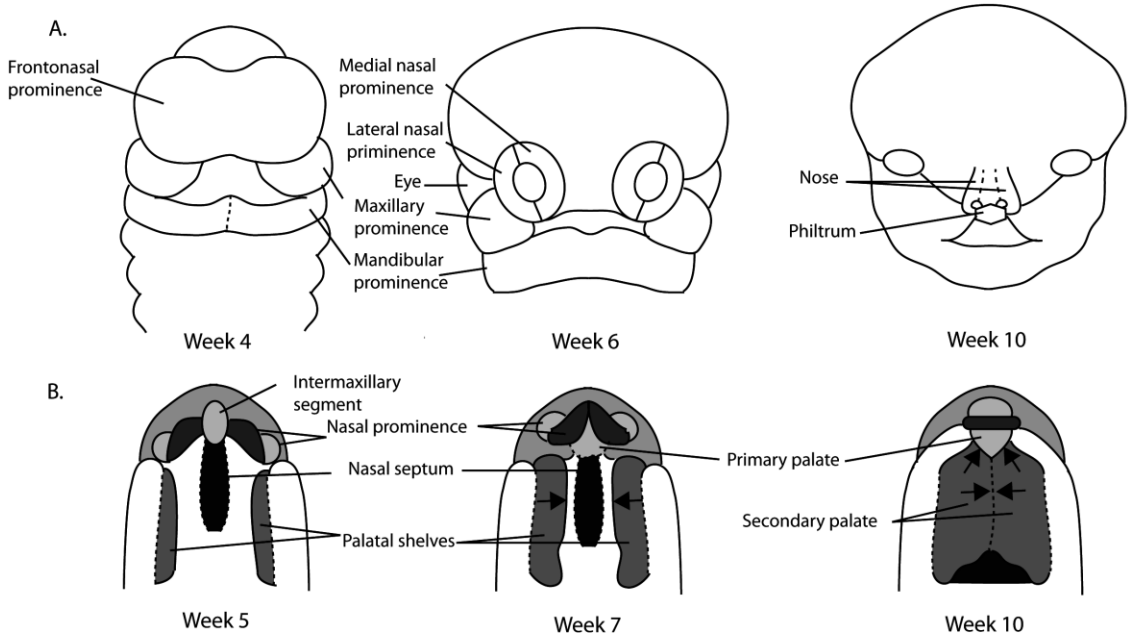

Figure 1.4: Development of the face and the palate in humans.

(A) Frontonasal, maxillary, and mandibular prominences form in 4th week. By 6th week, nasal prominences develop from frontonasal prominence. (B) Ventral view of palate development. Around 5th week palatal shelves from maxillary prominences grow downward on the either side of the tongue. Growing palatal shelves start elevating medially in the 7th week. By 10th week, secondary and primary palates fuse together to form complete palate.

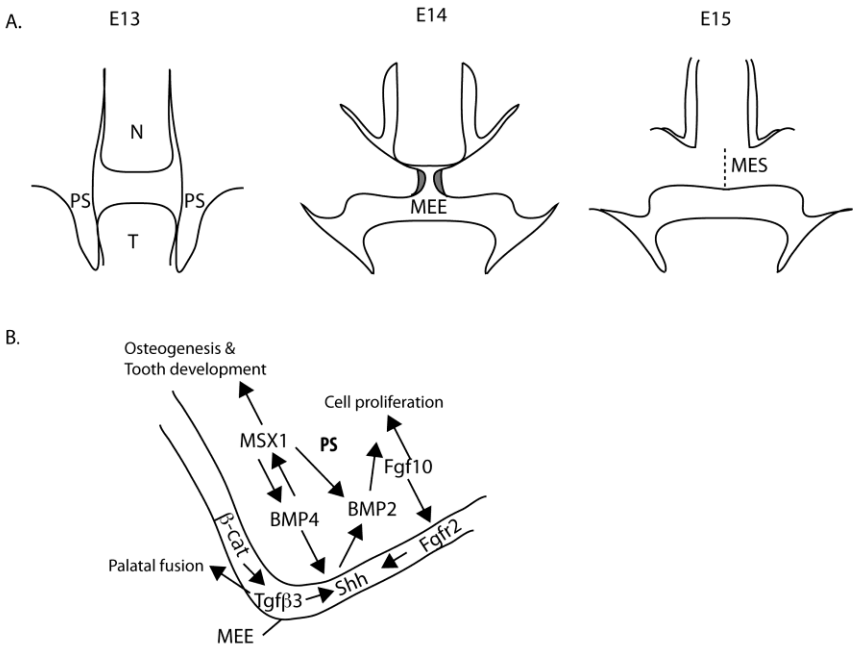

Figure 1.5: Coronal view of palatogenesis and gene networks during palatogenesis.

(A) Palatal shelf (PS), nasal septum (N), tongue (T), medial edge epithelium (MEE), medial edge seam (MES). (B) Complex gene networks in the palatal shelves. Molecular signaling events during epithelial-mesenchymal interactions of palatogenesis are depicted.

1.2.3 Orofacial cleft

Orofacial clefts, among the most common congenital malformations, result from failure in the joining of bilateral facial structures during development. They are divided in three large groups, cleft lip with cleft palate (CL/P), cleft lip (CL) only and CP only. Approximately half of the CL patients also manifest CP, considered a secondary consequence of the primary imperfection of premaxillary fusion. Thus, CP only may be etiologically distinct from CL/P. CP emanates from defective unification of the palatal shelves. Mechanisms leading to this failure include defects in palatal shelf growth, palatal elevation, and palatal shelf adhesion.

CP is subdivided into hard palate cleft, soft palate cleft, complete palate cleft, and bilateral palate cleft (Fig. 1.6). Patients often suffer from complications causing speech and feeding difficulties, frequent ear infections, dental problems as well as problems in psychological development (Stanier and Moore, 2004). About 70 percent of orofacial clefts arise as an isolated form where no other anomalies are associated in those patients, while the remaining cases occur in syndromes; about 400 syndromes are known to cause orofacial clefts (Zucchero et al., 2004). Recent studies show that genes causing syndromic CL/P have a significant overlapping etiology with non-syndromic clefting (Stanier and Moore, 2004). Studying those genes and related molecular pathways will help us further understand pathogenesis of human facial clefts.

In addition to genetic factors associated with orofacial clefts, numerous non-genetic risk factors have been identified. Maternal smoking during periconceptional period increased incidence of CL/P and CP by twofold (Honein et al., 2007). Smoking during pregnancy also increases the chance of causing orofacial clefts in fetuses with certain susceptibility loci (Lammer et al., 2004). In addition, the Food and Drug Administration (FDA) recently announced that certain types of antiepileptic medications increase the risk of CL/P and CP.

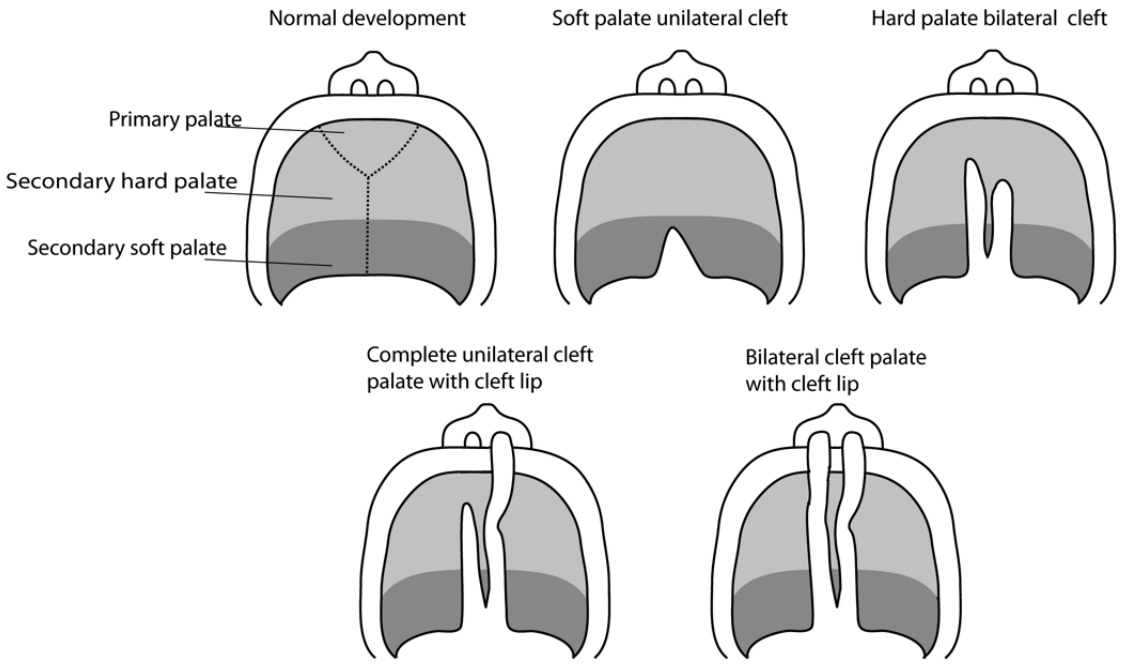

Figure 1.6: Types of cleft palate and cleft lip.

Normal palate morphology and types of cleft palate. The palate is composed of the primary palate and secondary palate. The secondary palate is further subdivided into the hard palate and the soft palate. The degree of severity varies case by case, some only affect the soft palate while others affect both the secondary and primary palates as well as lip formation.

1.2.4 Mandibular development

The mandible develops through unique steps. Bilaterally symmetric mandibular buds of PA1, stuffed with mesenchymal NCCs and paraxial mesoderm and enclosed by endodermal and ectodermal epithelial layers, dramatically grow and fuse to each other at the midline (Chai et al., 2000b). Within this fused mandibular process arises Meckel's cartilage (MC), a rod-shaped transient structure that functions as a template for mandibular formation. NCCs surround MC to form a membranous sheath, which later undergoes intramembranous ossification to form the mandible proper (Fig. 1.7). The distal portion of MC undergoes endochondral ossification to become a part of the mandibular bone supporting the incisors, whereas the proximal portion contributes to the inner ear ossicles. The central part of MC disappears soon after birth (Frommer and Margolie.Mr, 1971). MC degradation may be induced by feed-forward secretion of interleukin-1β by infiltrating macrophages and chondrocytes (Tsuzurahara et al., 2011).

Proper mandibular morphogenesis requires signaling interactions between mesenchyme and epithelial cells in PA1. In addition, signaling from pharyngeal endoderm plays a significant role in mandibular growth. Survival of mesenchyme, Meckel's cartilage outgrowth and osteogenesis of mandibular bones are closely regulated by stage-and region-specific roles of BMP and FGF signaling pathways (Mina et al., 2007; Mina et al., 2002; Wilke et al., 1997). For example, ectopic BMP4 application

to mandibular explants increases apoptosis and represses Fgf8 transcription. Fgf8 signaling is considered as a source of survival signaling for mesenchyme in PA1. Mouse embryos lacking the BMP antagonists Chordin and Noggin show reduced Fgf8 in the pharyngeal ectoderm and increased apoptosis, resulting in a whole spectrum of mandibular outgrowth defects (Stottmann et al., 2001). Perturbing FGF receptor 3 (FGFR3) in Meckel's cartilage before chondrogenic and osteogenic condensations results in defects in development of the mandibular process and Meckel's cartilage and a lack of mandibular bones (Mina et al., 2007).

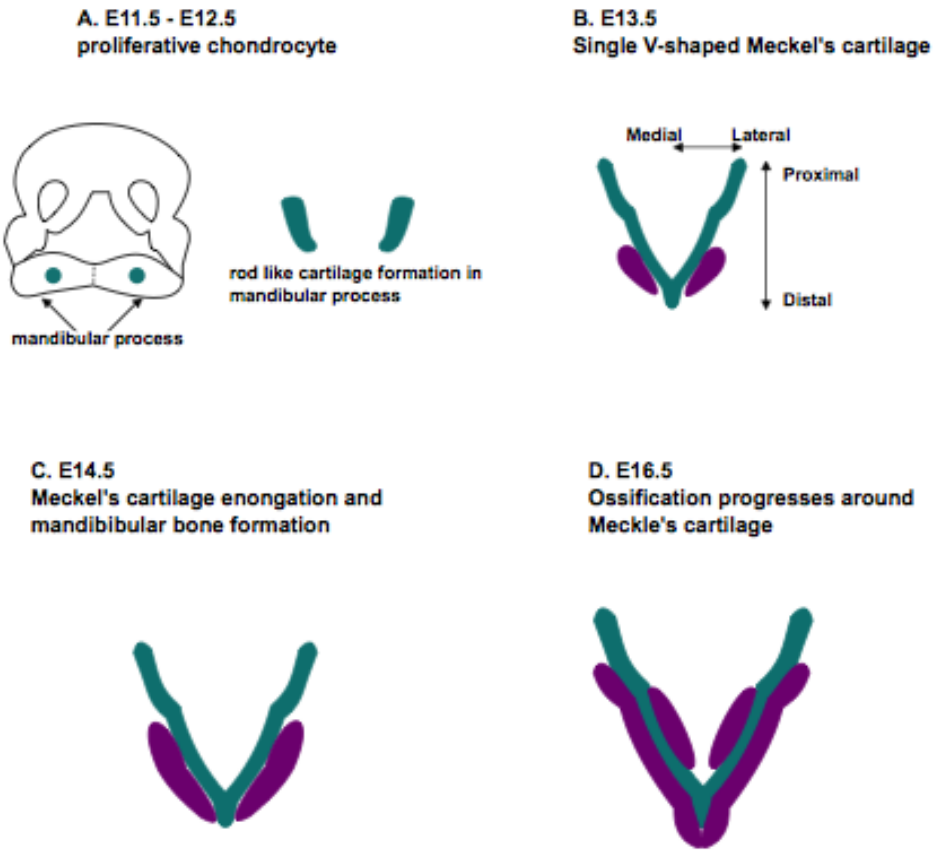

Figure 1.7: Meckel's cartilage and mandibular development

(A) chondrocyte condensation begins in the mandibular process between E11.5 and E12.5. (B) "V" shaped Meckel's cartilage forms around E13.5. (C) Meckel's cartilage elongates in proximal-distal direction and osteogenesis begins at E14.5. (D) Ossification progresses around Meckel's cartilage using Meckel's cartilage as a template at E16.5.

1.2.5 Micrognathia

Micrognathia, characterized by mandibular hypoplasia, is another example of a common craniofacial structural malformation. It is generally considered a defect in which too few NCCs populate PA1, due to insufficient production or migration during the fourth week of human gestation. Such NCC defects are often caused by misregulation of signaling pathways elicited by genetic and environmental factors. Affected patients show a wide range of malformation, from almost normal to agnathia, a complete lack of the lower jaw. While multiple syndromes include micrognathia, isolated micrognathia may cause sequential deformities. Hypoplastic mandible can displace the tongue posteriorly, which in turn prevents elevation of palatal shelves, leading to CP or CL/P as in Pierre Robin sequence (Weseman, 1959). Children with micrognathia often have problems of feeding and upper airway breathing as well as sleep apnoea. In severe cases, surgical intervention may be required to allow the mandibular bone to elongate (Figueroa, 2002). Although it has been believed that in some cases of mandibular hypoplasia, outgrowth may eventually attain normal proportions during childhood, recent findings suggest the underdeveloped mandible generally remains small (Daskalogiannakis et al., 2001; Suri et al., 2010).

1.2.6 Development of the neurocranium

The neurocranium is composed of two parts: the skull vault and the base. The skull vault consists of multiple separate membranous bones - frontal, parietal, and a part of the occipital bones. The frontal bones are derived from NCCs, while others are mostly derived from mesoderm cells (Jeong et al., 2004; McBratney-Owen et al., 2008). Connective tissues called cranial sutures articulate these bones, resulting in formation of fontanelles at the boundaries of cranial bones (Fig.1.8A). These sutures are the primary sites of osteogenesis during skull development. Cranial sutures are formed between neighboring membranous bones when cells at the osteogenic front proliferate. Tissue and molecular signaling interactions with underlying dura mater influence development and maintenance of cranial sutures. Dura mater releases and takes up cytokines, mediates biochemical signaling and contributes cells to suture mesenchyme. FGFs are expressed in dura mater just below the forming sutures; FGF signaling is critical for cranial suture biology (De Coster et al., 2007; Ogle et al., 2004). Maintenance of suture patency at birth helps the skull of a baby go through the birth canal and, until 12-18 months, is essential for proper brain growth and development (Richtsmeier et al., 2006).

The skull base includes midline structures such as the ethmoid, sphenoid, basioccipital bones, and parts of the temporal bones. These bones play an important role in supporting the brain. The anterior-most skull base is derived from NCCs, while the

posterior skull base is derived from paraxial mesoderm (Couly et al., 1993). The timing of growth, ossification and maturation of the anterior and posterior skull base is not synchronous. A distinct feature of skull base bones is that, unlike other craniofacial skeletal elements, these bones develop through endochondral ossification. The skull base first forms from multiple paired cartilaginous anlagen from caudal to rostral. These grow, extend and fuse together resulting in formation of skull base sutures between each cartilaginous element. Eventually, they form a single perforated base plate. Chondrogenesis in neural crest derived cartilages requires Sox9. Mesoderm-derived occipital bone is present while NCC-derived sphenoid bone is absent in mice lacking Sox9 (Mori-Akiyama et al., 2003). The development of the skull base is also critical for facial growth. The size and shape of the skull base affect the position of mandible, and may cause consequential craniofacial deformities such as CP (Bastir et al., 2010; Harris, 1993; Lieberman et al., 2000; Nie, 2005).

1.2.7 Craniosynostosis and skull base deformities

Premature suture fusion, craniosynostosis, occurs 1 in 2500 human births (Cohen and MacLean, 2000) (Table 1.2). The form of craniosynostosis depends on the affected suture(s) (Fig.1.8B). Nature of the alteration in cranial vault shape depends on which sutures are fused prematurely. Different types of craniosynostosis involve distinct etiology. Primary craniosynostosis is caused by premature ossification of the skull vault,

and union of one or more cranial sutures. Accordingly, abnormal shape of the cranial vault and/or premature closure of the fontanelles result. In contrast, secondary craniosynostosis is caused by insufficient brain growth, that is usually caused in turn by failure of cephalic neural tube closure in the first month of human embryonic development. More than 180 syndromes include craniosynostosis in humans, including Apert, Crouzon, and many others (Hennekam and Van den Boogaard, 1990) (Table 1.2). Mutations in FGFs, genes involved in FGF signaling, and the osteogenic transcription factor Runx2 have been identified as the molecular lesions underlying syndromes with craniosynostosis (Kimonis et al., 2007).

Table 1.2: Syndromes with craniosynostosis and implicated genes.

Gene	Syndromes
Fgfr1	Jackson-Weiss syndrome, Kallmann syndrome2, Pfeiffer syndrome
Fgfr2	Apert syndrome, Crouzon syndrome, Jackson-Weiss syndrome, LADD syndrome, Saethre-Chotzen syndrome
Fgfr3	Crouzon syndrome, LADD syndrome, Muenke syndrome
Twist1	Saethre-Chotzen syndrome
Fbn1	Marfan syndrome, MASS syndrome
Tgfbr1 & Tgfbr2	Loeys-Dietz syndrome

The frequency of deformities in the skull base is less than that of defects in other parts of the craniofacial skeleton. The NCC-derived anterior skull base is more susceptible to defects than the posterior mesoderm-derived skull base (Nie, 2005). Abnormalities of the skull base can affect the position of the jaws. A recent study has suggested correlations between anterior skull base morphology and midfacial retrusion (Lozanoff et al., 1994). Some cases of skull base deformities are also observed in the syndromes causing craniosynostosis (Nie, 2005). Research so far has been unable to conclude if skull base abnormalities are the cause or consequences of craniosynostosis or craniofacial deformities. Defects in the skull base are often observed in skull base sutures and cartilage growth plate called synchondroses. The location and timing of premature skull base fusion and synchondroses can influence the craniofacial symmetry of a child. Premature skull base closures and abnormal growth in synchondroses are recognized in many syndromes such as Crouzon and Apert (Goodrich, 2005). However, as Goodrich suggests, the development of each unit, the skull vault, facial skeleton, and the skull base influences the other units of the head skeleton. Thus, it is critical to maintain proper regulation of gene expression, tissue growth, and patterning for development of craniofacial skeletal elements.

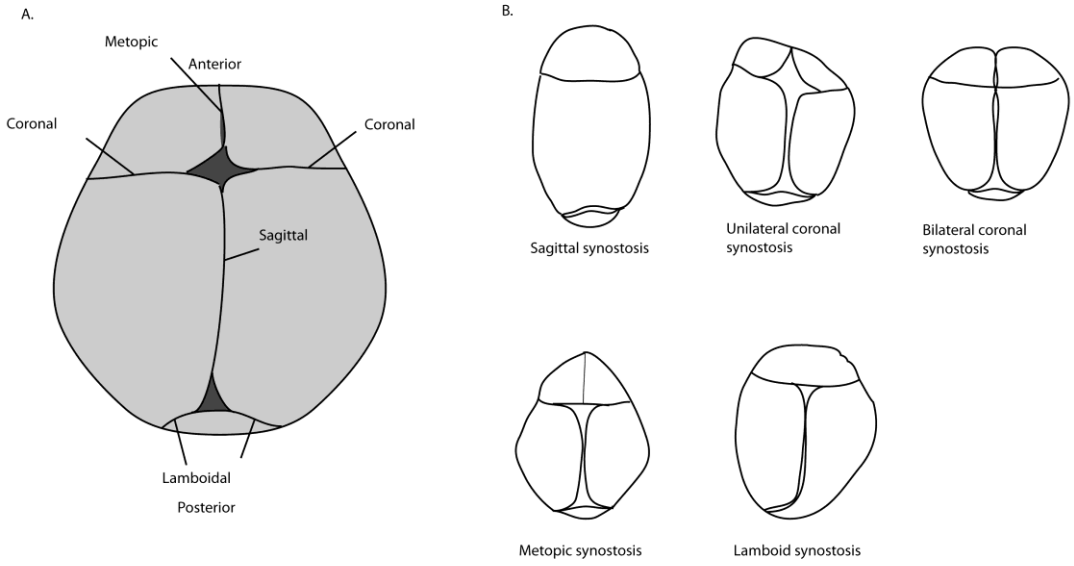

Figure 1.8: Cranial sutures and types of craniosynostosis viewed from above.

(A) Positions of the major cranial sutures. (B) Diagnostic features of craniosynostosis. Sagittal synostosis results in a long and narrow head. Right unilateral coronal synostosis shows flattened forehead on affected side. Bilateral coronal synostosis causes flattened head. Metopic synostosis dysplays hypotelorism and pointy forehead. Lamboid synostosis causes a flattening of the back of the head.

1.3 Development of neural tube

Neural tube is the dorsally located epithelial tubular structure found in the early vertebrate embryo. Neural tube is originated from the neural ectoderm and the precursor to the central nervous system. Mammalian neural tube first develops from a flat sheet called the neural plate. The neural plate will turn into the neural tube through two major events; primary neurulation and secondary neurulation. Primary neurulation during which the brains and most part of spinal cord form occurs rostrally to future sacral level of the spine (Copp et al., 1989). Secondary neurulation occurs more caudally by condensation and epithelialization of mesenchymal cells to form the sacral and all of the coccygeal regions of the spinal cord. In primary neurulation, cells in the neural plate elongate and both edges of the neural plate elevate to form the medial hinge point (MHP) right above the notochord and the neural folds at the lateral sides of the neural plate. Because of its distinct mechanism of development, the lower spinal neural tube that is derived through secondary neurulation does not have MHP. In addition to MHP, formation of dorsolateral hinge points (DLHPs) is critical in certain parts of neural tube including intermediate spine and cranial neural tube (Fig. 1.9). In addition to proper HP formation, neural tube closure involves adhesion and fusion of epithelial sheets. Convergent extension of the neural folds allows midline epithelium of the apposing neural folds to happen, resulting in hollow tube formation.

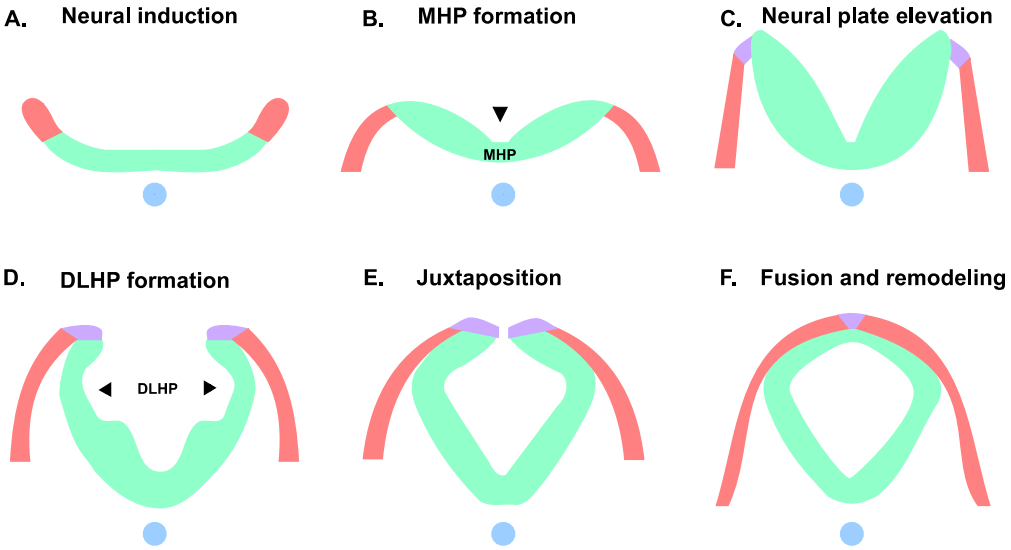

Figure 1.9: Neural tube development

(A) Neural induction begins in the flat neural plate. (B) MHP (black arrow head) forms at the future midline of the body. (C) Both sides of the neural plate elevate dorsally to form the neural fold. (D, E) DLHP (black arrow heads) formation allows neural folds to juxtapose to each other. (F) The neural folds meet at the dorsal midline to fuse, completing neural tube closure.

1.3.1 Human neural tube defects and animal models of studying NTDs

Neural tube defects (NTDs) are one of the most common congenital deformities in humans. Every year, approximately 300,000 babies are born with NTDs (Botto et al., 1999). Since the report of folic acid effectiveness by the Medical Research Council Vitamin Study Group was released in 1991, many countries have recommended periconceptional intake of folic acid. Moreover, improved technologies such as high-resolution ultrasonography for in utero fetal examination, and termination of affected pregnancies also have helped reduce the prevalence of NTD considerably (Kondo et al., 2009). However, according to the International Clearinghouse for Birth Defects Surveillance and Research, among G8 countries (8 developed countries), Germany and Japan exceed the average rate of prevalence -approximately 3 to 4 per 10,000 live births and stillbirths with or without termination of pregnancy between 2000 and 2004. There are several reasons to explain this result. First, accuracy of the diagnosis may differ from a country to country. Second, public awareness of importance of periconceptional consumption of folic acid for preventing NTDs may be lower in some countries. In addition, folic acid may not be effective to prevent all the NTDs because etiology of NTDs may be diverse. It is critical to understand etiology of different types of NTDs to prevent this serious human health problem.

Studies using animal models such as zebrafish and mice have contributed to identify mechanisms underlying the NTDs. In human, variants of VANGL1, a planner cell polarity gene, are associated with NTDs. Two variants were tested in zebrafish and led to defective convergent extension phenotype. Thus, this study demonstrates conserved function of the gene that causes NTDs and zebrafish as a useful animal model. Mouse studies concerning NTDs also have been extensively carried out and provided valuable insight for us to understand genetic, cellular and molecular mechanisms of NTDs.

1.3.2 Mechanisms of HP formation and neural tube closure

Neural tube closure involves a sequence of dynamic cellular change in the neural plate. The key event of neural tube closure is formation of hinge points. There are two types of hinge points in neurulation, MHP and DLHPs (Fig. 1.9). MHP and DLHPs have distinct roles in neural tube closure at different levels of spinal axis in mice (Shum and Copp, 1996). First hinge point, MHP, appears at the center of the neural plate, dividing future left and right. MHP is the only HP required in the upper spinal region of the neural tube (Ybot-Gonzalez et al., 2002). Induction from the notochord is critical for MHP formation (Smith and Schoenwolf, 1989). The coordinated morphogenesis of epithelial tubing has been implicated in active regulation of apicobasal epithelial polarity (Andrew and Ewald, 2010). Upon induction from the notochord, cells in the

neural plate where the notochord is apposed elongate along an apicobasal direction and become columnar from cuboidal and then transform into wedge-shaped, which in turn form MHP and the neural groove, while adjacent cells in the neural plate maintain their spindle-shape (Schoenwolf and Franks, 1984). To accomplish cell elongation, centrosomal microtubule consisting of alpha- and beta-tubulin, one of the major cell cytoskeleton, plays an important role. Randomly oriented microtubules mainly around cell cortex in the columnar cells polymerize and assemble, while non-centrosomal gamma-tubulin is localized apically in the cells undergoing apicobasal elongation (Lee et al., 2007). Interestingly, Shroom3, which was previously identified to cause NTD when it was mutated, is an actin binding protein and was reported to recruit gamma-tubulin to the apical region in the Xenopus neural tube (Haigo et al., 2003; Lee et al., 2007). Another study suggests that Shroom3 regulates neuroepithelial apical constriction through recruitment of ROCK1 to the apical junctions, which leads to phosphorylation of Myosin light chain (MLC) required for actomyosin contraction (Nishimura and Takeichi, 2008). Recent studies in chick show that the shape change of the cells in the MHP of the midbrain neural tube are regulated by a dynamic modulation of cell behaviors, namely apical constriction and basal nuclear migration closely regulated by BMP signaling (Eom et al., 2011; Eom et al., 2012). According to their model, in the presence of canonical BMP signaling, pSmad interacts with the PAR3-PAR6-aPKC that is associated with the apical

tight junctions, while local inhibition of BMP in the cells at the presumptive MHP destabilize apical PAR complex, disrupting tight junction. This allows apical localization of LGL, resulting in apical constriction and basal nuclear migration. However, it is still unknown if cellular and molecular mechanisms found in MHP formation are applicable to DLHP formation (Eom et al., 2011; Eom et al., 2012).

The other HPs are paired DLHPs which appear at the junction between the neural ectoderm and surface ectoderm. Bending of DLHPs allows both sides of neural folds to juxtapose to each other (Fig. 1.9D). This allows neural tube fusion to occur. As MHP receives induction from the notochord, induction from non-neural surface ectoderm is required to form DLHPs (Ybot-Gonzalez et al., 2002). The members of Grainy head-like (Grhl) family of developmental transcription factors, Grhl2 and Grhl3 are expressed in non-neural ectoderm. In mice, ablating Grhl2 causes a split face and exencephaly, while loss of Grhl3 results in spina bifida in the lower spine. In both cases, the phenotypes were associated with defective DLHP formation (Rifat et al., 2010). Cytoskeletal rearrangement is also important for DLHP formation. Members of zinc-finger transcription factors, zic2a and zic5 are expressed at the border of future DLHPs. Zic2a and zic5 are the downstream targets of the canonical Wnt signaling pathway (Nyholm et al., 2007). Loss of zic2a and zic5 by morpholino treatment causes a defect in DLHP formation due to lost apical junction integrity with disrupted actomyosin

organization in zebrafish (Nyholm et al., 2009). Interestingly, Zic2 mutant mouse embryos lack dorsal BMP antagonist expression and DLHP formation, resulting in severe spina bifida (Ybot-Gonzalez et al., 2007b). Although these studies suggest that similar molecular and cellular mechanisms in DLHP formation found in zebrafish also regulate mouse DLHP formation, further study is still required. Hh signaling is another important signaling pathway in neurulation. BMP signaling and Hh signaling often antagonize each other in multiple different contexts such as neural fate specification in the early neural tube. In neurulation, Shh acts as a negative regulator of *Noggin* (*Nog*) (Ybot-Gonzalez et al., 2007). Shh is expressed ventrally in the notochord. However, the strength of Shh expression correlates with the presence or absence of DLHPs along the spinal axis. Hh signaling inhibits DLHP formation by antagonizing dorsal genes such as *Nog*. Its expression is markedly weaker at the lower spinal levels where DLHPs are formed (Ybot-Gonzalez et al., 2002). However, detailed cellular and molecular mechanisms of how Hh signaling prevents DLHP formation remain unclear.

The final step in neural tube closure is contact and fusion of epithelium, which are observed in many other morphogenetic events such as palatal shelves and eyelids. This step is followed by more stable union and epithelial remodeling. During neural tube closure, first contact of apposing neural folds is initiated by cellular protrusions comprising of lamellipodia and filopodia. Deleting Ena/VASP, which regulate

lamellipodia and filopodia, resulted in exencephaly (Furman et al., 2007). Surprisingly, there is not much information about requirement of adhesion molecules in fusing neural tube. However, it is likely that combination of initial contact by cellular protrusion and molecular adhesion from apposing neural epithelium induce following epithelial remodeling, ensuring fusion and neural tube closure. Further studies of this area will be awaited.

The final step in neural tube closure is contact and fusion of epithelium, which are observed in many other morphogenetic events such as palatal shelves and eyelids. This step is followed by more stable union and epithelial remodeling. During neural tube closure, first contact of apposing neural folds is initiated by cellular protrusions comprising of lamellipodia and filopodia. Deleting Ena/VASP, which regulate lamellipodia and filopodia, resulted in exencephaly (Furman et al., 2007). Surprisingly, there is not much information about requirement of adhesion molecules in fusing neural tube. However, it is likely that combination of initial contact by cellular protrusion and molecular adhesion from apposing neural epithelium induce following epithelial remodeling, ensuring fusion and neural tube closure. Further studies of this area will be awaited.

1.4 BMP signaling

Bone morphogenetic proteins (BMPs) are a group of secreted proteins that belong to transforming growth factor beta (TGF-beta) superfamily. BMPs consist of more than 15 ligands in mammals. While BMPs were first identified as bone/cartilage-inducing molecules, later studies found BMP signaling acts in organogenesis and maintenance of many tissues and organs, especially in dorsoventral and/or antero-posterior patterning formation. Homo- or hetero-dimers of BMP ligands bind to and signal through their receptors to induce expression of downstream target genes influencing cell proliferation, survival, and differentiation. BMP signaling pathway is evolutionally conserved and critical for multiple stages of embryogenesis and tissue homeostasis.

BMP signaling intensity is regulated by multiple mechanisms. One of the most important concepts is so called "sink-source model". BMPs act as morphogens that diffuse from and travel away from the cells in which they are synthesized (source), creating morphogen gradient. In a simple model, the morphogen gradient directly correlates with the level of BMP signaling. However, BMP signaling is also regulated by other players in the signaling pathway. BMP inhibition by antagonists, such as Nog, ensures the level of BMP signaling required for proper development or maintenance of the tissues and organs. Nog, a major BMP antagonist, binds to BMPs in the extracellular

space, and prevents them from binding to their own receptors (Fig. 1.10). In contrast, inhibin and BMP3 are the BMP receptor antagonists; they bind to BMP receptors instead of binding to ligands to block BMP signaling. Level of BMP receptor expression also affects intensity of BMP signaling. As such, fine tune of BMP signaling is assured by multiple mechanisms.

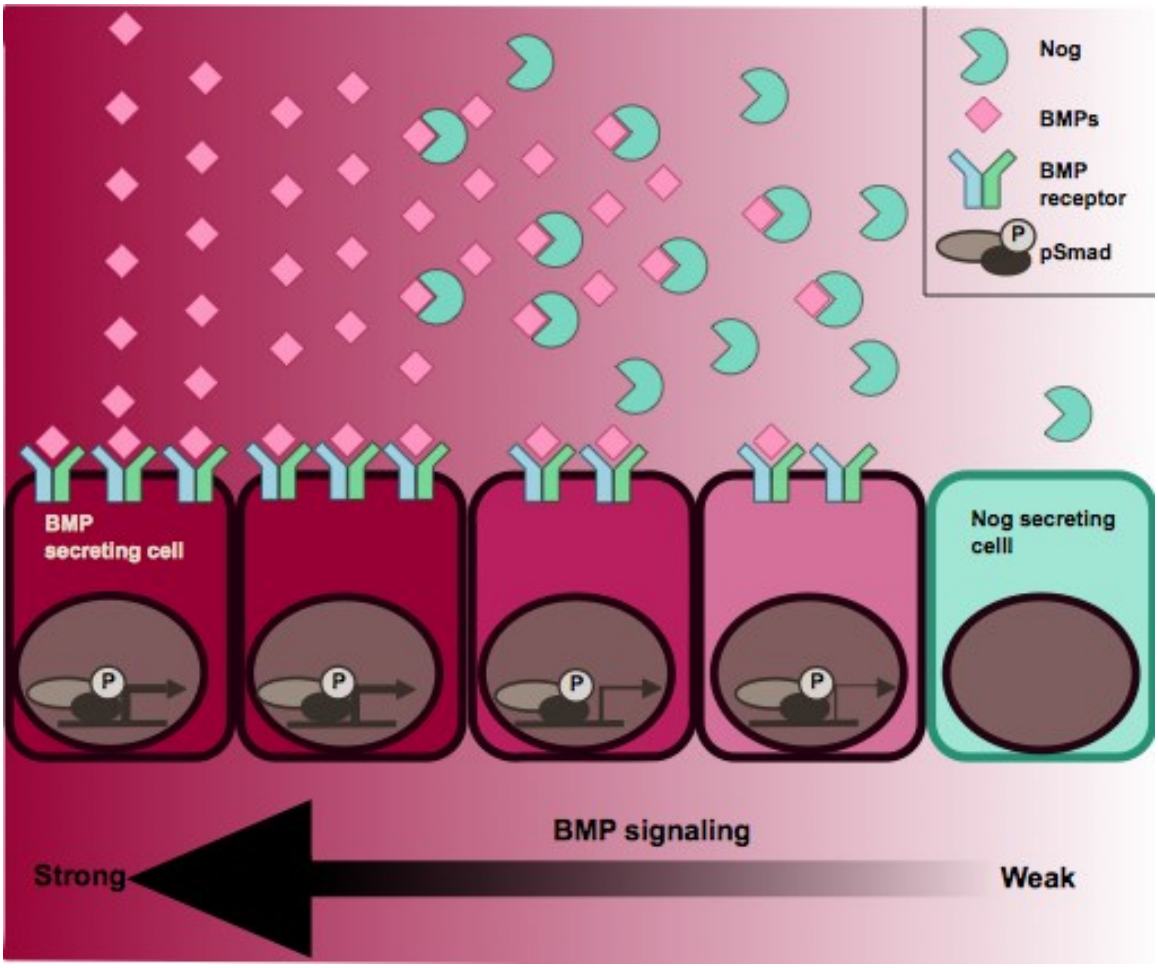
Nog
BMPs
BMP receptor
P
pSmad
BMP secreting cell
Nog secreting cell
P
P
P
P
BMP signaling
Strong
Weak

Figure 1.10: Canonical BMP signaling and gradient formation

BMPs (pink) are a secreted molecule in the extracellular space. They bind to and signal through the receptors at the cell surface. Binding BMPs to their receptors causes phosphorylation to Smads, and translocation of pSmads to the nucleus, resulting in transcription of downstream target genes. Nog (green) is also a secreted molecule. Nog inhibits BMP signaling transduction by binding to BMPs in the extracellular space, preventing BMPs from binding to their receptors. Nog antagonism is important for creating the BMP gradient, which is critical in multiple processes during embryonic development.

1.4.1 BMP signaling pathways

Among BMP ligand-activated signaling pathways, Smad pathway is the most well studied pathway. Both classes of transmembrane receptors, type I and type II, are required for BMP signaling transduction. Upon binding of BMPs to heterotetrameric complex of type I and type II receptors, type II receptor kinase phosphorylates the type I receptor, which in turn phosphorylates receptor Smad 1/5/8 (R-Smads). Phosphorylated Smad 1/5/8 form complexes with co-Smad (Smad4), which translocate into the nucleus and induce downstream target gene expression. Phosphorylated Smad 1/5/8 is often used as a readout for BMP signaling activity. Smad6 and Smad7 (I-Smads) act as antagonists of Smad signaling pathway by binding to type I receptors and prevent activation of R-Smad. Expression of I-Smads is regulated by R-Smads, creating a negative feedback loop.

In addition to the canonical Smad signaling pathway explained above, BMPs activate multiple kinase signaling pathways, including p38 and Erk MAP kinase, PI3, and PKC pathways (Kishigami and Mishina, 2005; Xu et al., 2008). Both canonical BMP signaling (Smad4) and p38 MAP kinase are activated in mediating TGF-beta/BMP signaling during tooth and palate development (Xu et al., 2008). These signaling pathways induce cell proliferation and differentiation.

1.4.2 Nog, a BMP antagonist in development

Nog is a secreted molecule that is encoded by the single-exon Nog gene. It was first discovered as a neural inducer in Xenopus (Smith and Harland, 1992). It is evolutionally conserved. Nog's function as a BMP antagonist was confirmed in evolutionally primitive species such as hydra. When Nog mRNA isolated from hydra was microinjected into Xenopus embryos, a secondary dorsoventral body axis developed (Chandramore and Ghaskadbi 2011). Contrary to expectation, Nog is not found in Drosophila melanogaster (Holley et al., 1996). Nog acts as a BMP antagonist by binding to BMPs in the extracellular space and masking the epitopes that are important for BMPs to bind to their cell surface receptors for activating downstream target genes. In addition to Nog's role as a BMP antagonist, it is found that Nog can bind to non-BMP TGF-beta ligands and XWnt8 and inhibit Activin/Nodal and Wnt signaling in Xenopus embryos during forebrain development (Bayramov et al., 2011). Nog may regulate non-BMP signaling pathways in mammals.

Early Nog expression also plays an important role in left-right axis establishment during somitogenesis stages. Nog regulates expression of Nodal that is a critical left-side determinant in the node and lateral plate mesoderm (Mine et al., 2008). Proper left-right set-up at this stage is crucial for subsequent morphogenesis and alignments of organs.

Importance of Nog in the skeletogenesis has been extensively studied. Nog mutations in humans are found in association with several dominant autosomal syndromes due to haploinsufficiency of the gene dosage. Affected individuals manifest skeletal defects and synostoses such as symphalangism, craniofacial defects and stapes fixation (Rudnik-Schoneborn et al., 2010; Hwang and Wu, 2007). Mouse studies revealed that Nog heterozygous mice exhibit conductive hearing loss similar to human patients with Nog mutations. The conductive hearing loss was caused by a synostosis between the stapes and styloid process resulting from ectopic bone formation during development (Hwang and Wu, 2007). Nog null mice show multiple craniofacial deformities including cleft palate and micrognathia (Stottmann et al., 2006; He et al., 2010). We will discuss more details about Nog's role in development of craniofacial skeletogenesis in a later chapter. Other roles of Nog during development are found in skeletal muscle generation (Smith and Harland, 1992) and differentiation of hair follicles (Botchkarev et al., 1999).

1.4.3 BMP signaling and Hh signaling in development

BMP signaling is involved in the most cellular processes throughout the life of an organism. One reason that BMP signaling can cause different cellular processes is signaling cross-talk in which BMP signaling together with other signaling creates distinct cellular responses. Depending on the partner signaling, the signaling cross-talk

gives diverse outcomes. One of such partner signaling pathways is Hh signaling. Like BMP signaling, Hh signaling is also involved in various types of cellular processes including cell proliferation and survival.

Hh signaling was first identified in Drosophila embryonic patterning, and now it has been known as one of the key signaling pathways in the development of multicellular organisms. Genetic studies in different organisms revealed most of the components in Hh signaling pathway are highly conserved throughout the species. Hh ligands consist of three secreted lipid molecules, Sonic hedgehog (Shh), Indian hedgehog (Ihh), and Desert hedgehog (Dhh) in chick and mammals.

Cross-talk between BMP signaling and Hh signaling is highly context dependent. They work together synergistically or antagonistically. Importantly, BMP and Hh signaling pathways can directly regulate each other by binding to the promoter region of key factors of each other (Zhao et al., 2006; Guo and Wang 2009). In vitro study suggests that Gli activates human BMP4 and BMP7 gene promoters (Kawai and Sugiura, 2001). Smads modulates Hh signaling through regulation of Gli transcription directly or indirectly (Rios et al., 2004; Alvarez-Rodriguez et al., 2007).

In vivo studies support the interactions between BMP and Hh signaling in several developmental contexts. Disrupted Shh signaling in the ventral neural tube of a mouse with cilia defects causes abnormal dorsal neural tube patterning due to aberrant

BMP signaling (Honer and Caspary, 2011). In humans, *SATB2* causes severe palatal and mandibular defects. The expression of *satb2* in pharyngeal arches is mediated by both BMP signaling and Hh signaling in zebrafish (Sheehan-Rooney et al., 2013). BMP4 expression in the palatal mesenchyme is required for Shh expression in the medial edge epithelium (MEE) for proper anterior palatal shelf growth and development (Zhang et al., 2002).

Taken together BMP and Hh signaling pathways are highly interdependent in various cellular processes. Therefore, studying mutation of one signaling pathway often finds disruption of the other.

2. Multiple tissue-specific requirements for the BMP antagonist *Noggin* in development of the mammalian craniofacial skeleton

The following chapter is currently under review for publication.

Proper morphogenesis is essential for both form and function of the mammalian craniofacial skeleton that consists of more than twenty small cartilages and bones. Skeletal elements that support the oral cavity are derived from cranial neural crest cells (NCCs) that develop in the maxillary and mandibular buds of pharyngeal arch 1 (PA1). Bone Morphogenetic Protein (BMP) signaling has been implicated in most aspects of craniofacial skeletogenesis, including PA1 development. However, the roles of the BMP antagonist Noggin in formation of the craniofacial skeleton remain unclear, in part because of its multiple domains of expression during formative stages. Here we used a tissue-specific gene ablation approach to assess roles of *Noggin* (*Nog*) in two different tissue domains potentially relevant to mandibular and maxillary development. We found that the axial midline domain of *Nog* expression is critical to promote PA1 development in early stages, necessary for adequate outgrowth of the mandibular bud. Subsequently, *Nog* expression in NCCs regulates craniofacial cartilage and bone formation. Mice lacking *Nog* in NCCs have an enlarged mandible that results from

increased cell proliferation in and around Meckel's cartilage. They also show complete secondary cleft palate, most likely due to inhibition of posterior palatal shelf elevation by disrupted morphology of the skull base structure. Our findings demonstrate multiple roles of *Nog* in different domains for craniofacial skeletogenesis, and suggest a novel mechanism of secondary cleft palate that previous studies have not revealed.

2.1 Introduction

Among the most frequently occurring congenital defects in newborns are craniofacial deformities, such as cleft palate and micrognathia (Holder-Espinasse et al., 2001; Mossey PA, 2002). These malformations impact the quality of life due to functional difficulties as well as negative social responses (Pruzinsky, 1992). The causes of craniofacial deformities are diverse, including genetic and environmental factors. Yet the underlying genetic and cellular mechanisms behind the emergence of such deformities are not well understood.

Mammalian craniofacial skeletal elements consist of more than 20 small bones and cartilages, the size and shape of which are precisely determined during development (reviewed by (Matsui and Klingensmith, 2013). Most of these skeletal elements are derived from neural crest cells (NCCs), an ectoderm-derived multipotent cell population that migrates ventrally from the closing dorsal neural folds. NCCs take distinct migratory pathways, with some populating the pharyngeal arches. One such group of NCCs populating pharyngeal arch 1 (PA1) proliferates, differentiates and gives rise to most of the frontal facial structures such as Meckel's cartilage, the mandible and the maxilla including the bones of the palate. Although NCCs possess intrinsic information that promotes differentiation of the facial skeleton, interactions between NCCs and other tissues such as ectoderm or endoderm allow molecular signaling

between tissues to ensure proper morphogenesis and development of pharyngeal arch derivatives (Couly et al., 2002).

Bone morphogenetic protein (BMP) signaling has been implicated as a key regulator of development of NCCs and their derivatives (Baek et al., 2011; Bonilla-Claudio et al., 2012; Dudas et al., 2004; Goldstein et al., 2005; Kanzler et al., 2000). Mouse genetic manipulation studies revealed a requirement for precise regulation of BMP signaling in craniofacial development (Bonilla-Claudio et al., 2012; Li et al., 2013; Wang et al., 2013).

One important means of regulating BMP signaling is by extracellular BMP antagonists. *Nog* is a major BMP antagonist expressed in multiple domains during embryonic development. Noggin binds to BMP ligands in the extracellular space and prevents them from binding their receptors. Experimental work in mice indicates that *Nog* regulates various types of skeletogenesis, including appendicular bone, cartilage and joint formation (Brunet et al., 1998). Genetic studies in humans have also identified a role for *Nog* in regulating skeletal morphogenesis, with mild ectopic bone formation particularly in the digits, associated with heterozygous loss-of-function mutations (reviewed by (Potti et al., 2011).

As demonstrated primarily by analysis of the null phenotypes of mice lacking the *Nog* gene, this BMP antagonist also has important roles in regulating the

development of craniofacial structures (He et al., 2010; Stottmann et al., 2001; Stottmann et al., 2006; Wang et al., 2013). In postnatal stages of development, *Nog* expression in cranial sutures prevents the premature fusion of skull bones (craniosynostosis) (Warren et al., 2003). *Nog* null mice display cleft palate, a defect ascribed to compromised integrity of palatal epithelium due to the change in cell death and cell proliferation rate (He et al., 2010). Further roles of Noggin are betrayed in the absence of Chordin, another BMP antagonist which when lacking on its own has only very mild, non-lethal phenotypes (Choi and Klingensmith, 2009). Mice lacking one or both alleles of *Nog* display a range of craniofacial malformations of varying expressivity and penetrance. These sometimes include dramatic truncations of the rostral head, in association with holoprosencephaly (Anderson et al., 2002; Bachiller et al., 2000). These defects are due at least in part to defective Shh signaling from the prechordal plate and Fgf8 signaling from the anterior neural ridge, organizing centers of early forebrain patterning and growth (Anderson et al., 2002).

Independent of this early rostral requirement, these BMP antagonists also function to promote mandibular development. Whereas mice lacking the *Chordin* gene (*Chrd*) show a very low penetrance of mild micrognathia (Choi and Klingensmith, 2009), $Chrd^{-/-};Nog^{+/-}$ and $Chrd^{-/-};Nog^{-/-}$ exhibit a spectrum of mandibular hypoplasia, ranging from agnathia to micrognathia, as a result of insufficient NCC survival during mandibular

bud outgrowth PA1 (Stottmann et al., 2001). In contrast, in the absence of *Nog* alone, mandibles are enlarged, reflecting increased size of the transient Meckel's cartilage, around which mandibular bone is formed (Stottmann et al., 2001; Wang et al., 2013). The mandible forms via ossification of cells from the NCC-derived perichondrium at the periphery of Meckel's cartilage, which itself is composed of both neural crest derivatives and other mesenchymal cells (Chai et al., 2000a). Whereas the normal fate of chondrocytes in the main portion of Meckel's cartilage is to degenerate, in *Nog* mutants or in embryos expressing an activated BMP receptor transgene in chondrocytes, these cells over-proliferate, then differentiate and undergo ossification (Wang et al., 2013).

These phenotypes all reveal important roles for *Nog* in regulating development of the craniofacial skeleton, but the relevant spatiotemporal contexts of *Nog* expression are not clear for any of these roles. During early stages of head development, *Nog* is expressed in several potentially relevant domains (Anderson et al., 2002; He et al., 2010; Lana-Elola et al., 2011; Nifuji and Noda, 1999; Stottmann et al., 2001). Here we further probe the expression of *Nog* in relation to development of the viscerocranium. We then use a series of tissue-specific ablations of the *Nog* gene to elucidate the cellular mechanisms of Noggin function in mandibular and palatal development.

2.2 Materials and Methods

2.2.1 Mouse strains

The $Nog^{fx/fx}$ conditional (Stafford et al., 2011), $Nog^{lacZ/+}$ (Brunet et al., 1998), and constitutively active Bmpr1a conditional mice (*caBmpr1a*), conditional mice were maintained on the mixed background. *Wnt1-Cre* mice (Brewer et al., 2004; Chai et al., 2000b; Jeong et al., 2003; Jiang et al., 2000) were crossed with $Nog^{lacz/+}$ to generate *Wnt1-Cre;*$Nog^{lacz/+}$ male mice, which were subsequently crossed with $Nog^{fx/fx}$ to conditionally knockout *Nog* from neural crest cells. As a complement experiment, *caBmpr1a*, which have been described previously (Rodriguez et al., 2010), were crossed with *Wnt1-Cre* to activate BMP signaling only in NCCs.

2.2.2 Histology, immunohistochemistry, and X-gal staining

For histology, embryos were harvested from pregnant mice, fixed in 4% paraformaldehyde (PFA) at 4°C for 2 hours to overnight depending on gestation stage, dehydrated through graded alcohols, embedded in paraffin wax and sectioned at 10-um thickness. The sections were stained with hematoxylin and eosin for morphological observations.

Whole embryos are stained with X-gal overnight at RT. For section X-gal staining, embryos were fixed 2 hours to overnight embedded in OCT compound (Sakura

Finetek) after sucrose gradient (15% and 30% sucrose in PBST). Cryosections were made at 10 um thickness and stained with X-gal.

2.2.3 Skeletal preparations and in situ hybridization

For skeletal preparation, embryos were skinned, fixed in 95% ethanol overnight, stained with 0.05% alcian blue, washed in 95% ethanol for 6hours to overnight and cleared in 2% KOH. Further, to stain bone, embryos were placed in 0.005% alizarin red in 0.9 N acetic acid and 60% ethanol overnight at room temperature and cleared with 1% KOH for overnight followed by 20% glycerol in 1% KOH until cleared. For whole mount in situ hybridization, embryos were dissected from pregnant mice, fixed overnight in 4% PFA at 4°C. The fixed embryos were dehydrated through 25%, 50%, 75%, and 100% ethanol, and stored in 100% ethanol at -20°C. Whole mount in situ hybridization was carried out using previously described protocol (Belo et al., 1997) with hybridization temperature of 65°C.

2.2.4 Palatal shelf organ culture

Palatal shelves were cultured according to previously described methods (Brunet et al., 1995; Taya et al., 1999a). Palatal shelves were removed at E13.5 from wild-type and *Wnt1-Cre;Nog*$^{lacz/fx}$ embryos. Paired palatal shelves were placed on 0.3 um Millipore filters with medial edge epithelia (MEE) in contact. Initially, paired palatal shelves were cultured in Minimal Essential Medium with Earle's salts and L-glutamine (Gibco)

supplemented with 1% anti-anti (Gibco) at 37°C in a 5% CO_2 air environment. After 24 hours culture the paired palatal shelves were submerged in DMEM with Earle's salts and L-glutamine (Gibco) supplemented with 5% FBS for another 48 hours. After total 72 hours of culture, paired palatal shelves were fixed in 4% PFA and processed for paraffin blocks and sectioned 10-um thickness as described above.

2.2.5 Quantitative real-time reverse transcription-polymerase chain reaction (RT-PCR)

RNA was purified from E12.5 and E13.5 palatal tissue or mandibles from wild type and mutant using Trizol reagents (Invitrogen). Following RNA extraction, cDNA was synthesized using iScript™ cDNA Synthesis Kit (BIO RAD). Quantitative PCR amplifications were performed in a StepOnePlus real-time PCR machine (Applied Biosystems) using the SensiMix™ SYBR & Fluorescein Kit (Bioline). For each gene, the PCR reaction was carried out in triplicates and the relative levels of mRNAs were normalized to that of HPRT using the normalized expression method. Student's t-test was used to analyze the significance of difference and a P-value less than 0.05 was considered statistically significant.

2.2.6 Detection of cell proliferation

For detection of cell proliferation in the palatal shelves, pregnant female mice were injected once intraperitoneally at gestational day 12.5 and 13.5 with BrdU Labeling Reagent (50μg/g body weight; Roche). 30 min after injection, embryos were dissected,

fixed with 4% PFA overnight at 4°C and embedded in paraffin for 10um-thickness coronal sectioning. To detect BrdU, rat anti-BrdU (1:500; Accurate Chemical & Scientific) was used. Following BrdU immunostaining, cell counts were recorded for each of the bilateral palatal shelves of matching areas of anterior secondary palate and of posterior secondary palate regions in the wild type and mutant samples. The cell proliferation rate was calculated as the number of the cell nuclei with BrdU labeling. Alternatively, mouse anti-phosphorylated histone H3 (1:500; cell signaling) was also used to detect dividing cells. Data were collected from at least three pairs of mutant and wild type littermates at each developmental stage. Students' t-test was used to analyze the significance of difference and a P-value less than 0.05 was considered statistically significant.

2.3 Results

2.3.1 Expression of *Nog* during formative craniofacial development

To gain insight into its possible roles of *Nog* in development of tissues derived from PA1, we assessed its spatiotemporal expression using an assay for the expression of a *lacZ* reporter in the published *Nog* null allele (Anderson et al., 2002; Brunet et al., 1998; McMahon et al., 1998). *Nog* is expressed transiently in migrating and post-migratory NCCs from the earliest stages, with robust expression by at E8.5 (Fig. 2.1A, B). At E9.5 expression is observed in NCCs in PA1 (Fig. 2.1C). By E10.5, its expression is restricted in epithelium of PA1 (Fig. 2.1D). Over this timeframe *Nog* is also present in the notochord, the floor plate of the neural tube, the dorsal foregut endoderm (Fig. 2.1B, C), and the ventrolateral foregut endoderm in the laryngeal region. During palatal development, between E11.5 and E13.5, *Nog* is more strongly expressed in the palatal epithelium. *Nog* is also expressed in various cartilages; as previously observed (Wang et al., 2013), this includes Meckel's cartilage from E12.5 and later (Fig. 2.1E, F).

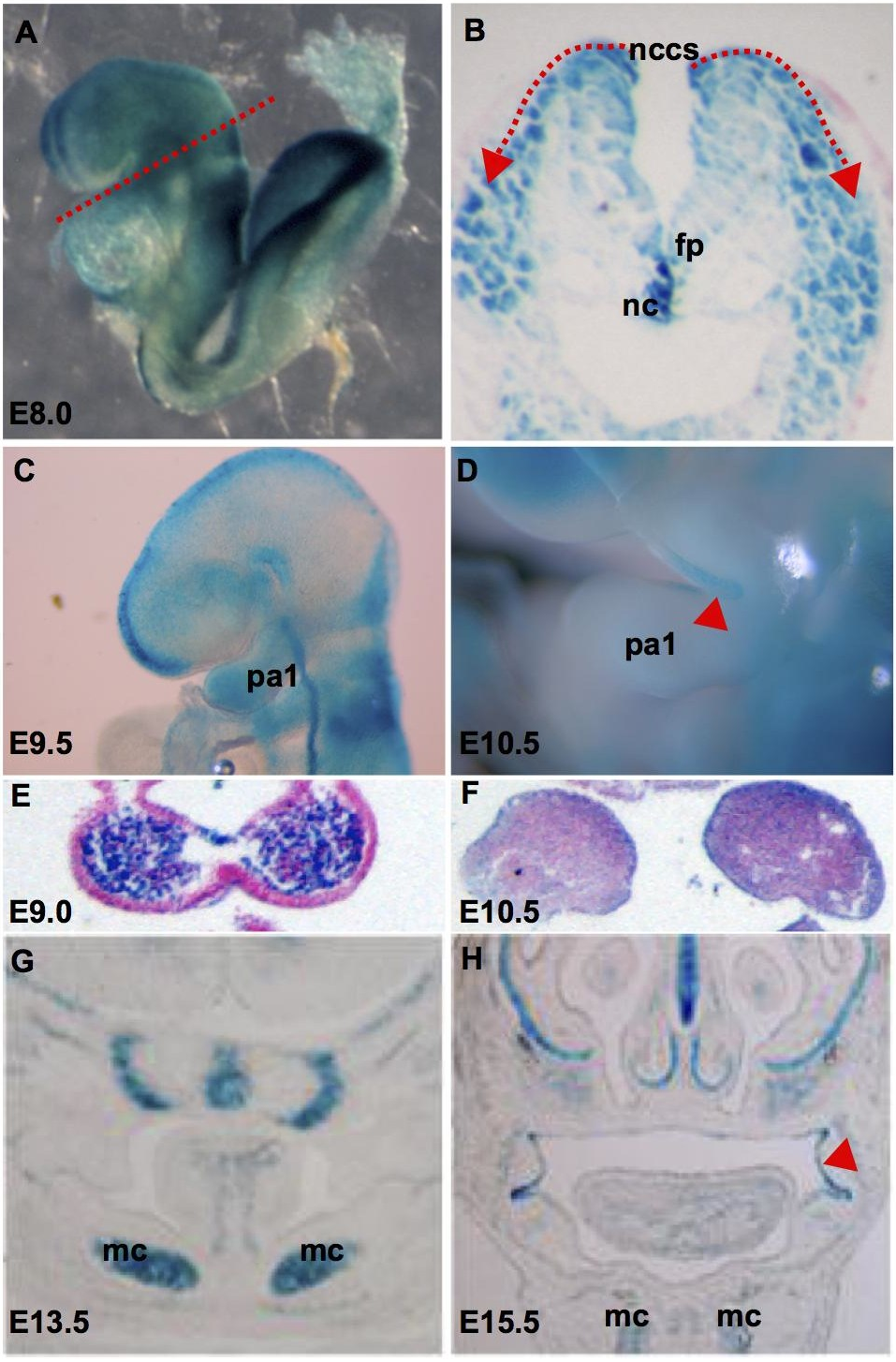
A
E8.0
B
nccs
fp
nc
C
pa1
E9.5
D
pa1
E10.5
E
E9.0
F
E10.5
G
mc
mc
E13.5
H
E15.5
mc
mc

Figure 2.1: Nog is expressed in multiple domains during craniofacial development.

(A, B) *Nog* is first expressed in the migrating NCCs around E8.0. (C) *Nog* is expressed in the NCCs of BA1. (D) By E10.5 *Nog* expression is restricted to the oral epithelium of BA1. (E, F) *Nog* is expressed in the cartilages in the head. pa1; pharyngeal arch 1, fp; floor plate of the neural tube, mc; Meckel's cartilage, nccs; neural crest cells, ns; nasal septum, oe; oral epithelium.

2.3.2 Loss of BMP antagonism from axial domains results in rostral hypoplasia but not cleft palate

Given that loss of BMP antagonism by *Nog*, specifically in the absence of *Chordin* (*Chrd*), can result in both micrognathia and holoprosencephaly (Anderson et al., 2002; Stottmann et al., 2001), we tested the role of axial *Nog* in craniofacial development by deleting *Nog* in the axial midline from early stages in the *Chrd* null background. To do this, we combined a conditional null allele of *Nog* (Nog^{fx}) (Stafford et al., 2011) with *Shh-GFP-Cre* (Harfe et al., 2004), a recombination driver for the late node, notochord, and floor plate. Because these are all sites not only of Nog expression but also Chrd, as well as the fact that either *Nog* null or *Chrd* null alone shows extremely low penetrance and very mild craniofacial phenotypes, we made *Shh-GFP-Cre;*$Nog^{lacz/fx}$ mutants with and without the presence of *Chrd*. Since we did not see any phenotypes in the mutant with the presence of *Chrd* (*Shh-GFP-Cre;*$Nog^{lacz/fx}$) (data not shown), we focused on the phenotypes of *Shh-GFP-Cre;* $Nog^{lacz/fx}$*;* $Chrd^{-/-}$ embryos. We observed that these mutants displayed a partially penetrant hypoplastic PA1 derivatives including the mandible and the maxilla (3/5), and some displayed holoprosencephaly as well (Fig. 2.2A-D). These data confirm what the models previously proposed - that is, underdeveloped PA1 derivatives and/or holoprosencephaly in $Chrd^{-/-}$;$Nog^{-/+}$ mutants result from a lack of rostral axial BMP antagonism (Anderson et al., 2002; Stottmann et al., 2001). These data

collectively indicate that BMP antagonism in axial midline tissues promotes mandibular outgrowth, though none of these tissues contribute to the mandible.

In contrast, none of the mutants showed two relevant defects of the *Nog* null. None exhibited a thickening of the mandible, implying some other deficit of *Nog* underlies the thickened mandible phenotype of the null (Stottmann et al., 2001; Wang et al., 2013). Moreover, the embryos lacking axial *Nog* did not display cleft palate. This indicates that the fully-penetrant cleft palate defect of *Nog* null mutants (He et al., 2010) does not result from a lack of axial BMP antagonism, but instead implies another tissue type must make Noggin protein for proper development of craniofacial structures, including palatogenesis.

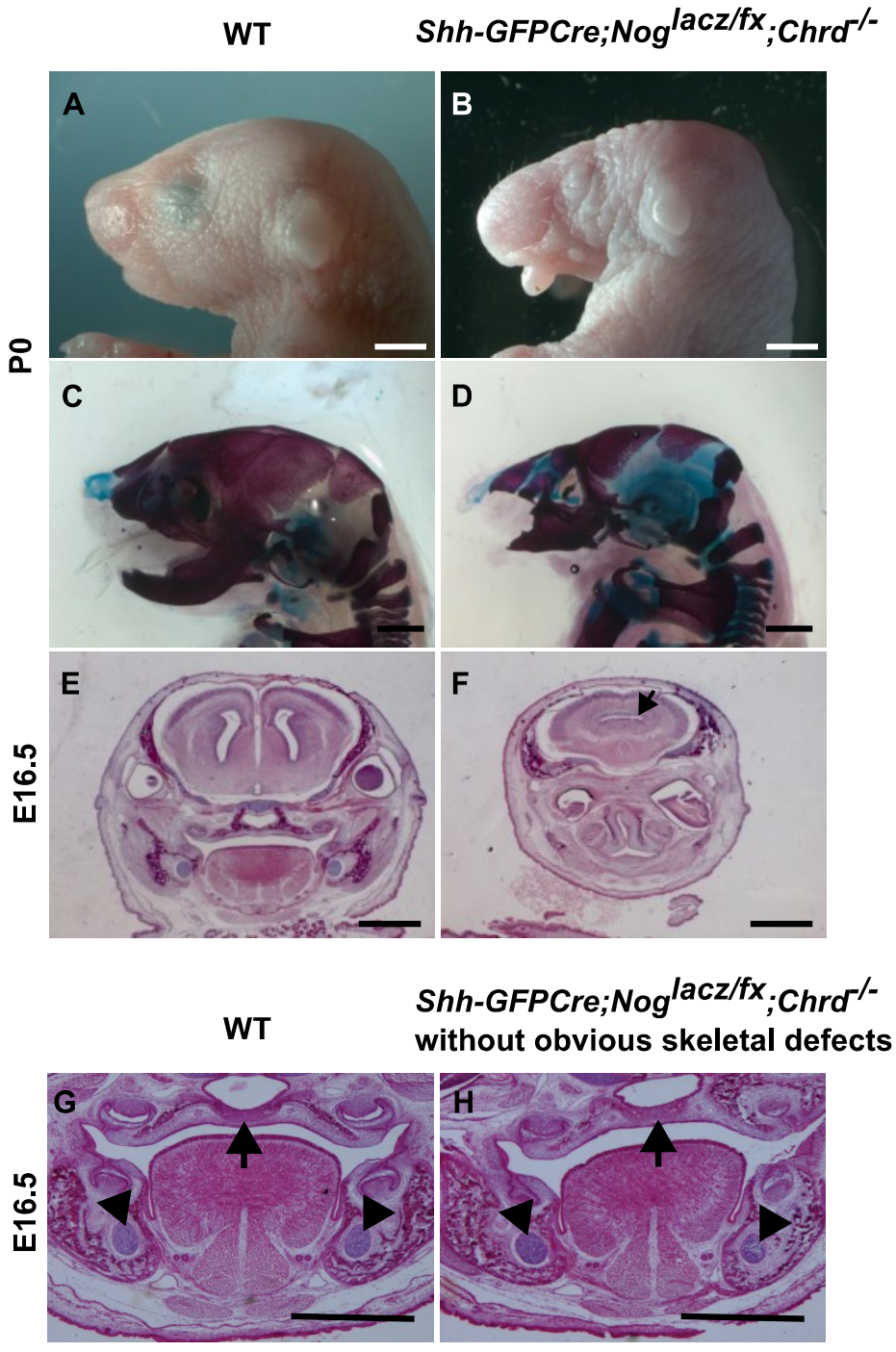
WT
Shh-GFPCre;Nog lacz/fx ;Chrd -/-
A
B
P0
C
D
E
F
E16.5
WT
Shh-GFPCre;Nog lacz/fx ;Chrd -/-
without obvious skeletal defects
G
H
E16.5

Figure 2.2: BMP antagonism in axial domain is critical for development of PA1 derivatives.

(A-D) Lateral view of wild-type (A, C) and *Shh-GFPCre;Nog*$^{lacz/fx}$*;Chrd*$^{-/-}$ (B, D) mutant whole-mount and skeletal-prep heads at P0 stage showing lack of *Chrd* and *Nog* in *Shh-GFPCre* domain results in hypomorphic PA1 derivatives compared with wild-type littermate. Scale bars = 2 mm. (E, F) Example of holoprosencephaly in mutant embryo at E16.5 (F). (G, H) Mutant embryos without obvious phenotypes showing relatively normal development of palate indicated with an arrow and Meckel's cartilage indicated with arrowheads (H). Scale bars = 1 mm.

2.3.3 Loss of *Nog* in neural crest cells results in an enlarged mandible

Since many craniofacial skeletal elements are derived from NCCs, in which *Nog* is expressed (Stottmann et al., 2001), we assessed potential roles of *Nog* in NCCs using *Wnt1-Cre*, an NCC specific Cre driver (Danielian et al., 1998), in the development of craniofacial structures. In the head region, *Wnt1-Cre* is expressed in the dorsal neural folds from early stages of cranial NCC development, as well as in newly migrating NCCs (Jiang et al., 2000; Stottmann and Klingensmith, 2011). Given that *Chrd* is redundant with *Nog* in many developmental contexts (reviewed by (Klingensmith et al., 2010), and that PCR data suggest *Chrd* is expressed at low levels in NCCs (M. Choi and JK, unpublished results), we tested the role of *Nog* in NCCs with and without wild-type allele(s) of *Chrd*. We found that the craniofacial phenotypes of *Wnt1-Cre; Nog*$^{lacz/fx}$ animals were not noticeably different from *Wnt1-Cre;Nog*$^{lacz/fx}$*;Chrd*$^{-/-}$ (Fig. 2.4). Regardless of *Chrd*'s presence or absence, embryos lacking Nog from NCCs resulted in multiple craniofacial defects as described below. As a demonstration, the samples in Figure 2.3 and 2.4 are from mutant animals of the genotype *Wnt1-Cre; Nog*$^{lacz/fx}$*;Chrd*$^{-/-}$, whereas all other figures depict results from mutants that were *Wnt1-Cre; Nog*$^{lacz/fx}$.

A striking phenotype in embryos lacking *Nog* in NCCs is an enlarged mandible (Fig. 2.3 & 2.7A, B) very similar to that of *Nog* null mice (Stottmann et al., 2001; Wang et al., 2013). Other craniofacial skeletal derivatives of NCCs, including laryngeal structures

such as hyoid and thyroid cartilages, were also hypermorphic in the mutant embryos (Fig. 2.5). Our results indicate that the thickened mandible phenotype of *Nog* mutants is due specifically to a lack of Noggin in NCCs, implying that attenuation of BMP signaling in the immediate environment of NCCs is necessary for proper mandibular morphogenesis.

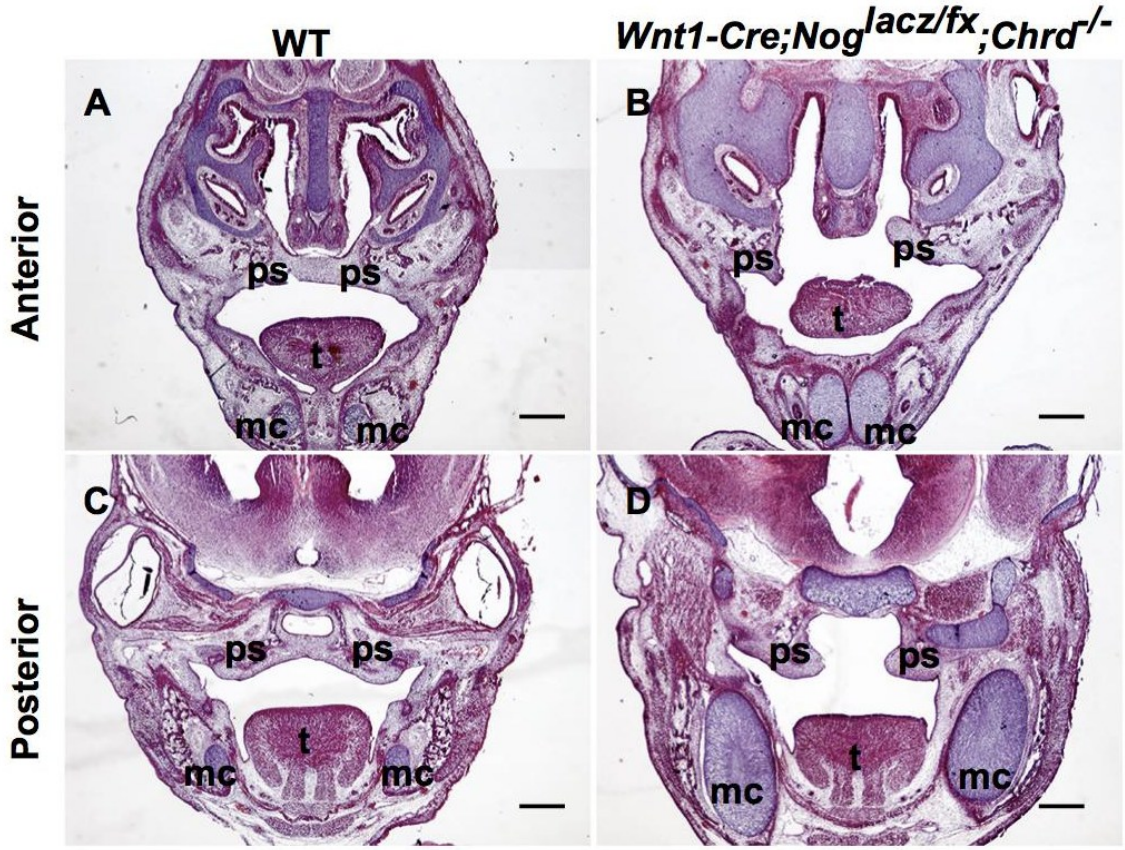

Figure 2.3: Absence of Nog in NCCs causes craniofacial defects.

(A, C) Anterior and posterior coronal sections through E15.5 wild-type embryonic head showing fusion of the palatal shelves and normal development of cartilages in the head. (B, D) Anterior and posterior coronal sections of *Wnt1-Cre;Nog*$^{lacz/fx}$ *;Chrd*$^{-/-}$ mutant embryos showing cleft palate and enlarged cartilages at E15.5. ps; palatal shelves, t; tongue, mc; Meckel's cartilage. Scale bars = 400 μm.

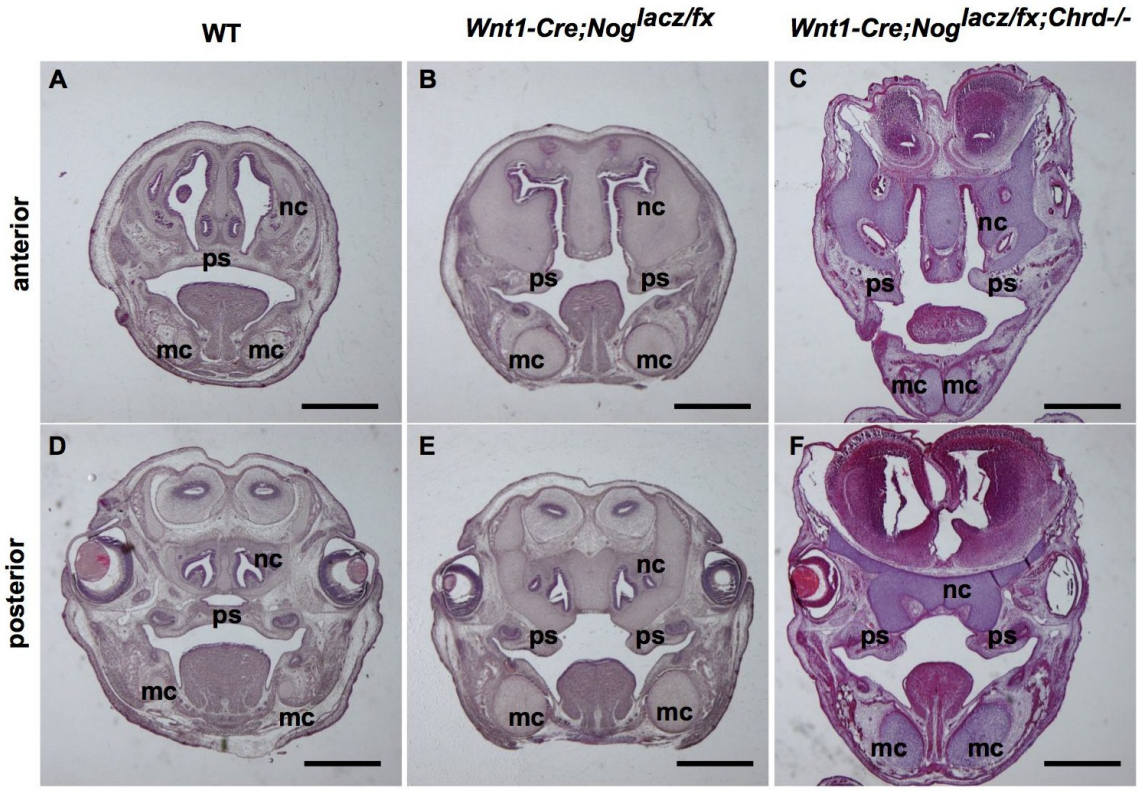
WT
Wnt1-Cre;Nog lacz/fx
Wnt1-Cre;Nog lacz/fx;Chrd-/-
anterior
posterior
A
B
C
D
E
F
nc
ps
mc

Figure 2.4: Lack of *Nog* in NCCs in the presence or absence of *Chrd* leads to an enlarged Meckel's cartilage and cleft palate.

(A-B) Anterior coronal sections of E15.5 wild-type (A), *Wnt1-Cre;Nog*$^{lacz/fx}$ (B), *Wnt1-Cre;Nog*$^{lacz/fx}$*;Chrd*$^{-/-}$ (C) heads. Regardless of presence or absence of Chrd, lack of Nog in NCCs results in an enlarged nasal and Meckel's cartilages and secondary cleft palate (B, C). (D-F) Posterior coronal sections of E15.5 wild-type (D), *Wnt1-Cre;Nog*$^{lacz/fx}$ (E), *Wnt1-Cre;Nog*$^{lacz/fx}$*;Chrd*$^{-/-}$ (F) heads. Both types of mutants (E, F) show not fully elevated palatal shelves and a wide gap between the palatal shelves. mc; Meckel's cartilage, nc; nasal cartilage, ps; palatal shelves. Scale bars = 1 mm.

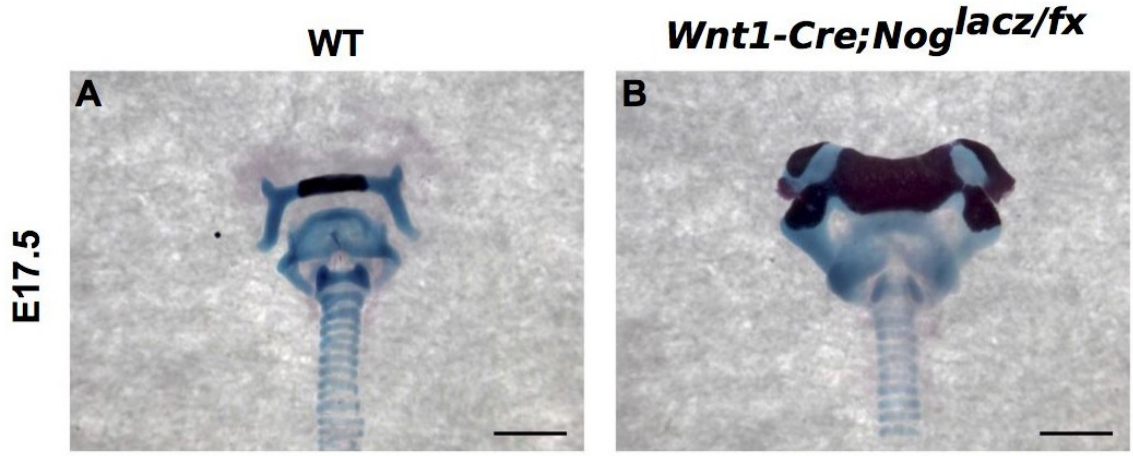

Figure 2.5: Laryngeal skeletal element in the *Wnt1-Cre;Nog*$^{lacz/fx}$ mutant embryos is hypermorphic.

(A) E17.5 wild-type laryngeal skeleton show normal development in which hyoid and thyroid structures are separated. (B) An enlarged hyoid skeleton is joined with thyroid cartilage in mutant. The hyoid structure is over-ossified. Scale bars = 1mm.

2.3.4 Neural crest migration into PA1 occurs normally in embryos lacking *Nog* in NCCs

We investigated the mechanisms underlying the enlarged mandibular skeletal element. A potentially relevant finding is that BMP signaling promotes delamination and collective migration of the NCCs (Burstyn-Cohen and Kalcheim, 2002; Hall and Erickson, 2003). In addition, in so far as *Chrd*$^{-/-}$;*Nog*$^{+/-}$ embryos has increased neural crest production from the neural tube (Anderson et al., 2006), we hypothesized that ablating *Nog* from NCCs may increase production and migration of NCCs into the pharyngeal arches. However, we observed that the size of the PA1 in mutant embryos was not noticeably larger than that in wild type littermates at E10.5, when NCC migration is completed as Fig. 2.6 shows. We also assessed the expression of pharyngeal arch markers, including *Dlx2*, *Dlx5*, *Msx1*, and *Barx1* (Fig. 2.6). Each marker was expressed similarly as in wild type embryos, suggesting normal patterning of the arch mesenchyme and ectoderm. These results suggest that altered NCC production and migration are not the primary cause of the enlarged mandibular skeleton observed in *Wnt1-Cre;Nog*$^{lacz/fx}$ mutants.

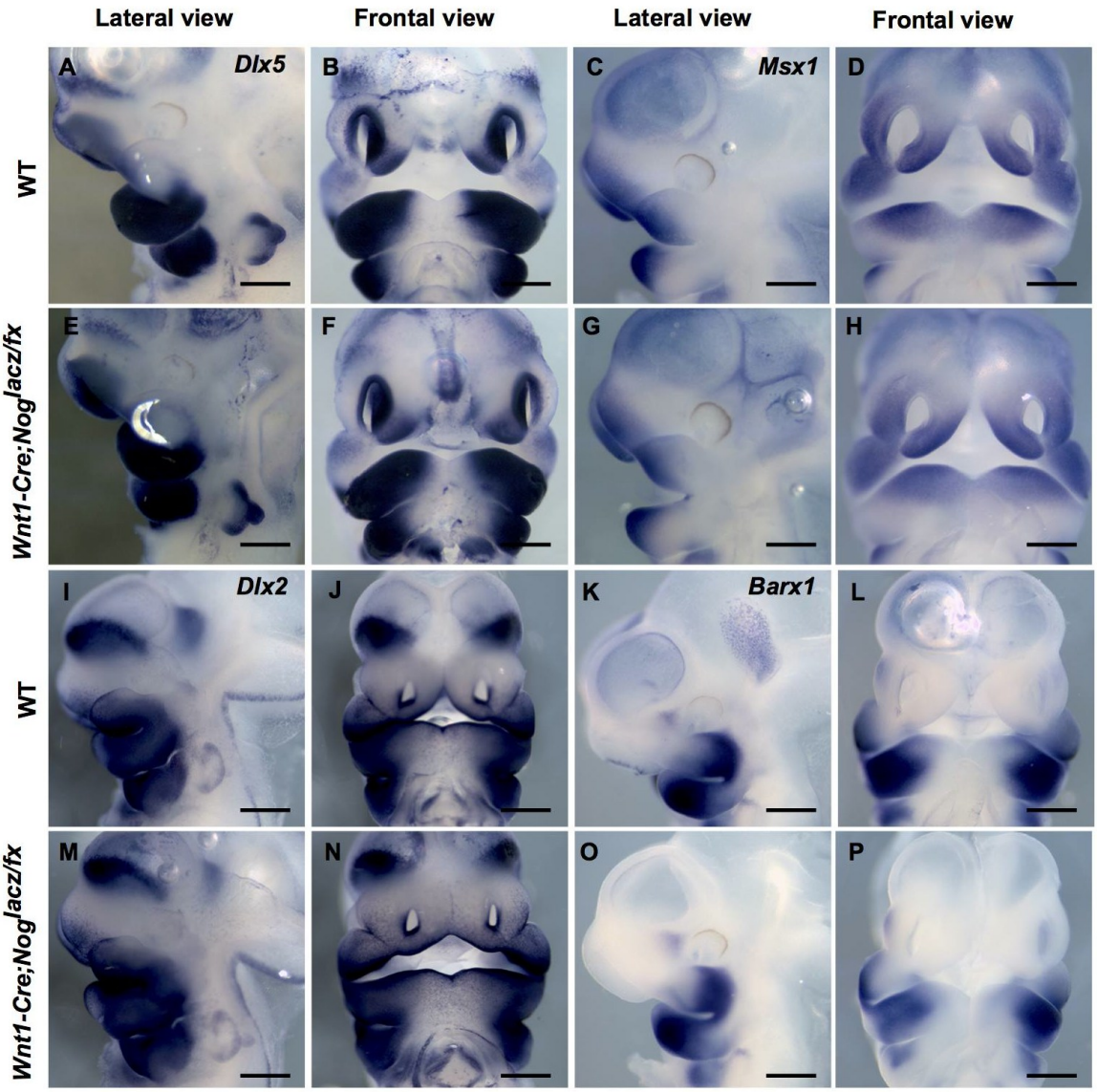
Lateral view
Frontal view
Lateral view
Frontal view
WT
Wnt1-Cre;Nog lacz/fx
WT
Wnt1-Cre;Nog lacz/fx
A
Dlx5
B
C
Msx1
D
E
F
G
H
I
Dlx2
J
K
Barx1
L
M
N
O
P

Figure 2.6: PA1 shows normal expresion of patterning markers in the *Wnt1-Cre;Nog*$^{lacz/fx}$ mutant embryos.

(A-D, I-L) Normal expression of pharyngeal arch markers was shown in wild-type embryos. (E-H, M-P) Expression of pharyngeal arch markers in *Wnt1-Cre;Nog*$^{lacz/fx}$ mutant embryos. (A, B, E, F) Expression of *Dlx5* mRNA in wild-type lateral and frontal views (A, B) and the similar expression pattern was observed in mutant lateral and frontal views (E, F). Expression of *Msx1* (C, D, G, H), *Dlx2* (I, J, M, N), and *Barx1* (K, L, O, P) showed normal expression both in wild-type (C, D, I, J, K, L) and mutant (G, H, M, N, O, P) embryos. The size of PA1 is not different between wild-type (A-D, I-L) and mutant littermates (E-H, M-P). Scale bars = 500 μm.

2.3.5 Cell proliferation in Meckel's cartilage and perichondrium is increased in the absence of Nog in NCCs

To probe the cause of the enlarged mandible in mutants lacking *Nog* in NCCs, we performed cell proliferation assays in Meckel's cartilage using a BrdU incorporation and detection to mark proliferating cells. Meckel's cartilage first forms as a cartilage condensation around E11.5. At this stage, the size of the condensation between wild-type and mutant does not show much difference (Fig. 2.7C, D). However, by E12.5, the mutant Meckel's cartilage grows much faster and larger (Fig. 2.7E, F and Fig. 2.8 G, H). We found that cell proliferation both in the mesenchyme and in the perichondrium of mutant Meckel's cartilage is increased at E12.5 and the diameter of the Meckel's cartilage persistently grows larger in the mutant until E15.5 than in wild type (Fig. 2.7C-F, 2.9B, C).

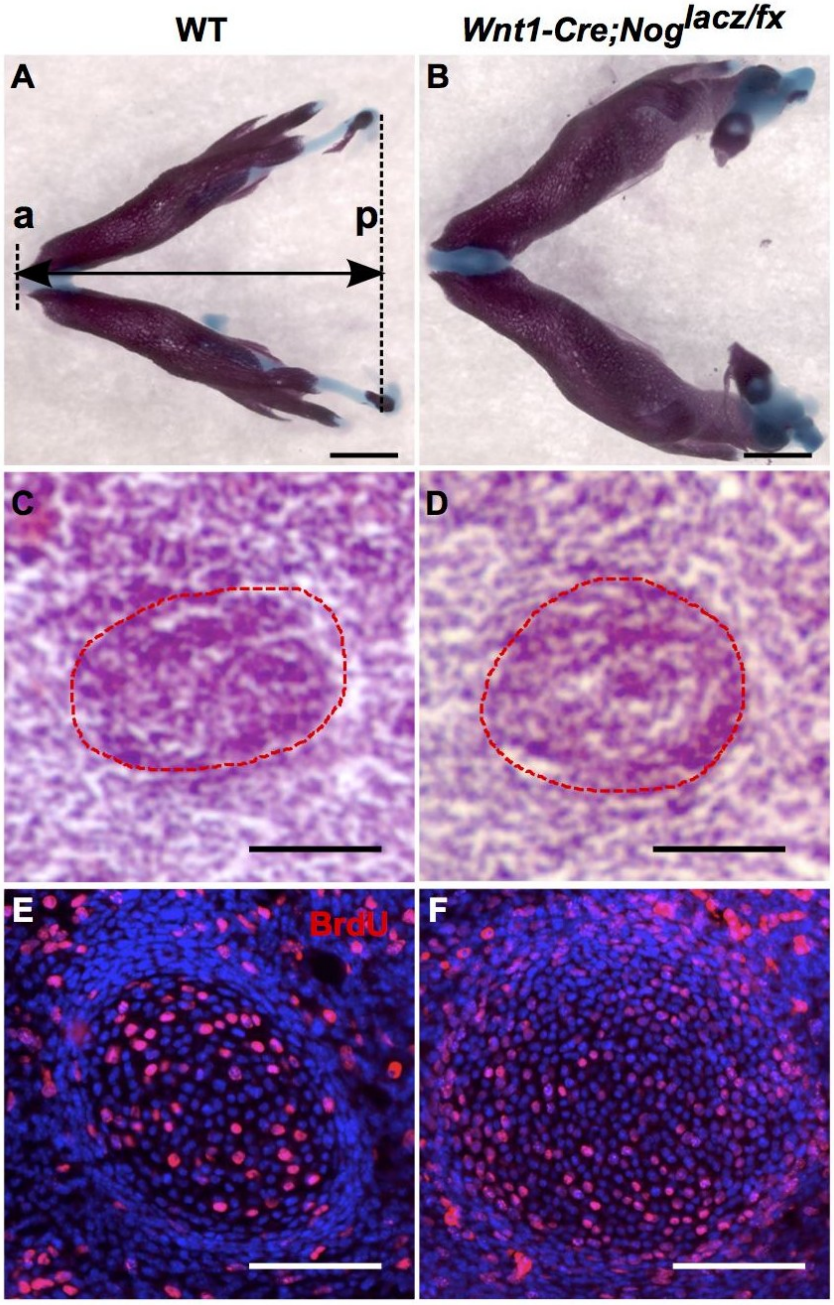
WT
Wnt1-Cre;Nog lacz/fx
A
B
a
p
C
D
E
BrdU
F

Figure 2.7: Increased cell proliferation causes Meckel's cartilage in *Wnt1-Cre;Nog*$^{lacz/fx}$ mice

(A, B) Mandibular skeletal preparations. Wild-type mandible (A) shows normal development of Meckel's cartilage (blue) and mandibular bone (purple) Double headed arrow shows antero- (a) posterior (p) direction of mandibular outgrowth. Enlarged Meckel's cartilage in *Wnt1-Cre;Nog*$^{lacz/fx}$ mutant (B) shows no obvious outgrowth defects. Scale bar = 1 mm. (C, D) Meckel's cartilage in red dotted line. The size of wild-type (C) Meckel's cartilage is similar to mutant (D) at E11.5. Scale bars = 100 μm. (E, F) Cell proliferation in the Meckel's cartilage. Cell proliferation was increased in the mutant (F) Meckel's cartilage at E12.5, compared with cell proliferation in wild-type (E) Meckel's cartilage. Scale bars = 100 μm.

Previous studies indicate that Hh signaling regulates mandibular development. For example, lack of Hh signaling in NCCs resulted in a hypoplastic mandible (Jeong et al., 2004; Jeong et al., 2003; Melnick et al., 2005), whereas activating Hh signaling in NCCs increased the size of facial primordial (Jeong et al., 2004). Accordingly, one hypothesis for the increased mandibular size and underlying cell proliferation is upregulation of Hh signaling when BMP receptor activation is increased in NCCs due to a loss of *Nog* from these cells. To investigate if activating BMP signaling induces ectopic Hh signaling in the developing mandible, we assessed the state of Hh signaling upon elevation of BMP signaling in NCCs. To do this, we drove expression of an activated BMP receptor 1A (*caBMPr1a*) transgene (Rodriguez et al., 2010) specifically in NCCs, and included a *Ptch1-lacz* transgene, an established, obligate reporter of Hh signaling (Goodrich et al., 1997). At E13.5, Ptch1-lacz staining was apparent in the Meckel's cartilage of these *Wnt1-Cre; caBMPr1a;Ptch1*^{lacz} mutants, while no blue cells were found in the wild-type Meckel's cartilage (Fig. 2.8).

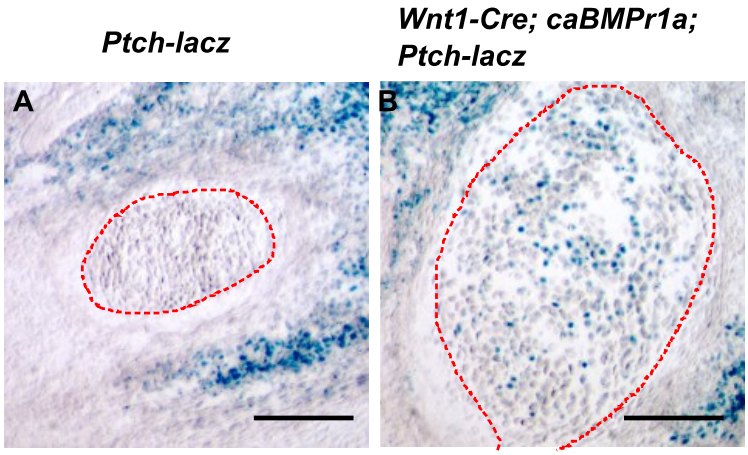

Figure 2.8: Hh signaling is upregulated in the Meckel's cartilage of mice with upregulated BMP signaling.

(A, B) Meckel's cartilage in red dotted line. Complementary experiment using constitutively active BMP receptor 1a (*caBMPr1a*) in combination with *Wnt1-Cre* showed overexpressing BMP signaling in NCCs caused ectopic expression of Hh signaling in mutant Meckel's cartilage, as revealed by Ptch-lacz (B). Wild-type (A) Meckel's cartilage showed no beta-galactosidase activity. Mutant (B) Meckel's cartilage showed beta-galactosidase activity (blue), indicating ectopic Hh signaling. Scale bar = 100 μm.

We also performed quantitative real time PCR (qPCR) to assess the level of Hh signaling and to determine if the increased Hh signaling activity might be reflected by increased expression of any Hh ligand. Our qPCR results showed increased expression of Hh transcriptional target genes (Fig. 2.9D). Moreover, we observed that *Indian hedgehog* (*Ihh*) expression is significantly increased in the mutant mandible. Together, these data suggest that in mandibular NCCs, increased BMP receptor activation leads to increased *Ihh* transcription, which then leads to increased Hh signaling, a known NCC mitogen. This in turn implies that the enlarged mandibular phenotype of embryos lacking *Nog* in NCCs may result from increased cell proliferation caused by elevated Hh signaling.

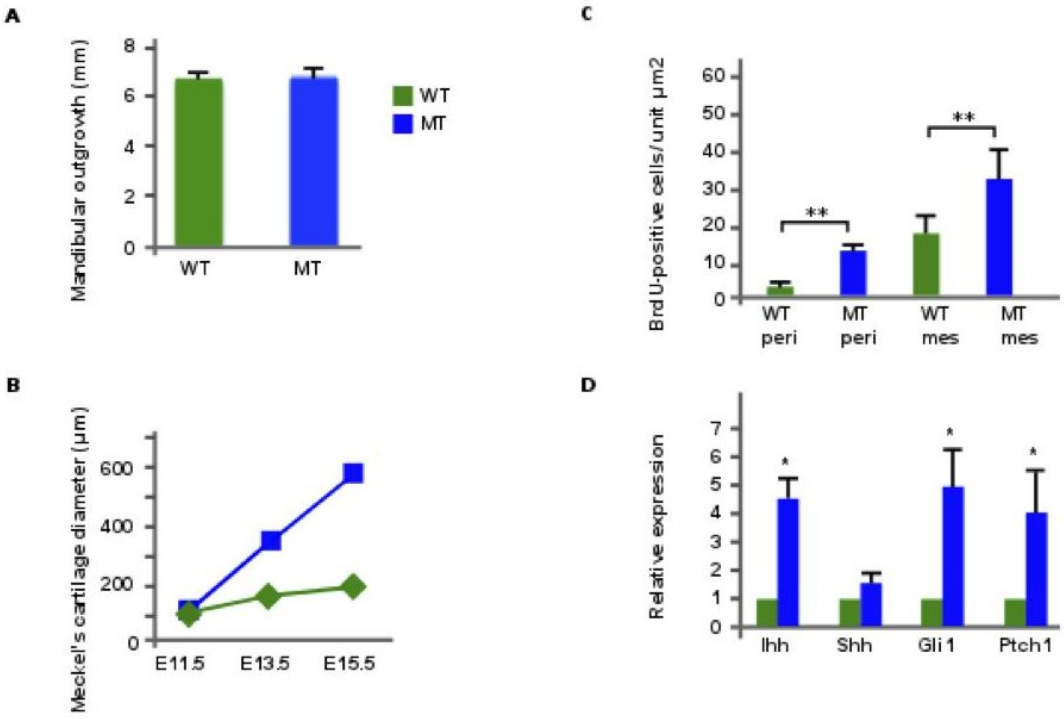
A
Mandibular outgrowth (mm)
8
6
4
2
0
WT
MT
WT
MT
B
Meckel's cartilage diameter (µm)
600
400
200
0
E11.5
E13.5
E15.5
C
BrdU-positive cells/unit µm2
60
50
40
30
20
10
0
**
**
WT peri
MT peri
WT mes
MT mes
D
Relative expression
7
6
5
4
3
2
1
0
*
*
*
Ihh
Shh
Gli1
Ptch1

Figure 2.9: Meckel's cartilage overgrowth and Hh signaling upregulation in mice lacking Nog from NCCs.

(A) Mandibular outgrowth in the anteroposterior direction as shown in (Fig. 3.7A) is not different between wild-type and mutant embryos. (B) The diameter of Meckel's cartilage showed similar size at E11.5 between wild-type and mutant. However, after E12.5 mutant Meckel's cartilage started rapidly growing and the growth persisted at E15.5, while growth rate in wild-type Meckel's cartilage was diminished. (C) Increased cell proliferation in both perichondrium (peri) and mesenchyme (mes) in Meckel's cartilage of *Wnt1-Cre;Nog*$^{lacz/fx}$ mutant was statistically significant at E12.5. (D) qPCR results indicate upregulated Hh signaling in the mutant Meckel's cartilage was due to upregulated *Ihh* expression. $P<0.05$.

2.3.6 Ablating *Nog* from NCCs results in secondary cleft palate

Beyond an enlarged mandible, loss of *Nog* expression in NCCs results in other craniofacial skeletal defects. While many defective skeletal elements are enlarged in mutants, (eg the nasal cartilage), hypoplasia occurs in a few membranous bones, such as the palatal bone (Fig. 2.17) and those of the cranial vault (data not shown). Although primary palatal development appeared unaffected in embryos lacking Nog specifically in neural crest derivatives, *Wnt1-Cre; Nog*$^{lacz/fx}$ embryos show overt secondary cleft palate (Fig. 2.10). Although the cause of cleft palate in Nog mutants was previously attributed to a lack of *Nog* expression in the oral epithelium (He et al., 2010), our results indicate that a key contributor to the cleft palate phenotype in Nog nulls is a lack of Nog in NCCs.

To investigate the etiology of the palatal defects in *Wnt1-Cre;Nog*$^{lacz/fx}$ mutant mice, we performed detailed morphological and histological analyses of palatal shelves at different stages of development. We first assessed the growth of the palatal shelves. At E13.5 palatal shelves of control and mutant embryos showed no clear differences in shape or size (Fig. 2.11A-F). We used BrdU incorporation assays to assess cell proliferation in the palatal shelf mesenchyme at this stage. We saw no significant difference between wild type and mutant embryos (Fig. 2.12). Thus both the gross size

and shape of the palatal shelves, as well as cell proliferation within the largely NCC-derived mesenchyme, show no difference.

We next tested whether patterning markers are correctly expressed in the mutant palatal shelves. During palatal development, specific genes are expressed along the anterior-posterior axis of the secondary palatal shelves. These markers are informative indicators to assess patterning defects in the mutant palatal shelves. *Shox2* is normally expressed in the anterior palatal shelves (Yu et al., 2005). *Shox2* null mice exhibit a rare form of cleft palate in which primary and secondary palatal shelves do not fuse properly (Yu et al., 2005). *Shox2* expression is greatly reduced in the anterior palatal shelves of *Nog* null embryos at E13.5 (He et al., 2010). However, *Shox2* expression was not altered in the palatal shelves of *Wnt1-Cre;Nog*$^{lacz/fx}$ embryos (Fig. 2.13A, E).

Besides being a patterning marker for the developing palate, *Tbx22* is also a context-dependent downstream target gene of BMP signaling (Higashihori et al., 2010). Explant culture experiments using facial primordia and palatal shelves suggest that *Tbx22* expression is regulated by BMP signaling (Fuchs et al., 2010). Its expression in the palatal shelves is found posteriorly. Loss of *Tbx22* results in submucous cleft palate in mice and human (Braybrook et al., 2001). *Tbx22* null mice show reduced palatal bone due to delay in the osteoblast maturation (Pauws et al., 2009). However, our results showed that *Tbx22* expression is not altered in the *Wnt1-Cre;Nog*$^{lacz/fx}$ mutant palatal

shelves at E13.5. qPCR analysis also indicates that expression level of *Tbx22* is unchanged in the mutant palatal shelves (Fig. 2.14), although the size of the palatal bone is greatly reduced (Fig. 2.13B, F, 2.17C, D). This is consistent with normal proliferation seen in the mutant palatal shelves (Fig. 2.12). These results, as well as the lack of evidence for change in cell proliferation in the mutant palatal shelves suggest that altered *Tbx22* expression in the *Wnt1-Cre;Nog*$^{lacz/fx}$ palatal shelves is not the main cause of the smaller palatal bone and cleft palate in this mutant. Expression of two other palatal shelf markers, *Barx1* and *Efnb2*, are also similarly expressed between wild-type and mutant embryos (Fig. 2.13C, D, G, and H).

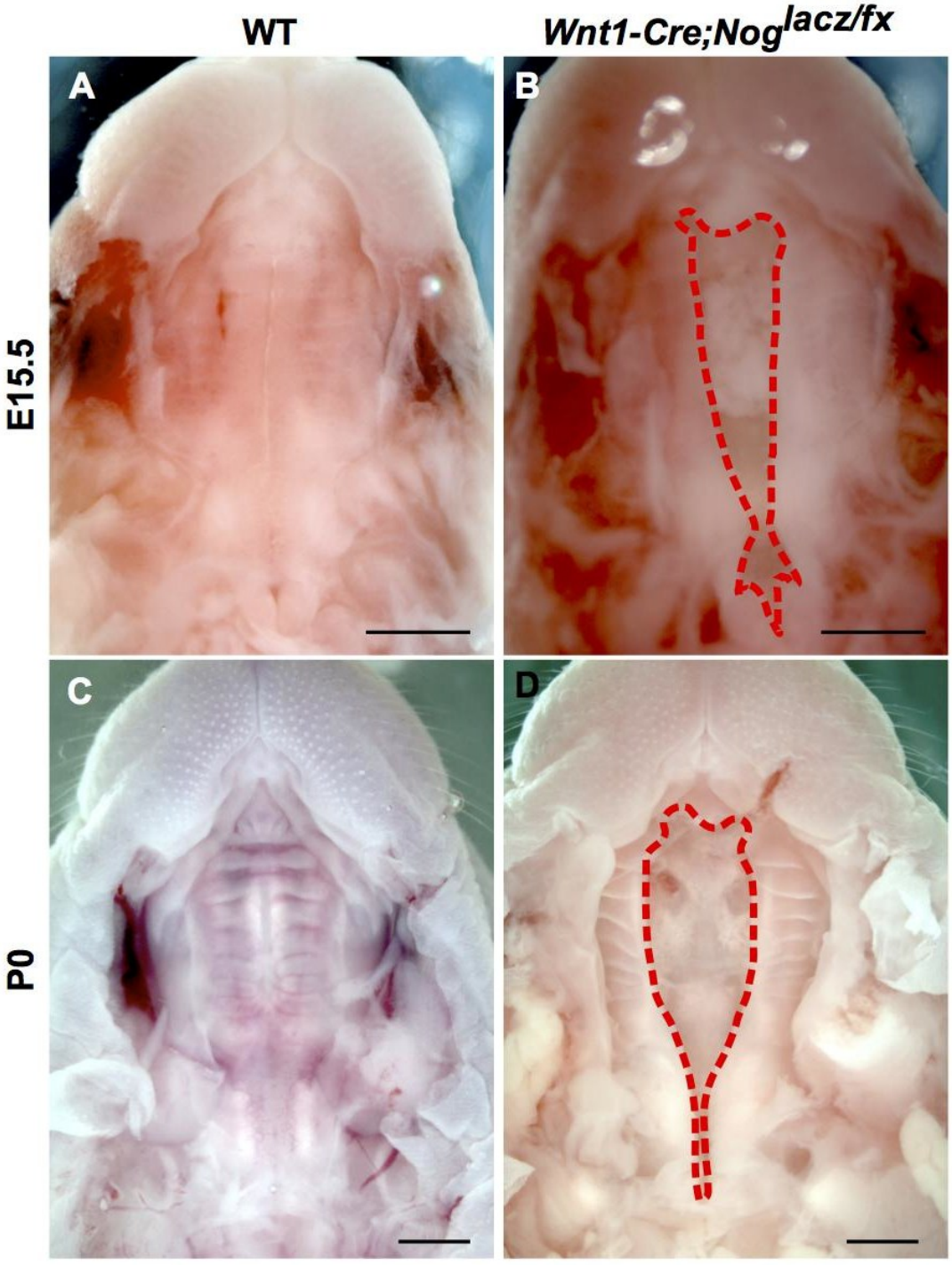
WT
Wnt1-Cre;Nog lacz/fx
A
B
C
D
E15.5
P0

Figure 2.10: *Nog* in NCCs is required for proper palatogenesis.

(A, B) A wild-type E15.5 mouse showing normal palatal development in which the palatal shelves fuse by this stage (A) compared with the secondary cleft palate in *Wnt1-Cre;Nog*$^{lacz/fx}$ (B). (C, D) A wild-type P0 mouse showing normal palatal development (C), overt cleft palate in *Wnt1-Cre;Nog*$^{lacz/fx}$ at P0 is obvious by this stage (D). Scale bars = 1 mm.

2.3.7 Nog in NCCs is not required for palatal fusion

One of the common causes of cleft palate is a defect in palatal fusion. For the bilateral palatal shelves to properly fuse, both sides need to come in close proximity for fusion, aided by secretion of extracellular matrix that helps bind the two sides (d'Amaro et al., 2012; Gato et al., 2002; Morris-Wiman and Brinkley, 1992). Upon contact of the opposing palatal shelves, dynamic tissue remodeling including apoptosis and changes in gene expression occur at the medial edge epithelium (MEE) (Huang et al., 2011; Nawshad et al., 2007; Xu et al., 2006). To test if Nog in NCCs is important for palatal fusion, we performed palatal shelf explant cultures. Palatal shelves were harvested from E13.5 embryos, and placed in contact with each other in culture medium such that their medial surfaces were juxtaposed. After 72 hours, both wild-type and mutant palatal shelves fused normally (Fig. 2.13I, J). These data indicate Nog in NCCs is not necessary for palatal fusion, in turn suggesting that failure of palatal shelf fusion is not the cause of the secondary cleft palate phenotype that occurs when Nog is absent from NCCs.

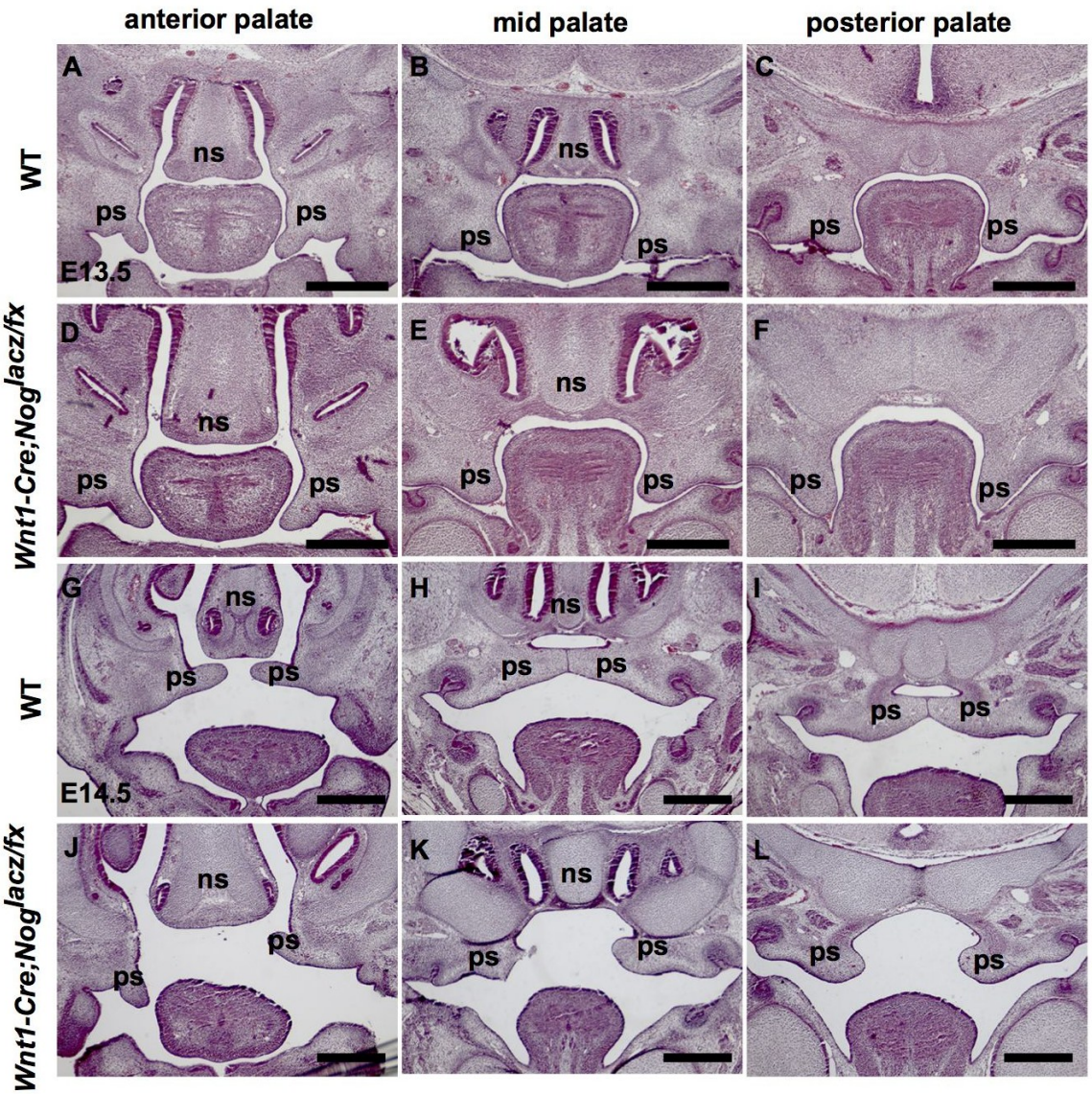
anterior palate
mid palate
posterior palate
WT
Wnt1-Cre;Nog lacz/fx
WT
Wnt1-Cre;Nog lacz/fx
A
B
C
D
E
F
G
H
I
J
K
L
ns
ps
E13.5
E14.5

Figure 2.11: Palatal shelf development in *Wnt1-Cre;Nog*$^{lacz/fx}$ is normal before elevation.

(A-F) Anterior to posterior level matched coronal sections of E13.5 control (A-C) and mutant (D-F) littermates. (G- L) Anterior to posterior level matched coronal sections of E14.5 control (G-I) and mutant (J-L) littermates. Sections shown in the left column (A, D) are anterior secondary palate. Sections shown in the left column (G, J) are from the elevated secondary palate region. Mutant palatal shelves (J) often show incomplete elevation of palatal shelves. Sections shown in the middle column (B, E, H, K) are from the middle of the secondary palate region. Sections shown in the right column (C, F, I, L) are from the posterior soft palate region. Scale bars = 400 μm.

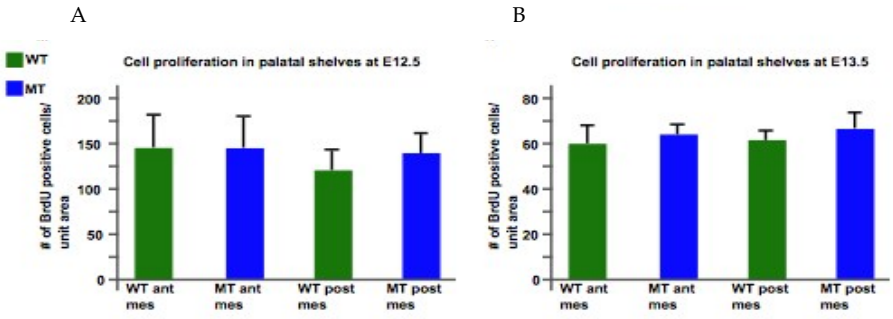

Figure 2.12: Cell proliferation in palatal shelves is not different from wild-type and mutant embryos.

(A, B) numbers of BrdU-positive cells per unit area in the palatal shelves of E12.5 (A) and E13.5 (B) were counted and compared between wild-type and *Wnt1-Cre;Nog*$^{lacz/fx}$ mutant littermates. They showed no statistically significant difference in cell proliferation. ns, nasal septum; ps, palatal shelf.

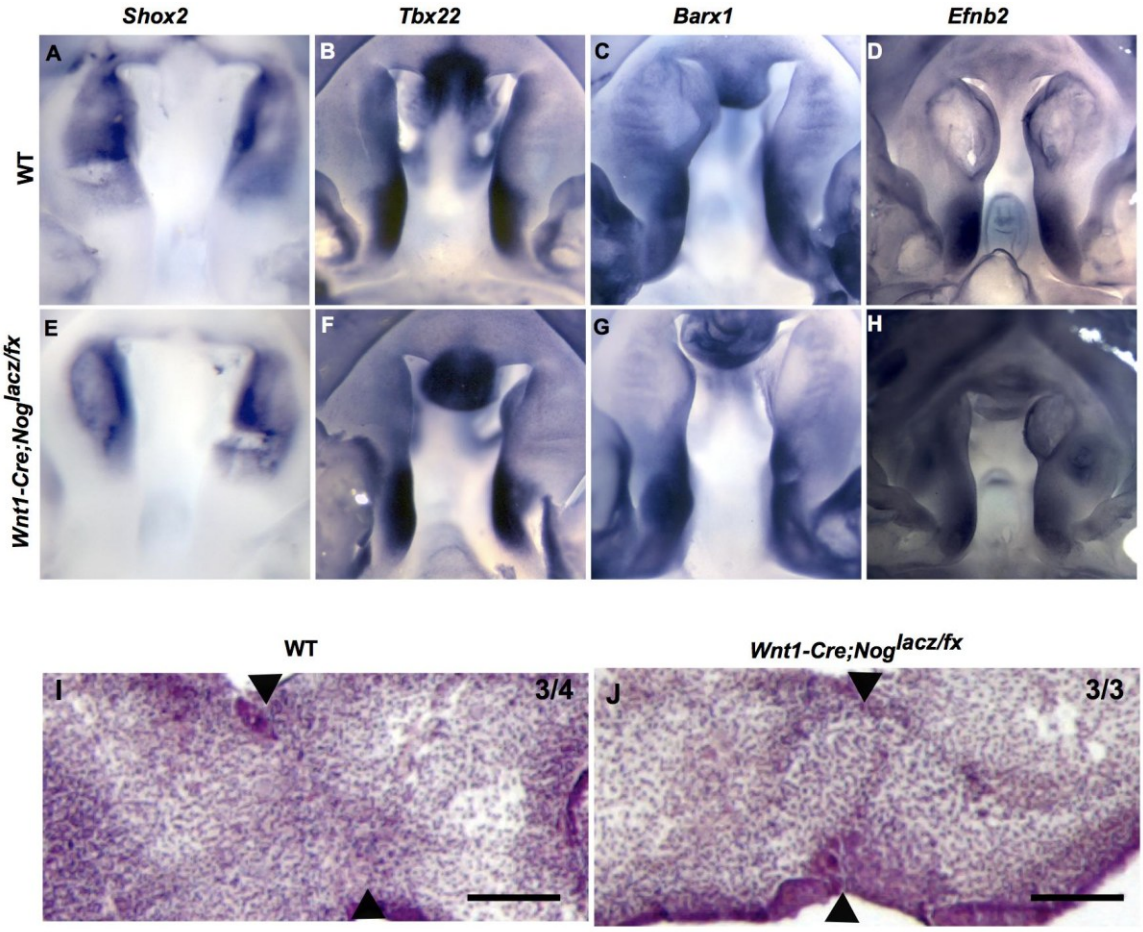
Shox2
Tbx22
Barx1
Efnb2
A
B
C
D
WT
E
F
G
H
Wnt1-Cre;Nog lacz/fx
WT
Wnt1-Cre;Nog lacz/fx
I
3/4
J
3/3

Figure 2.13: Growth and fusion steps of palatal development are not disrupted in *Wnt1-Cre;Nog*$^{lacz/fx}$ mutant mice.

(A-E) Anterior and posterior local characteristics in the secondary palatal shelves are not altered in the *Wnt1-Cre;Nog*$^{lacz;fx}$ mutant mice. (A, E) *Shox2* mRNA expression was restricted to the anterior palatal shelves in E13.5 wild-type (A) and mutant (E) littermates. (B-D, F-H) Expression of *Tbx22* (B, F), *Barx1* (C, G), and *Efnb2* (D, H) mRNA was restricted to the posterior region of the E13.5 palatal shelves in both wild-type (B-D) and mutant (F-H) embryos. (I, J) Arrowheads indicate the point where palatal shelf fusion has taken place. Palatal shelves in mutant (J) fuse normally as wild-type (I). Scale bars = 100 μm.

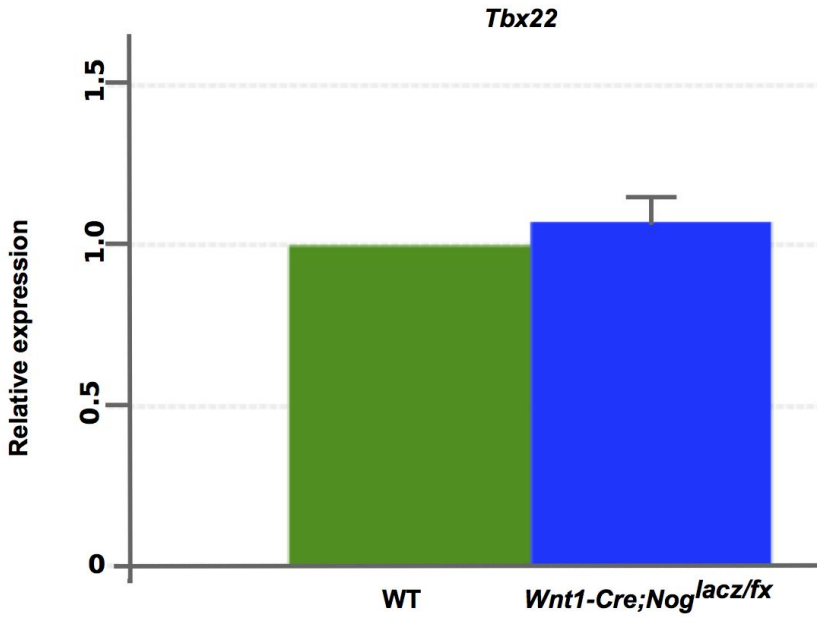

Figure 2.14: Expression of Tbx22 shows no difference between wild-type and mutant palatal shelves.

Quantitative real time PCR shows a similar level of *Tbx22* expression in the palatal shelves of wild-type and *Wnt1-Cre;Nog*$^{lacz/fx}$.

2.3.8 Failed palatal shelf elevation likely results from dismorphic skull base skeletal structure

As noted above, the size of palatal shelves in mutant embryos prior to palatal shelf elevation showed no overt differences relative to wild-type palatal shelves at E13.5. However, we noticed that by E14.5 anterior palatal shelves in mutants were elevated horizontally above the tongue, yet were not close to each other; by contrast, control palatal shelves were fusing at this stage (Fig. 2.11G-L). We observed that the angle of the mutant palatal shelves gets wider progressively from anterior to posterior (Fig. 2.15E, F). Surprisingly, we found ectopic skeletal element invasion into the further posterior palatal shelves of mutant embryos at E13.5 at which palatal shelf elevation has not started (Fig. 2.15A, B). By E14.5 the skeletal element occupied majority of the posterior palatal shelves (Fig. 2.15C, D). Analysis of stained skeletal preparations revealed that the overgrown skeletal element in the posterior palatal shelves was the pterygoid bone (Fig. 2.17). The pterygoid bone is derived from NCCs (McBratney-Owen et al., 2008). Further, the antero-posterior (AP) and medial-lateral (ML) lengths of skull base structure were compared, and we found that the AP length of mutant skull base was significantly shorter while the ML width of mutant skull base was longer than those of wild-type embryos (Fig. 2.17 & 2.18). We also found that the presphenoid and the basisphenoid in mutant embryos prematurely fused (Fig. 2.17). These results suggest that the shorter skull base caused by prematurely fused presphenoid and basisphenoid displaces an

enlarged pterygoid bone anteriorly, which in turn allows the enlarged pterygoid bone to invade into the posterior palatal shelves, preventing proper elevation of the palatal shelves in the mutant lacking Nog in NCCs. Similar phenotypes were observed in Nog null embryos (Fig. 2.21).

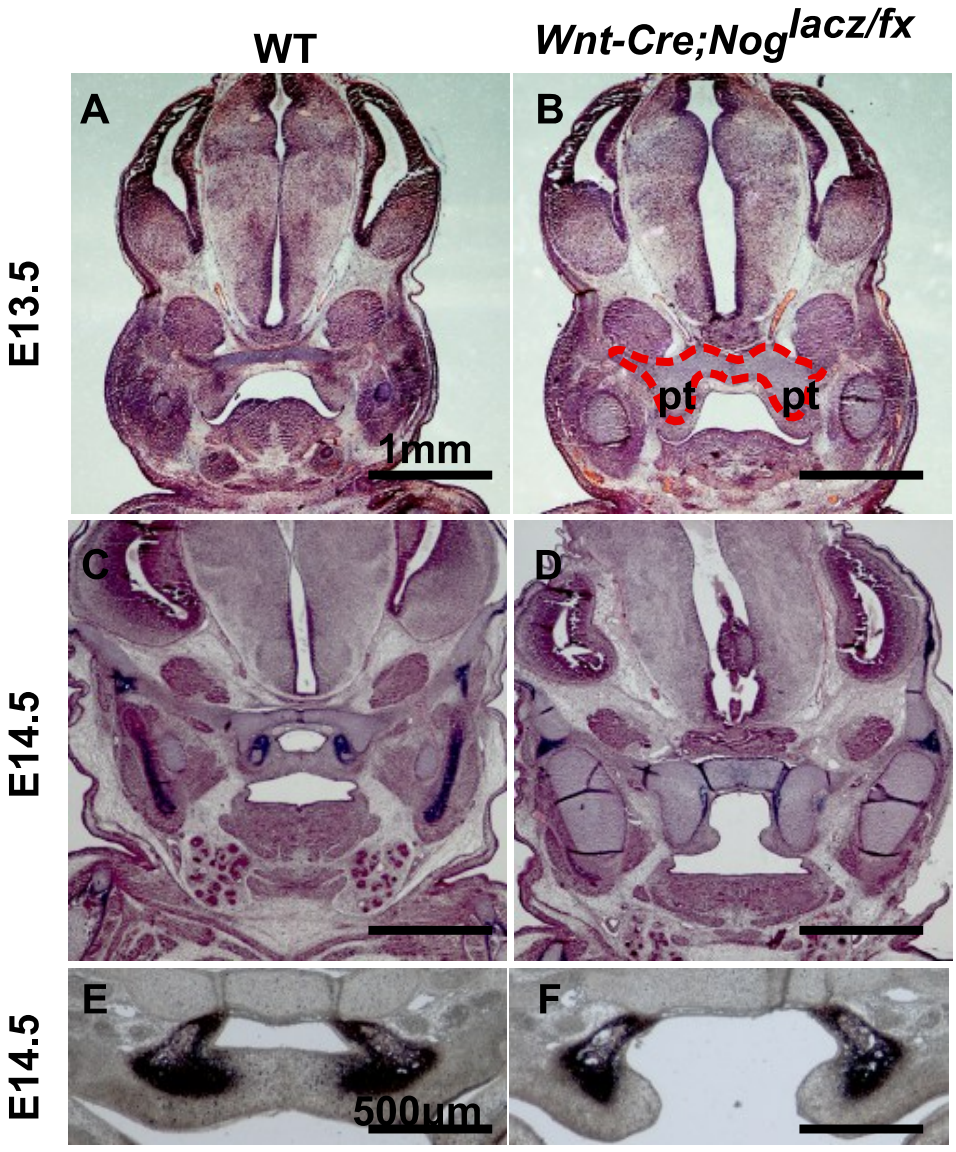
WT
Wnt-Cre;Nog lacz/fx
E13.5
E14.5
E14.5
A
B
C
D
E
F
1mm
pt
pt
500um

Figure 2.15: Pterygoid bone invades the posterior palatal shelves in the *Wnt1-Cre;Nog$^{lacz/fx}$* mutant palate.

(A, B) Before palatal shelf elevation at E13.5, pterygoid is not obvious in wild-type embryo (A), but it is already much larger in the *Wnt1-Cre;Nog$^{lacz/fx}$* mutant and it invades into the posterior part of palatal shelves (B). (C, D) Pterygoid bone appears in wild-type at E14.5 (C), while it is further growing in mutant palatal shelves (D). (E, F) Coronal sections of palatal bone region. Completely elevated and fused wild-type palatal shelves (E) and palatal shelves were elevated but the angle of elevation was wider in the *Wnt1-Cre;Nog$^{lacz/fx}$* mutant littermate (F). Scale bars = 100 μm for A, B, C, D, 500 μm for E, F.

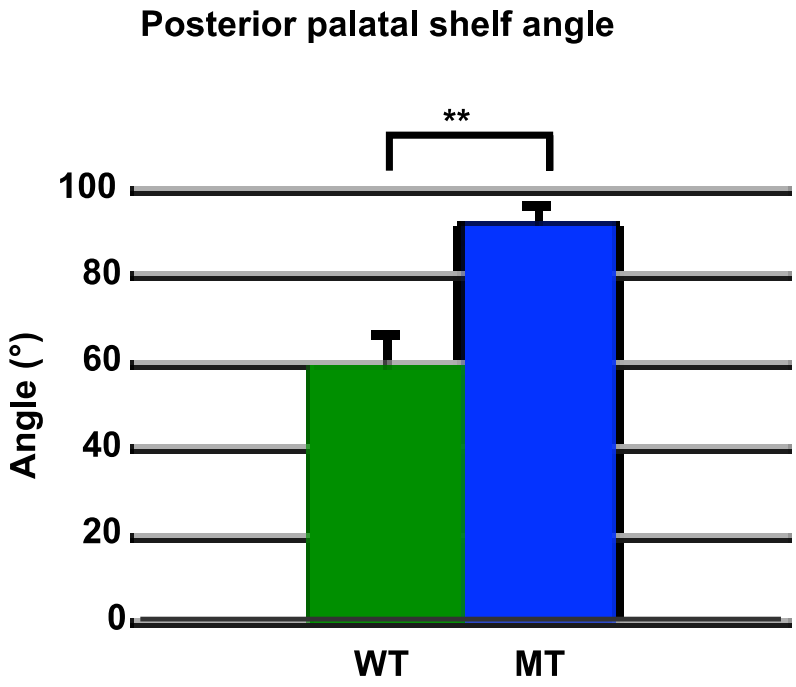

Figure 2.16: Posterior palatal shelf angle is wider in Wnt1-Cre;Noglacz/fx.

The angle of palatal elevation was recorded and compared between wild-type and mutant littermates.

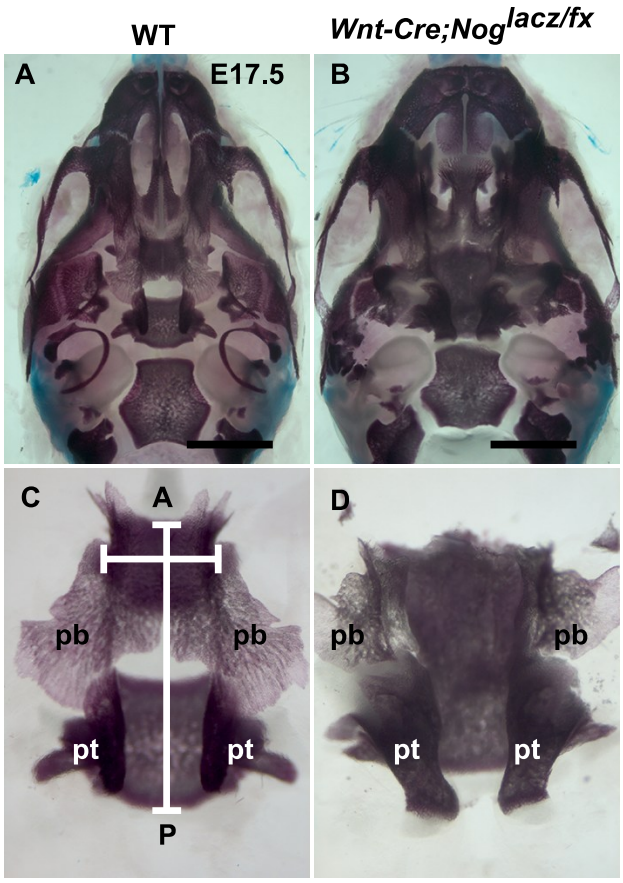
WT
Wnt-Cre;Nog lacz/fx
A
E17.5
B
C
A
pb
pb
pt
pt
P
D
pb
pb
pt
pt

Figure 2.17: Skull base bones in mutant are dysmorphic.

(A, B) skeletal preparation showing posterior view of the skull base and palate. Compared with the width of wild-type skull (A), the width of mutant skull is wider (B). (C, D) Isolated skull base and the palatal bone region from the skeletal preps. The bilateral palatal bones are in contact in wild-type embryo at E17.5 (C). The palatal bones are smaller and far apart. Pterygoid bone is enlarged and dysmorphic in the skeletal prep of mutant littermate at E17.5 (D). pb, palatal bone; pt, pterygoid; prs, presphenoid; bs, basisphenoid; a, anterior; p, posterior; ml, medial-lateral.

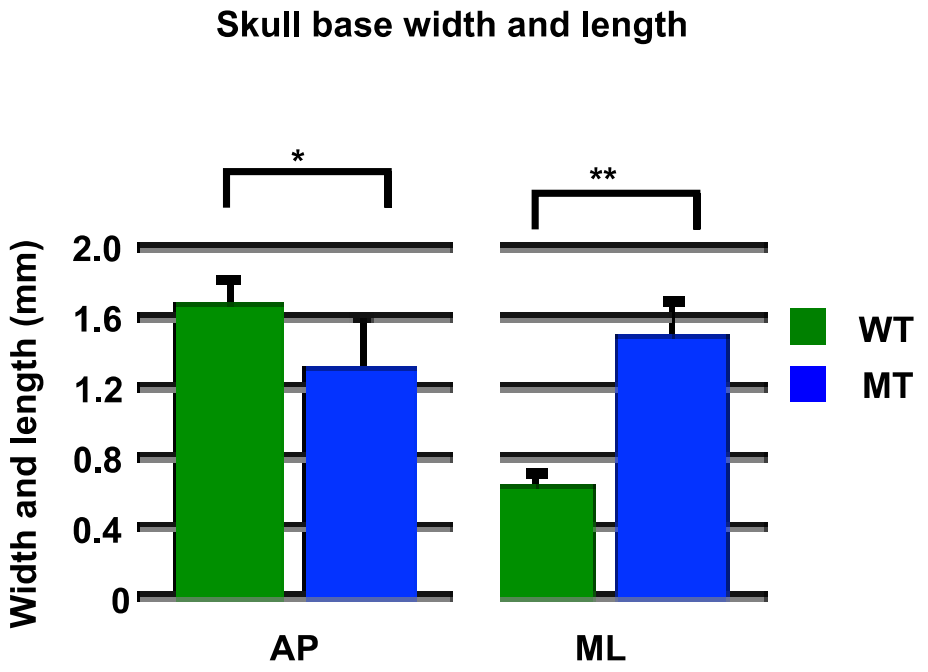

Figure 2.18: The sizes of skull base width and length are statistically different between wild-type and mutant embryos.

The length and width of the skull base were recorded and compared between wild-type and mutant skeletal preparations at E17.5. pb, palatal bone; pt, pterygoid. *P-value < 0.05, **P-value < 0.01.

2.4 Discussion

In this study, we used tissue specific gene knockout mouse models to probe the roles of two distinct domains of *Nog* in regulating craniofacial development. We found that the axial midline domain of BMP antagonism is critical for outgrowth of the mandibular bud of PA1, which swells with the immigration of NCC cells. Our data suggest an indirect effect of axial *Nog* in promoting the survival of these NCCs. Later, in NCCs and their derivatives, *Nog* activity regulates development of mandibular and maxillary craniofacial skeletal elements that are derived from NCCs. By upregulating BMP signaling in NCCs, we found that Meckel's cartilage became strikingly enlarged as a result of greatly increased cell proliferation; this was accompanied by increased Hh signaling, a possible mitogenic cue for some NCC derivatives. We also found that mutants lacking *Nog* in NCC derivatives show secondary cleft palate, likely due to defects in bones of the skull base, particularly an enlarged pterygoid. Together, these results reveal distinct roles of *Nog* in axial domains for early PA1 development and in the NCC lineage for regulating later development of craniofacial skeletal elements.

2.4.1 BMP antagonism by *Nog* and *Chrd* from the axial midline promotes mandibular outgrowth

Our previous studies with $Chrd^{-/-};Nog^{-/-}$ and $Chrd^{-/-};Nog^{+/-}$ embryos revealed a requirement for these BMP antagonists in proper generation of the NCCs that populate PA1 (Anderson et al., 2006; Stottmann et al., 2001). Lowering the genetic dosage of *Nog*

in the absence of *Chrd* caused a somewhat increased emigration of NCCs from the dorsal neural folds, but instead of expanded mandibular buds, they were deficient; this was because a high level of NCC apoptosis in the pharyngeal region (Anderson et al., 2006). One possibility was that lack of expression of these BMP antagonists in NCCs causes their death and the resulting mandibular hypoplasia. This is not the case, because we saw no outgrowth defect when we ablated *Nog* specifically in NCCs, regardless of whether *Chrd* was present or not. Instead, we found that in the absence of *Chrd*, ablating *Nog* from the axial midline (notochord and floor plate) results in mandibular hypoplasia very similar to that observed in *Chrd;Nog* mutants. If *Chrd* were present, loss of *Nog* from the axial midline had no such effect. The axial midline domain of *Nog* is therefore the relevant source of expression.

Our results imply that decreased BMP antagonism at the axial midline leads to a failure to attenuate BMP signaling in the pharyngeal environment as NCCs migrate through to populate the mandibular arch. One possibility is that increased BMP signaling in NCCs causes their apoptosis. If this were true, then expression of an activated BMP receptor in NCCs should cause their apoptosis. When we did this experiment, by expressing an activated BMP receptor (Rodriguez et al., 2010) in migratory NCCs, we saw the opposite phenotype - an enlarged mandible. Therefore, it is more likely that increased BMP activity caused by loss of axial BMP antagonism is

leading to lower levels of an NCC survival cue. *Fgf8* has been shown to promote NCC survival during mandibular outgrowth. We previously found that pharyngeal *Fgf8* expression is reduced in *Chrd;Nog* mutants, and that beads soaked in BMP caused decreased expression of *Fgf8* in mandibular arch explants, whereas beads soaked in carrier had no effect (Stottmann et al., 2001). Together with these earlier results, our data further support a mechanism in which reduced axial BMP antagonism leads to increased pharyngeal BMP activity, which in turn reduces expression of *Fgf8* in the pharyngeal ectoderm and endoderm. This in turn results in less NCC survival as these cells colonize and populate the mandibular bud (Fig. 2.19 & 20).

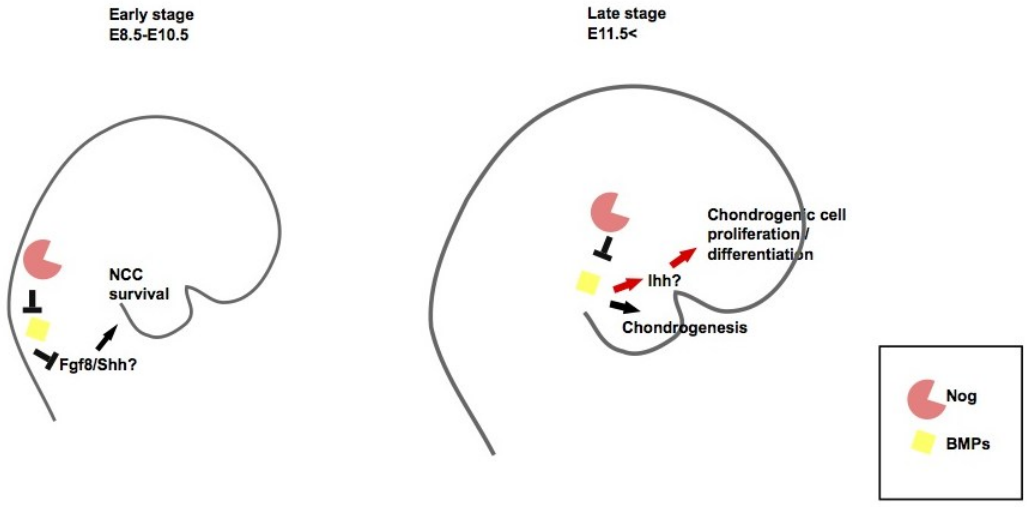

Figure 2.19: Model of the roles of *Nog* in development of craniofacial development.

Earlier expression of *Nog* in axial domains promotes NCC survival by inducing secondary signaling such as Fgf8 and Hh signaling. However, in later stages, *Nog* regulates skeletogenesis by balancing level of BMP signaling. In chondrocytes, *Nog* regulates size of cartilage by suppressing cell proliferation. When BMP attenuation is not enough, chondrocyte proliferation/ differentiation is promoted possibly through ectopic *Ihh* expression.

2.4.2 *Nog* expression in NCCs regulates Meckel's cartilage and mandibular development

As noted above, loss of *Nog* expression from the NCCs, via tissue-specific gene ablation with *Wnt1-Cre*, resulted in an enlarged mandible. The enlarged mandibular phenotype is very similar to that seen in *Nog* nulls (Fig. 2.21) (Stottmann et al., 2001; Wang et al., 2013), and was not noticeably different from *Wnt1-Cre;Nog*$^{lacz/fx}$;*Chrd*$^{-/-}$. Thus in mandibular development per se, as opposed to mandibular bud outgrowth, there appears to be no redundancy of *Nog* with *Chrd*. Our results are consistent with a recent study which reported that BMP4 overexpression in NCCs at E10.5 also resulted in micrognathia (Bonilla-Claudio et al., 2012). Earlier in development, embryos lacking *Nog* in NCCs (*Wnt1-Cre;Nog*$^{lacz/fx}$ mice) showed normal size pharyngeal arches, and several arch markers that are also BMP downstream target genes showed normal expression patterns at E10.5 (Fig. 2.6). These results further suggest that *Nog* activity in NCCs is not necessary for early stages of mandibular development, but rather is necessary for proper skeletogenesis within the developing mandibular prominence.

We found that the enlarged mandible phenotype occurred not only when *Nog* was ablated from NCCs via *Wnt1Cre*, but also when the same recombination driver was used to express an activated BMP receptor in NCCs. This result suggests that the NCCs themselves, and their derivatives, need attenuation of BMP signal transduction to undergo proper development in the mandibular bud. These derivatives are likely to be

chondrocytes, as expression of an activated BMP receptor construct in these cells results in a similarly enlarged mandible as a result of expanded Meckel's cartilage (Wang et al., 2013).

Our studies with *Wnt1-Cre;Nog*$^{lacz/fx}$ mutants indicated greatly increased cell proliferation in the perichondrial area of Meckel's cartilage relative to normal controls. A similar increase in cell proliferation was noted in embryos expressing an activated BMP receptor in chondrocytes (Wang et al., 2013). Consistent with studies suggesting the ability of BMP signaling upregulation in NCCs to cause increased cell proliferation in Meckel's cartilage (Hu et al., 2008; Wang et al., 2013), the increased size of the mandible may be a direct effect of an increased level of chondrocyte proliferation triggered by less attenuation of BMP signaling by *Nog*. An alternative explanation is that the increased proliferation results form some other cue. We found that a known positive cytokine regulator of chondrocytic cell proliferation, Indian hedgehog (*Ihh*) (Minina et al., 2001), was expressed at increased levels when BMP signaling was upregulated in the NCC lineage. Accordingly, a second possibility is that in the context of the developing Meckel's cartilage, BMP signaling in NCCs positively regulates *Ihh* activity, which in turn promotes chondrocyte proliferation. At least in endochondral ossification, BMP signaling is reported to positively regulate *Ihh* expression which, in turn, promotes cell proliferation (Minina et al., 2002). This may be true in Meckel's cartilage as well. A

caveat to this model is that in the absence of *Ihh*, in mutants lacking the gene, the size of the mandible is not greatly diminished (St-Jacques et al., 1999). We would thus posit that *Ihh* can promote chondrocyte proliferation in Meckel's cartilage, but is not essential for it. In any case, we suggest that a key function of *Nog* in chondrocytes derived from NCC cells is to limit proliferation by attenuating BMP activity (Fig. 2.20).

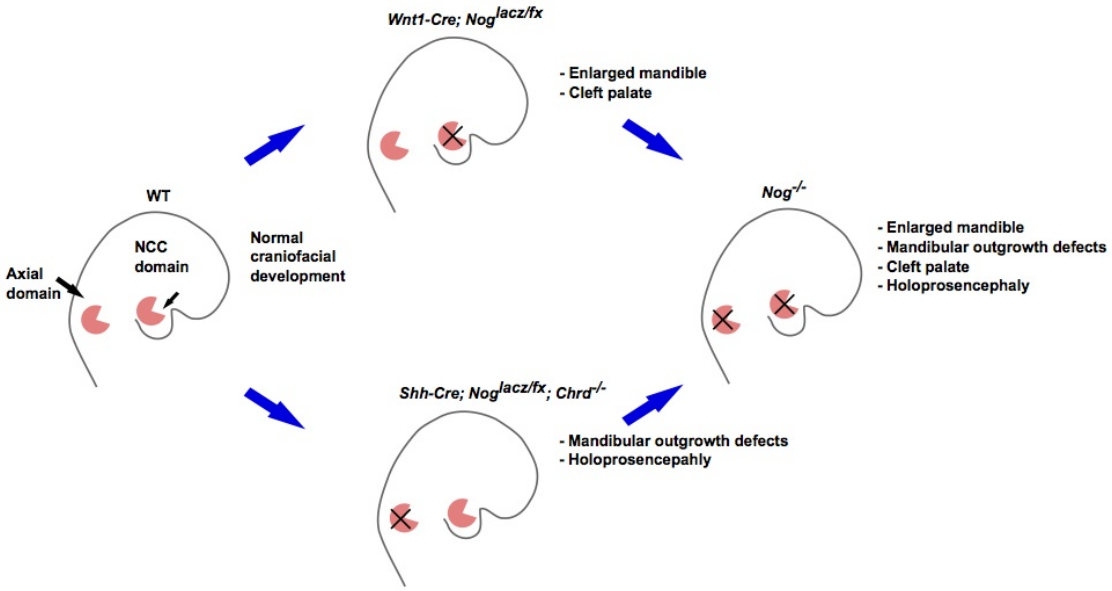

Figure 2.20: Summary of the roles of Nog in development of craniofacial development.

Nog is expressed in two relevant domains for craniofacial development – NCCs and axial domains. When *Nog* is ablated in NCCs, an enlarged mandible and cleft palate result without mandibular outgrowth defects. When axial domain of BMP antagonism is absent, mandibular outgrowth defects and holoprosencephaly occur. *Nog* null mutant embryos exhibit phenotypes of two mutants combined, which are an enlarged mandible, cleft palate, mandibular outgrowth defects, and holoprosencephaly.

2.4.3 Noggin activity and the regulation of palatal development

In addition to an enlarged mandible, *Wnt1-cre;Nog*$^{lacz/fx}$ embryos exhibited almost fully penetrant secondary cleft palate. A previous study characterized the cleft palate of the *Nog* null (He et al., 2010), which also includes primary cleft palate. *Nog* is expressed in the oral epithelium, which showed increased cell death in *Nog* null mutants. He et al (2010) expressed activated BMP receptor in the epithelium, and found that the resulting embryos had cleft palate. These findings suggested that the cleft palate of *Nog* mice results from increased BMP signaling in the oral epithelium. By contrast, we have found that ablation of *Nog* exclusively in the NCC lineage, which contributes to the mesenchyme but not the epithelium of the forming palate, also causes severe secondary cleft palate. Together, these studies suggest that *Nog* plays multiple tissue-specific roles in palatal development (Fig. 2.19).

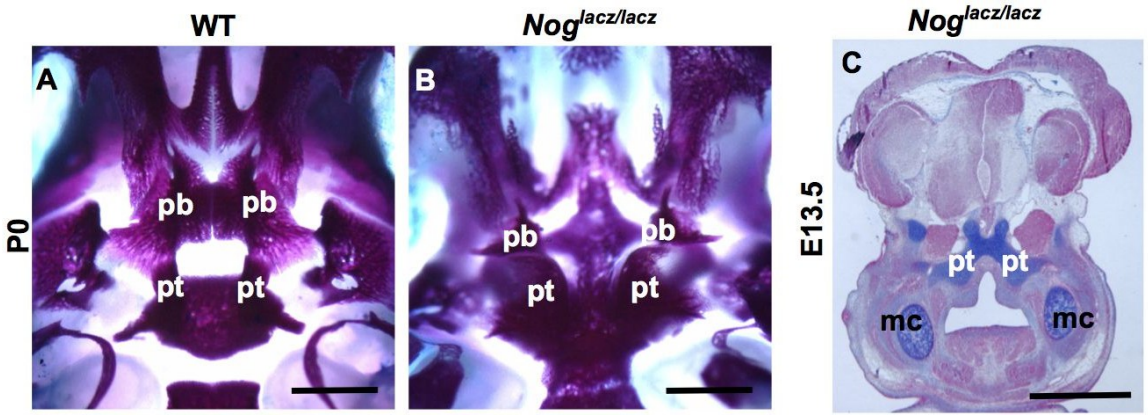

Figure 2.21: Nog null embryos exhibit an enlarged pterygoid.

(A, B) Skeletal prep showing skull base skeletal element at P0. Wild-type embryos show normal development of palate and pterygoid bone (A), while small palatal bone and an enlarged pterygoid bone in *Nog* null embryos (B). (C) Pterygoid bone invades in the posterior palatal shelves in *Nog* null at E13.5. Scale bars = 1 mm.

In embryos lacking Noggin activity in NCC derivatives, the mutant palatal bones were hypomorphic, which in principle could directly cause submucous cleft palate. However, the primary cause of overt cleft palate in *Wnt1-cre;Nog*$^{lacz/fx}$ embryos is most likely due to a defect in posterior palatal elevation. The palatal shelf elevation was likely inhibited by the presence of an enlarged pterygoid bone that is located posterior to the palatal shelves. Pterygoid cartilage is derived from NCCs and develops through endochondral ossification (McBratney-Owen et al., 2008). We found that in culture the mutant palatal shelves could fuse seemingly as well as in wildtype, but in the context of the rest of the mutant viscerocranium they likely never get close enough. These data suggest that a dysmorphic skull base component can greatly influence palatogenesis.

We further observed that in mutants lacking Nog in NCC derivatives, the mutant mouse skull base was shorter and wider than in wild type embryos. Studies concerning human patients show great correlations between morphological anomalies in the skull base and the incidence of cleft palate. For example, in 3-month-old children with complete cleft, there was an increased width of the cranial base, and an increased width of the spheno-occipital synchondrosis - the cartilaginous junction between the basisphenoid and basioccipital bones - in newborns, compared with patients with incomplete cleft (Molsted et al., 1993; Molsted et al., 1995). Although a correlation between complete clefts and skull base anomalies was found, it is difficult to establish

etiology from these results. However, our mouse model suggests a novel mechanism of cleft palate. The skeletal elements of the skull base are structurally complex and intricately interconnected. We suggest that an abnormally formed bone outside those directly involved in palatal development can influence overall structural development of the skull base and indirectly cause cleft palate. It is likely that morphological anomalies in the skull base that affect palatal development are overlooked as part of the etiology of cleft palate.

2.5 Acknowledgements

The *caBMPr1a* mouse and the *Nog*^{fx} strains were generously provided by Dr. Fan Wang and Dr. Richard Harland, respectively. We thank our lab colleagues for helpful discussion and comments, and special thanks to our lab technician, Kathy Carmody. This work was supported by grants from the NIH to J.K.

3. Roles of *Noggin* in Neural Tube Closure

The following chapter is now being prepared in preparation for submission. Adhesion assay in this study was the collaborative effort of Rebecca Thomason, Manuel Lopez (McClay lab) and Andy Ravanelli (Klingensmith lab).

3.1 Introduction

Neural tube defects (NTDs) are common human birth defects, occurring 6% of all births worldwide (Wallingford et al., 2013). NTDs result from one or more failures during neurulation. Causes of NTDs include genetic and environmental factors including maternal alcohol consumption and smoking (Grewal et al., 2008). Among human NTDs, spina bifida (unfused spine) and exencephaly (open brain) are the most prevalent defects. Numerous mouse models of NTDs have been identified so far. However, genetic, cellular and molecular mechanisms of proper neural tube development and the causes of NTDs are still poorly understood.

The neural tube that consists of pseudostratified neuroepithelium is the precursor to the central nervous system. Proper neural tube closure is a prerequisite for the following organogenesis. Previously, we showed that *Nog* null mice exhibit fully penetrant spina bifida and to a much lesser extent exencephaly (Stottmann et al., 2006). When Nog or Chrd is absent, expression of several BMP transcriptional target genes is

upregulated in the dorsal neural folds (Anderson et al., 2006). Furthermore, the incidence of exencephaly in *Nog* null embryos greatly depends on genetic background. For example, $Nog^{-/-}$ in a 129/Sv background exhibits 100% exencephaly while $Nog^{-/-}$ in a mixed background of 129:C57BL show 65% penetrance of exencephaly (Stottmann et al., 2006).

In our model of neural tube closure, there are mechanistic differences between caudal (spinal) neural tube closure where spina bifida occurs and cranial neural tube closure where exencephaly occurs. In the cranial neural tube closure, dorsolateral hinge points (DLHPs), as well as median hinge point (MHP) formation, are necessary for both edges of elevated lateral neural plate meet to fuse to each other. For instance, in *Nog* null mutants, exencephaly results due to the defective of DLHP formation (Stottmann et al., 2006). Studies show that when a Shh-soaked bead was placed near a neural fold, DLHP formation was inhibited (Ybot-Gonzalez et al., 2002). In addition, Hh signaling is ectopically expressed in the roof plate of neural tube of exencephalic *Nog* null mutant embryos without inducing Shh ligand expression while no Hh signaling upregulation was observed in the non-exencephalic *Nog* null embryos (Stottmann et al., 2006). It has also been shown that *Shh* acts as a negative regulator of *Nog* during neurulation. *Nog* expression in the neural fold was abolished when Shh soaked beads were implanted. Further, dorsal *Nog* expression was extended ventrally in *Shh* null embryos (Ybot-

Gonzalez et al., 2007). These data suggest that *Nog* and Hh signaling interact and the precise regulation of these genes is essential for proper formation of DLHP and by extension neural tube formation. However, whether just activating Hh signaling in the roof plate of the neural tube is sufficient to cause exencephaly in $Nog^{-/-}$ mutant mice remains as yet unexamined.

In contrast, our model of caudal neural tube closure suggests that proper paraxial mesoderm formation is essential to maintain closing caudal neural tube. In addition to this model, there is another potential mechanism for spinal NTD in *Nog* null mice. Spina bifida in *Nog* null mice occurs at full penetrance regardless the background. Surprisingly, when embryos were dissected between E8 and E9, mutant neural tube at the spinal region was closed. However, after E11, the neural folds spread apart, resulting in spina bifida (Stottmann et al., 2006). These results suggest that neural folds normally elevate and come into contact, but the closing neural folds do not remain closed in *Nog* null embryos. Our hypothesis here is that *Nog* mutant embryos are not capable of maintaining the closing neural tube due to insufficient adhesion between neural folds. This hypothesis is consistent with several recent findings that BMP signaling regulates expression of cadherins (Eom et al., 2013; Eom et al., 2011, 2012; Shoval et al., 2007). Interestingly, Grainy head-like (*Grhl*) family of developmental transcription factors, *Grhl2* regulates expression of the adherens junction gene E-cadherin and the tight

junction gene claudin 4 (*Cldn4*) in different types of epithelia (Werth et al., 2010). *Grhl2* and *Grhl3* have region specific and cooperative roles in neural tube closure; *Grhl2* mutant mice show exencephaly, *Grhl3* mutants result in spina bifida, and *Grhl2*$^{+/-}$;*Grhl3*$^{-/-}$ compound mutant embryos exhibit more severe phenotypes than either mutant alone (Rifat et al., 2010). One study indicates that BMP-signaling dependent *Grhl1* expression is required for epidermal differentiation in *Xenopus laevis* (Tao et al., 2005). However, the association, if any, between BMP signaling pathway and *Grhl2*/*Grhl3* genes in neurulation remains unknown.

Here, we used conditional gene ablation to generate tissue-specific *Nog* mutants to identify the domain(s) important for neural tube closure because *Nog* is expressed multiple domains which are potentially relevant for proper neural tube formation. We also assessed adhesiveness in the *Nog* heterozygous neuroepithelium, and examined the expression of *Grhls* in *Nog* null mutant embryos. Finally, we investigated if ectopic upregulation of Hh signaling in *Nog* null embryos causes exencephaly. We used Cre-mediated activation of a constitutively active form of Smo (*caSmo*) to ectopically upregulate Hh signaling in the roof plate of the neural tube (*Wnt1-Cre;c-Smo*) to see if the mutant mice recapitulate NTDs in *Nog* null mice.

3.2 Materials and Methods

3.2.1 Mice

The mutant mice used in the detection of domains important for NTDs are the same crosses (*Wnt1-Cre;Nog$^{lacz/fx}$, ShhGFP-Cre;Nog$^{lacz/fx}$;Chrd$^{-/-}$, and Wnt1-Cre;caBMPr1a)* used in the previous chapter.

For activation of Hh signaling in the roof plate, conditional activation of Smo floxed mice (*caSmo*) was used in combination with *Wnt1-Cre* mice. All these mice were maintained on a random outbred ICR genetic background.

3.2.2 Gene expression assays

For whole mount in situ hybridization, embryos were dissected from pregnant mice, fixed overnight in 4% PFA at 4°C. The fixed embryos were dehydrated through 25%, 50%, 75%, and 100% ethanol, and stored in 100% ethanol at -20°. Whole mount in situ hybridization was carried out using previously described protocol (Belo et al., 1997) with hybridization temperature of 65°C. Primers for making *Grhl2* and *Grhl3* probes were designed using Primer3 (Koressaar and Remm, 2007). Standard techniques were used for β-galactosidase staining (Hogan, 1994).

3.2.3 Adhesion assay

This experimental technique was established and performed by Rebecca Thomason, Manuel Lopez (McClay lab) and Andy Ravanelli (Klingensmith lab).

384 well plates with flat polystyrene/coverglass bottom (Nunc #142761) were prepared in advance. Each test was run in triplicate. For cell-substrate adhesion experiments, fibronectin was deposited on the well bottoms with the concentrations determined empirically as the concentration required for reference standards to achieve maximum initial binding at 4°C (Lotz et al., 1989). Three types of cell lines were prepared for cell-cell adhesion experiments. Stably transfected N-CAM expressing CHO lines were obtained from Urs Rutishauser (Johnson et al., 2005). Cells that were harvested from culture were washed and diluted into serum-free DME medium. They were deposited to the bottoms of the wells of the 384-well plates by centrifugation at 50 xg rcf. It was confirmed that the substrate was largely covered by the unlabeled monolayers of cells, each containing ~ 50,000 cells. Similarly, an E-cadherin-expressing cell line (MDAMB-435 E435-E-cad cell line) (Meigs et al., 2002), or an A431D cell line transfected with N-cadherin (Lewis et al., 1997) was also deposited as a monolayer for measuring adhesion to E-cadherin or measuring adhesion to N-cadherin respectively.

Reference cells or neural tube cells that were stained either with RITC or cell tracker green as above were counted and diluted to approximately the same number with a desired final concentration of 5000 cells/ml and mixed. The cells were dispensed so that each test well of the 384 well Nunc plate received about 250-500 cells of each color. Finally, DME medium was poured into each well to form a slightly positive

meniscus at the top of the well after addition of the cells. Each well of the plate was sealed carefully with transparent packing tap. All of these steps were performed on ice to keep the cells and cultures at or below 4°C. The plates were centrifuged gently for 3 min so that all cells come into contact with the substrates (30x g, 3 min., 4°C). And then, the plates were inverted and spun at a speed predetermined to remove about 50% of the reference cell population (5 min., 4°C, force given for each experiment below). The plates were still kept inverted for analysis, cell counts, and imaging at 5X using Metamorph imaging software (Universal imaging). Each data point resulted from the average of at least three independent experiments that contained at least triplicate samples.

3.3 Results

3.3.1 Deletion of Nog using *ShhGFP-Cre* exhibits short tail phenotype, but does not show NTDs.

Nog null mice show fully penetrant spina bifida regardless of the background of the mice (Stottmann et al., 2006; Ybot-Gonzalez et al., 2007). *Nog* is expressed in the multiple domains that are potentially relevant to neural tube development (Fig. 2.1A, B, 3. 1A, B). In our model of *Nog* NTDs, spina bifida is caused by insufficient development of somite due to the lack of *Nog* from axial domains (Stottmann et al., 2006). To test this hypotheses, *ShhGFP-Cre*, axial domain specific Cre was used. *ShhGFP-Cre* is expressed in the axial midline including the floor plate of the neural tube and the notochord during neurulation. Although mutant embryos showed the characteristic *Nog* null phenotype of a short tail, neither obvious defects in somite development nor NTDs was present (Fig. 3.2A, B). The mutant embryos occasionally exhibited holoprosencephaly, and micrognathia as described in the previous chapter, but no cleft palate was found in the mutants (Fig. 2.2G, H). Additionally, they exhibited fused toes between the fourth and the fifth toes. The fused toe phenotype is not observed in *Nog* null embryos. This could be due to the high sensitivity of the genetic interaction between *Nog* and *Shh* in the toes (Fig. 3.2C-F). Taken together, these results indicate that axial domains of *Nog* are not critical for either caudal or rostral neural tube closure.

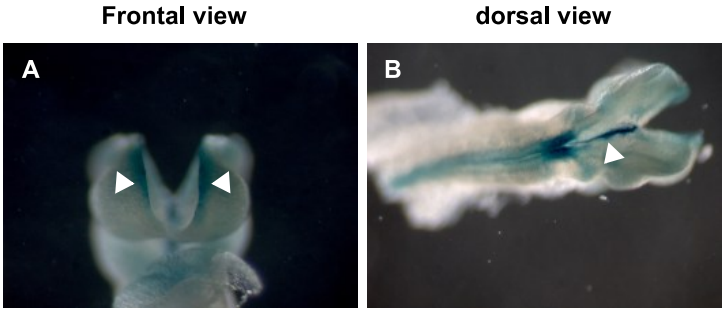

Figure 3.1: *Nog* expression during neurulation.

Nog is expressed in the roof plate of the closing neural folds (A). *Nog* is also expressed in the axial midline (B). More detailed *Nog* expression in axial midline is found in the Fig. 2.1B.

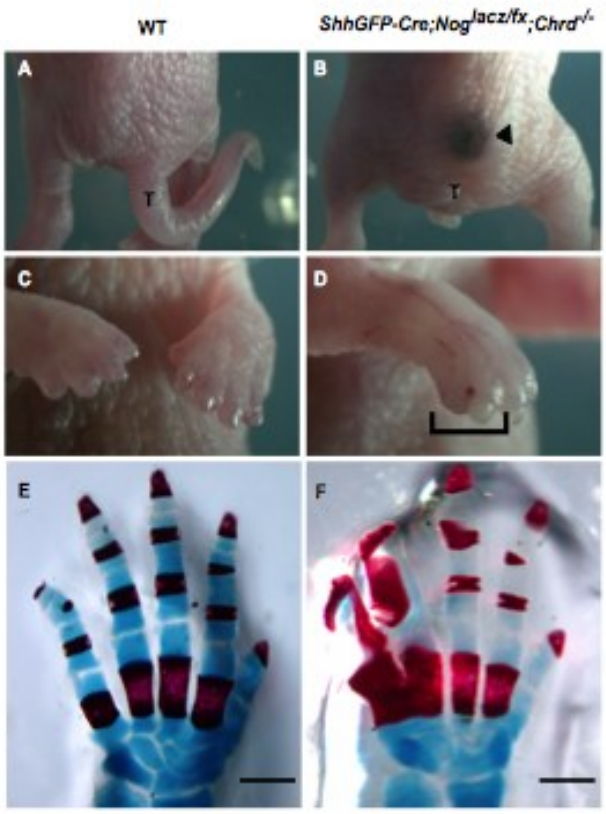

Figure 3.2: Short tail and fused toe phenotypes in *ShhGFP-Cre;Nog$^{lacz/fx}$;Chrd$^{-/-}$* embryos.

(A, B) Normal tail development in wild-type littermate (A). Ablating axial midline of BMP antagonists results in short tail. Because of the underdeveloped sacral structure, small amount of blood is accumulated (B). (C, D) within the bracket, 4th and 5th toes are fused in *ShhGFP-Cre;Nog$^{lacz/fx}$;Chrd$^{-/-}$* embryos (D) compared with normal development in wild-type embryo (C). (E, F) E17.5 skeletal prep showing normal toe development (E) and fused 4th and 5th toes in mutant embryos (F).

3.3.2 *Nog* heterozygous neural epithelium shows lower adhesion ability.

Our previous data showed that *Nog* null mutant embryos have a closed spinal neural tube at earlier stage around E9.5. However, after E11.5 it appeared reopened. However, *Nog* heterozygous embryos do not show visible NTDs. Therefore, we hypothesized that *Nog* heterozygous neuroepithelial cells have decreased adhesive ability than those in wild-type embryos, which in turn, cannot maintain the closing neural tube intact when both alleles of *Nog* are lost. To test if *Nog* is associated with adhesiveness in the developing neuroepithelium, we dissociated neuroepithelial cells from the neural plate and the neural tube of *Nog* heterozygous and wild-type control embryos between E8.5 and E9.5.

The technique employed for the adhesion assay is explained in detail in the Materials and Methods section of this chapter. Briefly, the adhesion assays include two parts - cell-cell and cell-substrate adhesion experiments. For cell-cell adhesion experiments, three different cell lines, stable neural crest adhesion molecule (N-CAM) expressing Chinese hamster ovary (CHO) cell lines (Johnson et al., 2005), E-cadherin-expressing cell line (Meigs et al., 2002), and an N-cadherin-expressing A431D cell line (Lewis et al., 1997) were employed. The cells were deposited into the 384-well plates so that they formed a monolayer of cells. For cell-substrate adhesion experiments, fibronectin was added on the bottoms of the plates with the concentration necessary to

achieve maximum initial binding at 4 °C (Lotz et al., 1989). Neuroepithelium harvested from embryos was stained either with rhodamine isothiocyanate (RITC) or cell tracker green and added on to the plates that contained either E-cadherin-, N-cadherin-, or N-CAM-expressing cells for cell-cell adhesion experiments, or fibronectin for cell-substrate adhesion experiments. The plates were spun gently for 3 minutes and the cells that remained attached to the substrate or the monolayers of the cells after centrifugation were counted. The results show *Nog* heterozygous cells exhibited less cell adhesiveness (Fig. 2.3). We found the largest difference in N-cadherin plate among all the adhesion molecules we tested. This is consistent with several other studies showing that expression of N-cadherin mRNA is upregulated by blocking BMP signaling while it is downregulated when BMP signaling is increased (Eom et al., 2011, 2012; Shoval et al., 2007).

As noted above, in these experiments, we used *Nog* heterozygous cells. Had we used cells from *Nog* null embryos, the effect would have been greater. Adhesiveness in the closing neural folds in *Nog* null embryos would be less than the hypothetical threshold of failure, leading to reopening the neural tube. The changes in adhesiveness could affect morphogenesis of neural tube development, which may in turn cause defects in maintaining the neural tube closure.

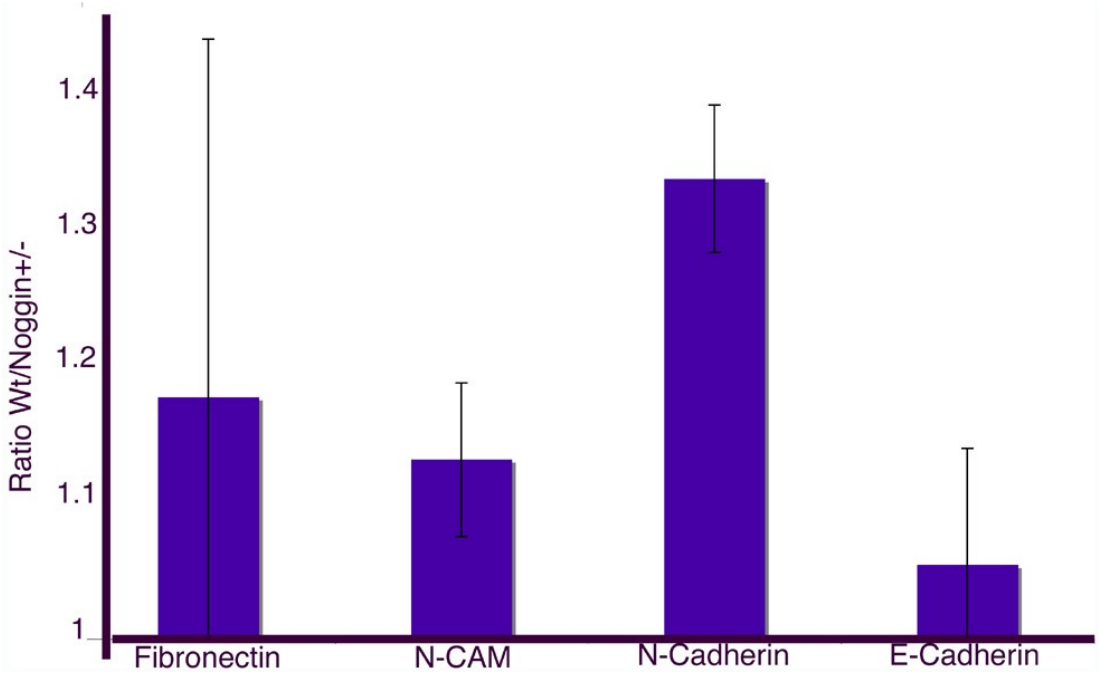

Figure 3.3: Nog heterozygous cells display an adhesive deficit relative to WT cells.

In multiple experiments wt cells showed better adhesiveness to fibronectin, N-CAM, N-Cadherin and E-Cadherin than Noggin $^{+/-}$ heterozygotic cells. Error bars include data from all experiments. The large error for fibronectin is due to the subtle differences in the stage of embryos. The adhesiveness to fibronectin changes dynamically in a short period of time. As neural tube folding proceeds, adhesion to fibronectin decreases in wild-type cells such that the difference between wild-type cells and Noggin $^{+/-}$ cells diminishes.

3.3.3 Expression of Grhl2 and Grhl3 is altered in the Nog null mutant embryos.

In our adhesion molecule experiment, *Nog* heterozygous neuroepithelium showed less adhesion levels. BMP signaling regulates expression of several adhesion molecules including Cadherins. *Grhl2* and *Grhl3* null mice exhibit region specific NTDs including exencephaly and spina bifida (Rifat et al., 2010), which are similar to *Nog* null NTDs. However, an *in situ* experiment shows that expression of *Nog* or *BMP2* was not altered in *Grhl3* null embryos (Rifat et al., 2010). These results indicate that BMP signaling is not the downstream target of *Grhl3* at least. It is still possible that *Grhl* genes are downstream targets of BMP signaling pathway. To investigate this possibility, we performed whole mount in situ hybridization against *Grhl2* and *Grhl3* in *Nog* null embryos. *Grhl2* was normally expressed in the front and midbrain region in the wild-type embryos. However, its expression was lost in the *Nog* null embryos at E9.5 (Fig 3.4A, B). Similarly, *Grhl3* expression was diminished especially in the lower spinal region where spina bifida occurs in the *Nog* null embryos at E10.5 (Fig 3.4C, D). These results suggest that potential regulation of *Grhl* genes by *Nog* in neurulation.

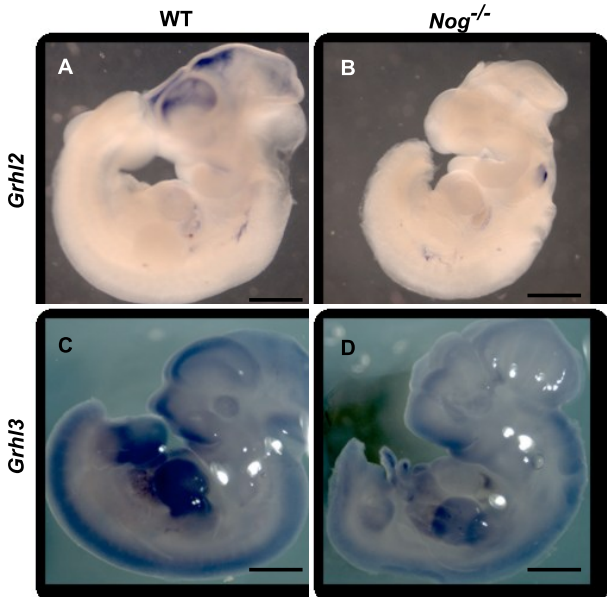

Figure 3.4: *Grhl* genes may be downregulated in the *Nog* null embryos.

(A, B) *Grhl2* expression is detected frontal part of the head in wild-type embryo (A), *Grhl2* expression is almost absent in the same area of mutant head (B). (C, D) *Grhl3* mRNAs were detected less in *Nog* null embryo (D). N=3, each.

3.3.4 Ablating *Nog* in the roof plate does not cause NTDs, but upregulating BMP signaling in the roof plate results in partially penetrant exencephaly.

Nog is expressed in another potentially relevant domain, the roof plate of the neural tube, for proper neural tube development. To examine if *Nog* in the roof plate of the neural tube is critical for proper neural tube development, we performed tissue specific *Nog* ablation using *Wnt1-Cre*. Mutant embryos lacking *Nog* from the *Wnt1-Cre* domain resulted in multiple craniofacial defects including fully penetrant cleft palate and an enlarged mandible shown in previous chapter (Fig. 2.3 & 2.4). However, there were no obvious defects, including NTDs, in the earlier stages. On the other hand, when BMP signaling is upregulated in the same domain using *Wnt1-Cre* and constitutively active BMP receptor 1a (*caBMPr1a*), approximately, half of the embryos exhibited exencephaly in addition to severe craniofacial defects including fully penetrant cleft palate and, to the lesser extent, cleft lip (Fig. 3.5). There was no consistent pattern between the severity of craniofacial defects and exencephaly. These results suggest that upregulating BMP signaling in the roof plate of the neural tube causes exencephaly, but ablating *Nog* from the roof plate does not upregulate BMP signaling high enough to cause exencephaly. Alternatively, *Nog* expression in the roof plate is not critical for proper neural tube development.

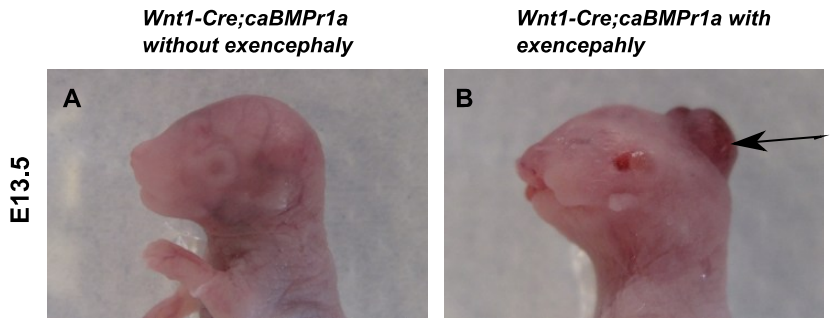

Figure 3.5: Activating BMP receptor 1a in the roof plate results in partially penetrant exencephaly.

(A, B) *Wnt1-Cre;caBMPr1a* embryos showing no exencephaly (A), however, about half of the mutant mice exhibit exencephaly with other craniofacial defects shown with black arrow (B).

3.3.5 Upregulating Hh signaling in the roof plate results in incomplete penetrance of exencephaly.

Previously, it was reported that *Nog* null embryos exhibited exencephaly. The phenotype was background dependent (Stottmann et al., 2006). However, one important finding is that exencephalic *Nog* null embryos always display ectopic Hh signaling in the roof plate of the neural tube although non-exencephalic *Nog* null embryos do not show ectopic Hh signaling upregulation (Stottmann et al., 2006). It is known that Hh signaling inhibits DLHP formation (Ybot-Gonzalez et al., 2007). Given the previous observations, we hypothesized that exencephaly in *Nog* null embryos is due to upregulating Hh signaling in the roof plate.

To test this hypothesis, we genetically upregulated Hh signaling in the *Wnt1-Cre* domain and compared the resulting phenotypes to those observed in *Nog* null embryos. We used Nog^{lacz} mice in undefined background in this study. *Wnt1-Cre* is expressed in the roof plate and NCCs. To upregulate Hh signaling, we used cre-inducible allele of constitutively active *Smo* (*caSmo*) in combination with *Wnt1-Cre*. We confirmed that *Wnt1-Cre;caSmo* embryos successfully upregulated Hh signaling in the roof plate of the neural tube by whole-mount in situ hybridization detecting expression of the *Shh* receptor and transcriptional target, *Ptch* (Fig. 3.7A, B) without upregulating *Shh* (Fig. 3.6).

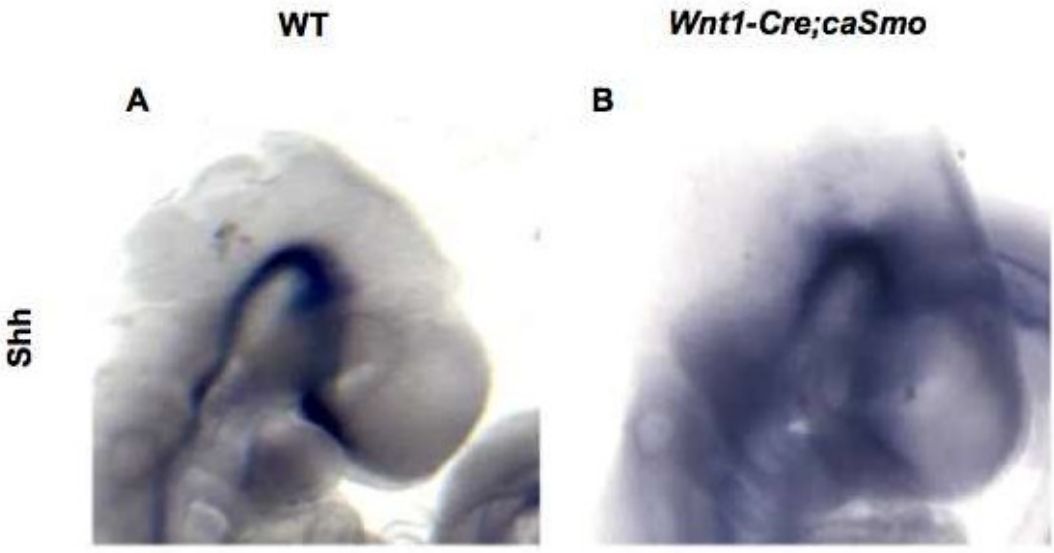

Figure 3.6: *Shh* is not upregulated in *Wnt1-Cre;caSmo* embryo.

Similar *Shh* expression pattern is detected in wild-type (A) and *Wnt1-Cre;caSmo* embryos (B) by whole mount in situ hybridization. (N=3, each)

Although penetrance of exencephaly was higher in *Wnt1cre;caSmo* (67%, N=9) at E9.5 than *Nog* null embryos (20%, N=6), it was not fully penetrant. Moreover, when dissected in later stage, the number of exencephalic embryos in *Wnt1cre;caSmo* was dramatically decreased (10%, N=10) (Fig. 3.9). In the later stages (E13.5~), only 10% of the *Wnt1-Cre;caSmo* embryos exhibited the open brain phenotype although the mutant embryos without exencephaly still showed an abnormally swollen head (Fig 3.9). Next, we measured angles of DLHPs and compared between *Wnt1cre;caSmo* and *Nog* null mutants (Table. 3.1). Angles of DLHPs in *Nog* null mutants are not different from those of *Wnt1cre;caSmo* (Fig. 3.8). Altogether these results suggest that upregulation of Hh signaling alone is not enough to cause exencephaly in *Nog* null embryos. It is also possible that variation of intensity in Hh signaling upregulation results in different phenotypic outcomes.

Table 3.1: Open NT phenotype in *Nog*$^{-/-}$ and *Wnt1-Cre;caSmo* mutants

	14-25 somites	25 somite <
WT	N=13, 0%	N/A
Nog$^{-/-}$	N=10, 20%	N/A
Wnt1-Cre;caSmo	N=9, 67%	N=10, 10%

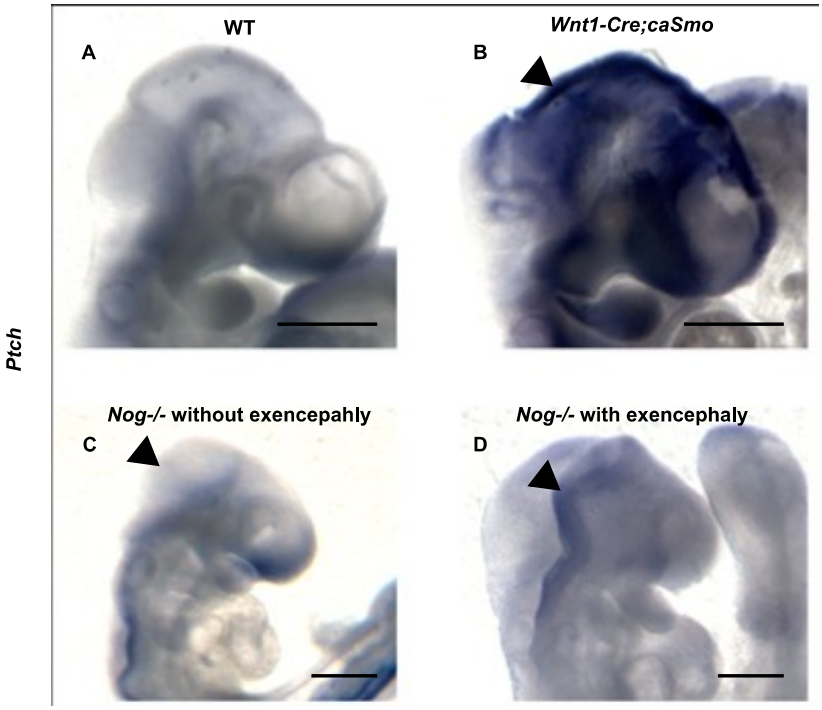

Figure 3.7: Ectopic Hh signaling is confirmed non-exencephalic *Wnt1-Cre:caSmo* mutant.

(A, B) Normal *Ptch* expression is found in the floor plate of the neural tube in wild-type embryo (A). Ectopic *Ptch* expression was seen in *Wnt1-Cre;caSmo* embryo to confirm upregulation of Hh signaling in non-exencephalic neural tube (B). (C, D) As previously shown, *Nog* null without exencephaly shows no Hh upregulation in the roof plate (C), while exencephalic *Nog* null shows ectopic *Ptch* expression in the roof plate (D). (N=3, each)

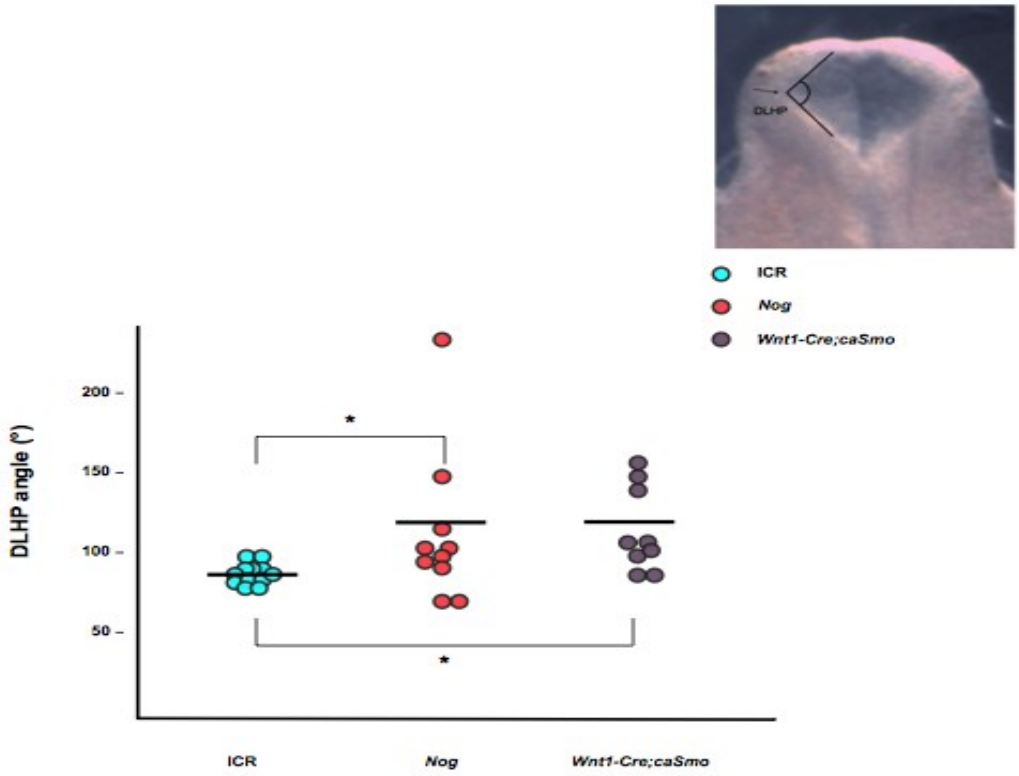

Figure 3.8: Angles of DLHP in *Nog* null and *Wnt-Cre;caSmo* were compared.

Angles of DLHP between wild-type (blue dots) and *Nog* null (pink dots) or between wild-type and *Wnt1-Cre;caSmo* (purple dots) are significantly different. However, difference is not observed angles between Nog null and *Wnt1-Cre;caSmo* embryos when one outlier in *Nog* null was discarded from the data point.

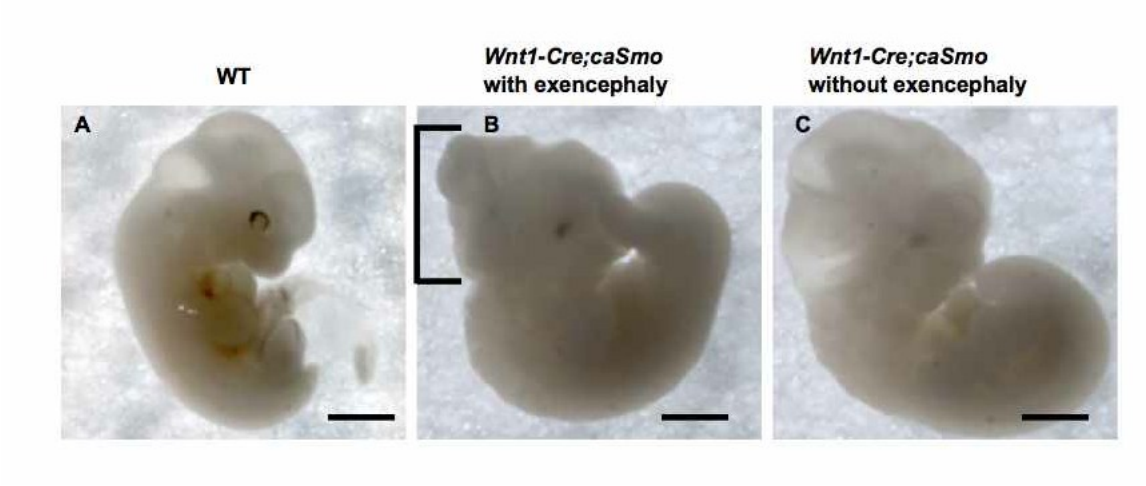

Figure 3.9: Upregulating Hh signaling in the roof plate cause partially penetrant exencephaly.

(A) Wild-type embryo showing normal neural tube development. N=20/20 (B, C) Upregulating Hh signaling in the roof plate results in partially penetrant exencephaly, N=1/10 (B), while some show no exencephaly, N=9/10 (C).

3.4 Discussion

In this study, we used tissue specific gene knockout mouse models to probe the roles of two distinct domains of *Nog* in regulating neural tube closure. When axial midline of BMP antagonists, *Nog* and *Chrd*, are absent, a short-tail like phenotype is present. However, no obvious NTDs were found in this class of mutant embryos. The other domain of *Nog* we tested was the roof plate of the neural tube using *Wnt1-Cre*. When *Nog* was ablated in the closing neural folds, which become roof plate of the neural tube, neural tube closure happens without any problem.

Since our previous study revealed that exencephalic *Nog* null mice exhibit ectopic Hh signaling upregulation in the roof plate of the neural tube, we hypothesized that upregulating Hh signaling in the roof plate can recapitulate exencephaly phenotype in *Nog* null mice. When constitutively active Smo was expressed in the roof plate, the resulting phenotype was partially penetrant exencephaly.

In our in vitro adhesion assay using neuroepithelium, *Nog* heterozygous cells showed decreased adhesion ability compared with wild-type cells. To further investigate molecular mechanisms underlying NTDs in *Nog* null mice, expression of *Grhl2* and *Grhl3*, which cause NTDs when one of them is absent, were examined. We found gene expression of both genes to be diminished in *Nog* null embryos. Together, our data and others suggest that *Nog* in other domain(s) than axial midline or roof plate,

such as somite-domain of *Nog*, or multiple domains of *Nog* are responsible for proper neural tube closure. *Nog* may regulate expression of adhesion molecules that are critical for neurulation, possibly through *Grhl* family genes.

3.4.1 Roof plate domain or axial midline domain of *Nog* alone does not cause NTDs.

Previous studies show that *Nog* null embryos exhibit fully penetrant spina bifida and to the lesser extent exencephaly. To investigate which domain of *Nog* is important for neural tube development, we used tissue specific gene ablation technique to knockout *Nog* from the roof plate of the neural tube. Although *Nog* is expressed in the roof plate of the closing neural tube, lack of *Nog* in the roof plate caused no NTDs. This result suggests *Nog* domain important for neural tube closure is not the roof plate. Alternatively, *Wnt1-Cre* expression may be too late to ablate *Nog* expression important for neural tube closure. *Nog* is also expressed in the axial midline including the notochord and the floor plate of the neural tube. One study suggests that axial domain of *Nog* is important for neural tube and somite development (McMahon et al., 1998). *ShhGFP-Cre* was used to ablate *Nog* from the axial midline. Although lack of *Nog* from axial midline in *Chrd* null background (*ShhGFP-Cre;Nog*$^{lacz/fx}$*;Chrd*$^{-/-}$) exhibited skeletal defects such as fused toes and micrognathia as well as small blood accumulation in the sacral area due to the caudal regression, no obvious NTDs were observed. One of the reasons that *ShhGFP-Cre;Nog*$^{lacz/fx}$*;Chrd*$^{-/-}$ did not show NTDs may be due to insufficient

Hh signaling upregulation in the mutant mice. *ShhGFP-Cre* was made by gene-targeting method to insert a gene that encodes *gfpcre* fusion protein into *Shh* locus (Harfe et al., 2004). *Shh* is a factor known to inhibit formation of DLHP that is critical for rostral neural tube folding (Ybot-Gonzalez et al., 2007). Exencephalic *Nog* null embryos always showed ectopic Hh signaling upregulation in the roof plate (Stottmann et al., 2006). Hh signaling upregulation by ablating *Nog* may be compensated by introduction of *ShhGFP-Cre*.

In the previous studies and our model of lumbar neural tube closure, axial domain of *Nog* is important for somite development, which in turn affects neural tube closure (McMahon et al., 1998; Stottmann et al., 2006; Wijgerde et al., 2005). However, ablating *Nog* from axial midline resulted in normal somite development. This result indicates that axial domain of *Nog* is not critical for somite development. Yet, whether proper somite development is required for subsequent neural tube closure remains unknown. Clearly *Nog* is necessary for somitogenesis. *Nog* regulates expression of somite patterning genes (Wijgerde et al., 2005). Importantly, *Nog* is expressed in the dorsal lip of the dermomyotome where *Pax3*-expressing cells first induce expression of *MyoD* and *Myf5* to develop myotomal cells (Reshef et al., 1998). The roles of this domain of *Nog* for neural tube development should be tested in the future study.

We found that *Nog* in the roof plate or axial domain alone does not cause NTDs or defects in somitogenesis. *Nog* expression in the somite itself may be directly responsible for somite development and indirectly for neural tube development. Alternatively, multiple domains, such as axial midline and somite domains, may act cooperatively in neurulation and somitogenesis. Further assessments are required for identifying *Nog* domain(s) important for proper neural tube development.

3.4.2 *Nog's* regulation of adhesion molecules in neural tube development.

Nog null mutant neural tube shows partially closed neural tube in the caudal spine before E10.5 and by E14.5 spina bifida becomes apparent by reopening of the neural tube (Stottmann et al., 2006). We hypothesized that *Nog* null mice do not have sufficient cell-cell and/or cell-substrate adhesion molecules that are essential for proper neural tube closure. To test this hypothesis, we performed adhesion assays that were described in detail in the Materials and Methods section of this chapter. The adhesion assay was originally established to measure hypothetical threshold of morphogenetic processes in the neural tube closure. It has been shown that natural genetic variations make one strain of mice more susceptible to a certain defect to occur over another strain of mice (Fleming and Copp, 2000). That is, using adhesion assay, we may be able to find "morphogenetic threshold of adhesiveness" beyond which it affects neural tube development.

We found that neuroepitheial cells from *Nog* heterozygous embryos, which do not exhibit NTDs, have less adhesiveness to fibronectin, N-CAM, N-cadherin, and E-cadherin, with significantly high adhesiveness to N-cadherin. These results suggest that *Nog* heterozygous embryos have, in total, adhesive ability above the threshold although they showed less adhesiveness to multiple adhesion molecules because *Nog* heterozygous embryos do not exhibit NTDs. Zebrafish Nodal signaling mutants display NTDs in the presumptive forebrain region. N-cadherin expression and localization to the membrane in the mutants are reduced (Aquilina-Beck et al., 2007). The adhesion assay experiments show that *Nog* heterozygous neuroepithelium exhibits reduced adhesiveness to N-cadherin although we still do not know how this adhesiveness affects neurulation in *Nog* embryos. It is likely that *Nog* homozygous neuroepithelium will show further reduction of adhesiveness. In addition to adhesion assay using *Nog* null neuroepithelium, it is also important to examine if localization and expression level of the adhesion molecules are altered in the closing neural folds of *Nog* null embryos.

We found that adhesiveness to cadherins was reduced in *Nog* heterozygous neuroepithelium. Yet, the genetic network regulating cadherins in the context of neural tube closure remains unknown. Interestingly, lack of *grainyhead-like* (*Grhl*) family genes results in region specific NTDs that are similar to the ones seen in *Nog* null mice. *Grhl2* mutant mice exhibit exencephaly with failed DLHP formation (Rifat et al., 2010), while

Grhl3 null mice show spina bifida due to defects in fusion of the neural folds (Copp et al., 2003; Rifat et al., 2010). One recent study in *Xenopus* demonstrates that *Grhl1* gene is regulated by BMP4 signaling cascade in development of epidermis (Tao et al., 2005). We hypothesized that BMP signaling negatively regulates expression of *Grhl* genes in the neural tube closure. To investigate if expression of *Grhl* genes is altered in *Nog* null embryos, whole-mount in situ hybridization was performed. The results suggest that the expression of both genes was greatly, but not completely, reduced in *Nog* null mutant ectoderm. Together, our data may indicate that BMP signaling regulation of cadherins in the neural tube closure is at least partially through *Grhl* genes. Further molecular analyses are awaited.

3.4.3 Hh signaling upregulation in the roof plate is necessary but not sufficient to cause exencephaly in *Nog* null.

Previously, our lab showed that *Nog* null embryos exhibit partially penetrant exencephaly, and the exencephalic embryos show Hh upregulation in the roof plate of the neural tube (Stottmann et al., 2006). *Shh* is a known inhibitor for DLHP formation (Ybot-Gonzalez et al., 2002). To examine if upregulating Hh signaling is the cause of exencephaly, we used constitutively active form of *Smo* mice (*caSmo*) in combination with *Wnt1-Cre* mice. Although we confirmed that Hh signaling was upregulated in the roof plate of *Wnt1-Cre;caSmo* mice by detecting a Shh receptor and transcriptional target

Ptch mRNA (Fig. 3.7), only 67% of embryos between 14 and 25 somite stages exhibited exencephaly (Table 3.1).

Hh signaling gradient from the ventral neural tube plays an essential role in the dorsoventral patterning of the neural tube in collaboration with BMP signaling gradient from the dorsal side of the neural tube. Precise regulation of gradient is the key step for proper patterning of the neural tube and subsequent generation of different types of neurons. Roles of Hh-signaling related genes in the neural tube development have been extensively studied. Loss of Shh causes craniofacial malformations and defects in development of the brain, but neural tube closure occurs normally (Chiang et al., 1996). NTDs' phenotypes in loss of function mutations of other Hh signaling components were described in various literatures. *Smo* mutants have defects in heart development and die around E9.5, but neural tube closure occurs normally (Zhang et al., 2001). Loss of other Hh signaling components such as *Dipatched1* or over-expression of *Ptch* reduces Hh signaling activity, preventing normal patterning in the neural tube, and yet, no defects in neural tube closure are observed (Goodrich et al., 1999; Kawakami et al., 2002).

On the other hand, activating Hh signaling often causes NTDs. Loss of *Ptch*, which causes Hh signaling activation, results in open neural tube (Goodrich et al., 1997). Loss of *Sufu*, another negative regulator of Hh signaling, results in defects in neural tube closure (Cooper et al., 2005). Both mutants show disrupted dorsoventral patterning in

the neural tube (Cooper et al., 2005; Goodrich et al., 1997). Notably, some studies indicate correlations between neural tube closure defects and degree of disruption in dorsoventral patterning in the neural tube of the mutant mice with Hh signaling upregulation (Ikeda et al., 2001; Murdoch and Copp, 2010; Norman et al., 2009; Patterson et al., 2009). Loss of a negative Hh signaling regulator, Tubby-like protein 3 (Tulp3) causes NTDs. Significantly, Tulp3 null embryos have higher degree of dorsoventral patterning defects with higher penetrance of NTDs than Tulp3 hypomorphs (Ikeda et al., 2001; Norman et al., 2009; Patterson et al., 2009).

Taken together, our results suggest that upregulating Hh signaling in the roof plate is a prerequisite for the exencephalic phenotype in *Nog* null embryos, but there may be critical threshold after which it affects neural tube development and causes fully penetrant exencephaly. Our studies did not extend to examine the degree of defects in dorsoventral patterning of *Wnt1-Cre;caSmo* and exencephalic *Nog* mutants. However, domains as well as intensity of Hh signaling activation will affect patterning of the neural tube. It is likely that wider area of Hh activation that causes severe dorsoventral patterning defects in the neural tube is required for increase the penetrance of exencephaly. *Nog* null mice in a 129/Sv background show fully penetrant exencephaly (Stottmann et al., 2006). Genetic variations may have distinct expressivity level of other BMP antagonists. This in turn could cause different level of Hh upregulation in *Nog* null

mice. Future studies that examine more precise interaction and regulation between BMP signaling and Hh signaling in neurulation will help us better understand about proper neural tube development.

3.5 Acknowledgement

We thank Urs Rutishauser, Rudi Juliano, Margaret Wheelock and Keith Johnson for supplying us with stably transfected cell lines. We also acknowledge the memory of Marcy Speer, a co-investigator on our Program Project, who provided sage advice and valuable insights into the complex issues in finding genes involved NTDs. Adhesion assay in this study was collaborative effort of Rebecca Thomason, Manuel Lopez (McClay lab) and Andy Ravanelli (Klingensmith lab).

4. Summary and future directions

BMP signaling has been implicated in numerous processes of embryonic development. Precise regulation of BMP signaling activity level is controlled by BMP antagonists. Our studies describe multiple roles of one such antagonist molecule, *Noggin* (*Nog*), in development of craniofacial skeleton and neural tube. The primary themes of this dissertation are (1) the elucidation of roles of distinct domains of *Nog*; axial midline and NCCs, in craniofacial skeletogenesis, (2) the identification of mechanisms of NTDs in *Nog* null mutant. These themes improve our understanding of normal development and etiology of defects in craniofacial skeleton and neural tube closure. This chapter summarizes our findings and discusses some implications for future research.

4.1 Nog in axial midline and pharyngeal arch 1 development.

Our original studies concerning mandibular outgrowth defects in BMP antagonist *Nog* and *Chrd* compound mutants ($Nog^{+/-};Chrd^{-/-}$) demonstrate that proper development of the derivatives of pharyngeal arch 1 (PA1) requires these antagonists (Stottmann et al., 2001). Although knockout of either gene, *Nog* or *Chrd*, only causes mild mandibular phenotypes, $Nog^{+/-};Chrd^{-/-}$ embryos exhibit a whole spectrum of mandibular truncation phenotypes ranging from almost normal to agnathia (no jaw) (Stottmann et al., 2001). In addition, explant culture experiments using PA1 suggest that upregulating

BMP signaling suppresses *FGF8* expression in ectoderm of PA1 and increases cell death in NCCs. *FGF8* is a NCC survival and patterning factor in populating NCCs in PA1 (Trumpp et al., 1999). However, during the development of craniofacial skeletal elements, *Nog* is expressed in multiple relevant domains including axial midline such as the notochord, the floor plate of the neural tube, and the foregut endoderm of the laryngeal region, and NCCs from which most of the craniofacial skeleton are derived. Therefore, it is important to identify which domain(s) of *Nog* are required for proper mandibular development. To address this, we first conducted a conditional genetic ablation experiment using Nog^{fx} (Stafford et al., 2011) allele in combination with axial-midline-specific *ShhGFP-Cre* (Harfe et al., 2004) carrying Nog^{lacZ} on a *Chrd* null background. We focused on the phenotypes of *ShhGFP-Cre;*$Nog^{lacz/fx}$*;*$Chrd^{-/-}$ embryos.

Ablation of *Nog* from the axial midline domain by *ShhGFP-Cre* on a *Chrd* null background resulted in high penetrance of micrognathia (3/5). The embryos that caused mandibular outgrowth defects were also accompanied with truncated maxilla. Additionally, some embryos exhibited holoprosencephaly – i.e., fused forebrain due to midline truncation. At earlier stage around E11.5, *ShhGFP-Cre;*$Nog^{lacz/fx}$*;*$Chrd^{-/-}$ embryos showed smaller PA1 than wild-type littermates. The smaller PA1 is often observed in other mutants with mandibular outgrowth defects. These studies allowed us to identify an important role of *Nog* in axial midline domain for development of PA1 derivatives,

indicating that *Nog*'s indirect role for proper craniofacial development because none of these tissues contribute to the craniofacial skeletal elements. Significantly, parietal bone which is a mesoderm derivative, also became smaller *ShhGFP-Cre;Nog*$^{lacz/fx}$*;Chrd*$^{-/-}$with mandibular outgrowth defects. In contrast to this indirect effect of *Nog* in axial midline to PA1 derivatives, this domain of *Nog* may also have direct effect on development of mesoderm derived craniofacial skeleton. Notably, other *No*g craniofacial phenotypes, such as thickened mandibular bone (Stottmann et al., 2006) and cleft palate (He et al., 2010) were not present in *ShhGFP-Cre;Nog*$^{lacz/fx}$*;Chrd*$^{-/-}$.

Our studies relied largely on analyses of histology and skeletal preparation. It is important to examine if the mandibular outgrowth defects seen in *ShhGFP-Cre;Nog*$^{lacz/fx}$*;Chrd*$^{-/-}$ embryos result from increased cell death in PA1 as previous studies of *Nog* null embryos suggested by immnohistochemistry (Stottmann et al., 2001). Indirect effect of *Nog* in axial midline domain likely alters secondary signaling that influences PA1 development. *Shh* and *FGF8* synergistically drive development of craniofacial cartilage by promoting NCC survival (Trumpp et al., 1999; Tucker et al., 1999). It would be more informative to identify which secondary signaling(s) are induced or suppressed by loss of *Nog* in axial domains, and upregulating BMP signaling in the mutant.

4.2 Nog in NCCs and craniofacial skeletogenesis.

Ablating *Nog* from axial midline caused hypoplastic PA1 derivatives including micrognathia and a shorter maxilla. These phenotypes resulted from loss of *Nog*'s indirect role in craniofacial development. However, previous studies indicate other roles of *Nog* in craniofacial development. *Nog* null embryos showed thickened mandibular skeletal structure (Stottmann et al., 2001). Lack of *Nog* also exhibited fully penetrant primary and secondary cleft palate (He et al., 2010). These phenotypes were not present in *ShhGFP-Cre;Nog*$^{lacz/fx}$*;Chrd*$^{-/-}$. However, craniofacial skeletal elements are mostly derived from NCCs. *Nog* is also expressed in NCCs. Therefore, it is essential to investigate *Nog*'s direct effect in the development of craniofacial skeleton. To assess this, we conducted another conditional genetic ablation experiment. This time, we used *Wnt1-Cre*, NCC-specific recombination driver, together with *Nog*^{fx} allele to ablate *Nog* in NCCs.

At the beginning of the genetic experiments, this genetic cross was done on a *Chrd* null background. *Wnt1-Cre;Nog*$^{lacz/fx}$*;Chrd*$^{-/-}$ embryos showed fully penetrant enlarged mandibular skeletal structure and secondary cleft palate. However, we found even when *Chrd* was present, *Wnt1-Cre;Nog*$^{lacz/fx}$ embryos exhibited the same phenotypes as *Wnt1-Cre;Nog*$^{lacz/fx}$*;Chrd*$^{-/-}$ embryos. Consequently, we decided to examine *Wnt1-Cre;Nog*$^{lacz/fx}$ embryos.

In addition to enlarged mandibular skeletal structure, other cartilages - such as nasal cartilage - were also hypermorphic in *Wnt1-Cre;Nog*$^{lacz/fx}$ embryos. Earlier studies show *BMP2* mutant mice lack detectable migratory cranial NCCs (Kanzler et al., 2000). In chick experiment, migration of transplanted melanoma cells was inhibited by *Nog* (Busch et al., 2007). Since BMP signaling is required in the multiple steps in the NCC development - starting from the generation and migration to proliferation and differentiation of NCCs, and *Wnt1-Cre;Nog*$^{lacz/fx}$ embryos showed enlarged NCC-derived craniofacial skeletal elements such as mandible and nasal cartilage, we hypothesized that increased NCC migration ventrally from the dorsal neural folds resulted in hypermorphic skeletal structures. However, embryos lacking *Nog* from NCCs showed normal size PA1 around E10.5 at which NCC migration should have completed. At this point, the size of the mutant head was not different from the wild-type head. Thus, NCC production and migration in *Wnt1-Cre;Nog*$^{lacz/fx}$ embryos were largely unaffected. We also tested several PA1 patterning makers, such as Dlx5, Barx1, Msx1, and Dlx2. No patterning markers were altered in *Wnt1-Cre;Nog*$^{lacz/fx}$ embryos. Notably, loss of *Nog* in NCCs did not exhibit micrognathia found in *Nog* null and *ShhGFP-Cre;Nog*$^{lacz/fx}$*;Chrd*$^{-/-}$. These data indicate that critical roles of *Nog* in NCCs for development of craniofacial skeleton occur after NCC migration.

Contrary to our hypothesis, *Nog* expression in NCCs was not necessary for NCC production and migration. There are several potential reasons for this. One reason is that other BMP antagonists such as *Gremlin* and *Twisted gastrulation* that are expressed during NCC formation and migration could compensate for the loss of *Nog* in NCCs (Hsu et al., 1998; Scott et al., 2001; Stafford et al., 2011). A second reason could be that *Nog* may not be the primary BMP antagonist at this stage. It would be useful to see whether expression of other BMP antagonists is increased during NCC production and migration in the embryos lacking *Nog* in NCCs.

4.3 Nog in NCCs and mandibular development.

A previous study showed that $Nog^{+/-};Chrd^{-/-}$ compound mutant mice displayed a whole spectrum of mandibular outgrowth defects (Stottmann et al., 2001). Our studies concerning roles of *Nog* in axial midline domain revealed that this domain of *Nog* is critical for mandibular outgrowth. In addition to the indirect role of *Nog* in axial domain, we also found that ablation of *Nog* from NCCs does not cause mandibular outgrowth defects. Instead, lack of *Nog* in NCCs resulted in a thicker mandibular structure formation. It is important to investigate what mechanism causes hypermorphic mandibular skeletal structure.

During mandibular development, Meckel's cartilage and mandibular bone are mostly derived from NCCs of PA1. Mandibular bone forms around Meckel's cartilage using Meckel's cartilage as a template. In mice, Meckel's cartilage first appears at E11.5 as a chondrocyte condensation, at E12.5 it starts forming rod-like shape, by E13.5 Meckel's cartilage becomes a single "V" shaped structure (Ramaesh and Bard, 2003) In our studies, we found the size of cartilage condensation was relatively similar between wild-type and *Wnt1-Cre;Nog*$^{lacz/fx}$ embryos. However, by E13.5 the diameter of the Meckel's cartilage became much larger in *Wnt1-Cre;Nog*$^{lacz/fx}$ embryos. We used BrdU to investigate if this was due to increased cell proliferation. We found that Meckel's cartilage in *Wnt1-Cre;Nog*$^{lacz/fx}$ embryos showed increase cell proliferation at E12.5. Activating BMP signaling in NCCs only by *Wnt1-Cre;R26R*$^{caBmpr1a/+}$ similarly exhibited thickened Meckel's cartilage as *Wnt1-cre;Nog*$^{lacz/fx}$. This result was consistent with a recent finding in which BMP receptor 1a was activated in the chondrocyte, and resulting phenotype was enlarged Meckel's cartilage due to increased cell proliferation (Hu et al., 2008; Wang et al., 2013).

While we identified that enlarged mandible in *Wnt1-Cre;Nog*$^{lacz/fx}$ embryos was due to increased cell proliferation in Meckel's cartilage, the mechanism causing increased cell proliferation was not clear. Previous studies show an association between BMP signaling and Hh signaling in skeletal development. BMP signaling promotes *Ihh*

expression which, in turn, positively regulates cell proliferation in chondrocytes (Minina et al., 2002). We hypothesized that upregulating BMP signaling in Meckel's cartilage induces Hh signaling upregulation. To assess this, *Ptch-lacz*, obligate reporter of Hh signaling, was incorporated in *Wnt1-Cre;R26R*$^{caBmpr1a/+}$. We found that Hh signaling was upregulated in Meckel's cartilage of *Wnt1-Cre;R26R*$^{caBmpr1a/+}$ embryos. Moreover, qPCR data suggested that Hh upregulation in Meckel's cartilage of *Wnt1-Cre;R26R*$^{caBmpr1a/+}$ was due to increased *Ihh* expression. These data may indicate that previous findings that BMP signaling induces Ihh signaling that promote chondrocyte proliferation in endochondral ossification also apply to mandibular development in which the structure is derived through non-endochondral ossification. However, it is important to examine whether increased Hh signaling in Meckel's cartilage promote cell proliferation in mice lacking *Nog* from NCCs. Hh signaling can be artificially blocked by adding cyclopamine. Mandibular explant culture *Wnt1-Cre;Nog*$^{lacz/fx}$ embryos with cyclopamine treatment followed by a BrdU incorporation experiment should reveal the answer to this question.

4.4 Roles of Nog in palatal development.

Nog null embryos previously showed primary and secondary cleft palate due to disrupted integrity of palatal epithelium (He et al., 2010). Cell proliferation was increased in the oral side of the palatal epithelium where ectopic pSmad activity was

observed in *Nog* null embryos, and palatal elevation was prevented by abnormal fusion between the posterior palate and the mandible (He et al., 2010). Activating BMP receptor 1a in epithelium using *K14-Cre* also recapitulated abnormal fusion of palatal shelves to mandible seen in *Nog* null embryos (He et al., 2010). These data indicate an important role of *Nog* expression in epithelium for palatal development. However, we found that lack of *Nog* from NCCs also resulted in secondary cleft palate. It was important to investigate mechanisms of the cleft palate phenotype in *Wnt1-Cre;Nog*$^{lacz/fx}$ embryos.

During palatal development in mice, at E13 palatal shelves grow vertically and at E14 both sides of palatal shelves rotate and elevate to meet at the midline. By E15 both sides of palatal shelves fuse and form a complete palate. To identify which step of palatal development was disrupted in *Wnt1-Cre;Nog*$^{lacz/fx}$ embryos, coronal sections of the head were carefully analyzed. We found normal growth of the mutant palatal shelves at E13.5 and the cell proliferation rate in the palatal shelves was not different between wild-type and *Wnt1-Cre;Nog*$^{lacz/fx}$ embryos. In addition, palatal patterning genes - such as Shox2, Tbx22, Barx1, and Efnb2 - were also detected similarly in the palatal shelves of wild-type and *Wnt1-Cre;Nog*$^{lacz/fx}$ embryos. Furthermore, explant culture of the palatal shelves showed palatal shelves of *Wnt1-Cre;Nog*$^{lacz/fx}$ embryos retained the ability of palatal shelf fusion as wild-type palatal shelves. From these experiments, we did not find any defective steps during palatogenesis of mice lacking *Nog* from NCCs. However,

we noticed ectopic bone growth in the further posterior palatal shelves at E13.5 of *Wnt1-Cre;Nog*$^{lacz/fx}$ embryos. This bone was strikingly large, and it invaded in the growing posterior palatal shelves so that elevation of the palatal shelves seemed prevented. Conducting skeletal preparation, this invading bone was identified as an enlarged pterygoid bone. Hypomorphic palatal bone, which is often considered as a cause of submucous cleft palate, was also found in *Wnt1-Cre;Nog*$^{lacz/fx}$ embryos. The cause of cleft palate in the mutant is likely due to disrupted elevation of the palatal shelves by ectopic pterygoid formation in the posterior palatal shelves. These results strongly suggest a novel mechanism of cleft palate, in which dysmorphic skull base component indirectly affects palatal development. Other craniofacial component may also influence palatogenesis. One study of patients with craniosynostosis, premature suture fusion of skull vault, found relatively wider cleft of soft palate in the patients (Iida et al., 1995). Understanding the distinct mechanisms underlying different types of cleft palate may help us find proper diagnosis, treatments, and prevention for cleft palate. Future research to understand the mechanisms is highly recommended, therefore.

4.5 Nog in DLHP formation.

It has been shown that formation of DLHPs is critical for cranial neural tube closure as exencephaly results if they do not form properly (Stottmann et al., 2006;

Werth et al., 2010; Ybot-Gonzalez et al., 2002). Our previous study also showed exencephaly in *Nog* null embryos resulted from disrupted DLHP formation (Stottmann et al., 2006). However, complete mechanisms of how the bending is formed are still uncertain. One recent study concerning chick neural tube development revealed that MHP, another important hinge point in the neural tube closure requires a two-dimensional canonical BMP activity gradient that creates a low and pulsed BMP activity in the MHP (Eom et al., 2011). This study also proposed a model that the MHP is formed through apical constriction caused by endocytosis of apical proteins, Par3 and N-cadherin, which associate with phosphorylated Smad5/8 in a BMP-dependent manner (Eom et al., 2011). The similar mechanisms may be also applicable to DLHP formation. Identifying mechanisms of DLHP formation is also a critical theme, since defective DLHP formation is often seen in exencephalic mice with different gene mutations.

DLHP formation may be also affected by the development of non-neural surface ectoderm. The surface ectoderm may have active role for neural tube closure, since removing the tissue surgically inhibits DLHP formation (Moury and Schoenwolf, 1995). Supporting evidence comes from studies of *Grhl* mutant mice (Pyrgaki et al., 2011; Rifat et al., 2010; Werth et al., 2010). Loss of *Grhl2* or *Grhl3* results in NTDs. *Grhl* genes are essential for development of non-neural epithelial cells. Interestingly, our in situ data indicate expression levels of *Grhl* genes in *Nog* null embryos may be reduced. Since *Grhl*

genes are expressed in the surface ectoderm, but not in the neural epithelium, it is unlikely that BMP signaling in *Nog* null directly regulates transcription of *Grhl* genes in the adjacent tissues. More detailed molecular analyses should reveal mechanisms of gene regulation and molecular control in DLHP formation.

4.6 Nog and Hh signaling in neural tube closure.

One of the original goals of our neural tube closure study was to determine if upregulating Hh signaling in the roof plate of the neural tube recapitulate exencephaly observed in *Nog* null embryos. Penetrance of exencephaly in *Nog* null embryos is greatly influenced by the genetic background, and exencephalic *Nog* null embryos always exhibited ectopic Hh upregulation (Stottmann et al., 2006). *Shh* is known to inhibit formation of DLHPs that are required for proper neural tube closure in the midbrain region (Ybot-Gonzalez et al., 2002). We hypothesized that upregulating Hh signaling in the roof plate results in exencephaly. To examine this, we conducted a genetic experiment that is activating *Smo* (*caSmo*) in the roof plate using *Wnt1-Cre*. We found that *Wnt1-Cre;caSmo* embryos cause partially penetrant (67%) exencephaly between 14 and 25 somite stages.

Ventral Hh is clearly important for neural tube development together with dorsal BMP signaling. These two signaling pathways synergistically and antagonistically act

together to form a correct neural tube. Importantly, ablating Hh signaling components affects neural tube patterning, but it does not cause NTDs (Goodrich et al., 1999; Kawakami et al., 2002). In contrast, activating Hh signaling components frequently causes defects in neural tube closure. Importantly, the degree of penetrance may depend on the level of ectopic Hh signaling upregulation. Tulp3 is a negative Hh signaling regulator. *Tulp3* null embryos exhibited highly penetrant exencephaly (77%) while *Tulp3* hypomorphs resulted in much lower penetrance of exencephaly (37%) at E12.5 (Ikeda et al., 2001; Patterson et al., 2009). The degree of Hh signaling activation may affect severity of defects in the neural tube patterning, which in turn cause NTDs.

Our findings of NTDs in *Wnt1-Cre;caSmo* embryos with previous studies suggest that Hh upregulation is a required factor, but just upregulating Hh signaling in the roof plate may not be sufficient to cause exencephaly in *Nog* null mice. Alternatively, the degree and domains of Hh signaling upregulation are also likely to influence the degree of perturbation in neural tube development. Since we used *Wnt1-Cre* to activate Hh signaling, ectopic Hh signaling was limited in the domain in which *Wnt1-Cre* was expressed. In *Nog* mutants with exencephaly may have Hh signaling upregulation in wider region that we may have missed. Future studies could examine dorsoventral patterning of the neural tube between exencephalic and non-exencephalic *Nog* mutant embryos to address this concern.

4.7 Nog and adhesion molecules in neural tube closure.

Neural tube closure involves dynamic tissue morphogenesis. Both edges of a flat sheet of neural plate roll up, and juxtaposed neural folds fuse together across the dorsal midline, resulting in complete neural tube closure. Failure of any step during neurulation may result in NTDs. It is critical that the cells in the neural plate to produce the correct cytoskeletal and adhesion apparatus for this active tissue movement to occur. In our previous study, we showed that *Nog* null mice exhibited NTDs including exencephaly and spina bifida. Despite severe NTDs seen in *Nog* null mice, *Nog* heterozygous embryos had no obvious NTDs. We hypothesized that neuroepithelial cells in *Nog* heterozygous mice retain adhesive ability above the threshold but lower than ones in wild-type neuroepithelium so that no NTDs result. Therefore, one of important goals was to establish an adhesion assay that would quantitatively evaluate adhesion of cells during neural tube closure (details of the experimental methods are found in the previous chapter). Using this adhesion assay, we found neuroepithelium in *Nog* heterozygous embryos exhibits less adhesiveness against several adhesion molecules including N-CAM and E-cad. Significantly, neuroepitheial cells in wild-type embryos showed 40% more adherent to N-cadherin than ones in *Nog* heterozygous embryos. These data suggest that *Nog* heterozygous neuroepitheial cells greatly reduce adhesiveness that in turn may be important for proper neural tube morphogenesis. One

study showed that removal of N-cadherin causes exencephaly with increased cell death (Luo et al., 2006). Extensions to this study should be aimed at determining if these adhesion molecules are regulated in the transcription level, translation level, or even localization level. These studies would serve as another step to more fully integrate BMP antagonism's contribution to neural tube development.

4.8 Conclusion

In this study, we focused on two most common and detrimental birth defects, craniofacial and neural tube defects and their development. Craniofacial skeletal structure is complex but elegant in that many distinct small bones and cartilages with different shapes come together and work cooperatively to function properly. The neural tube is a precursor to the brain and the spine. Correct development of these two organs is extremely important for ensuring quality of life as well as social acceptance. And yet, the processes of both craniofacial and neural tube development are unfortunately susceptible to genetic and environmental disruptions. Therefore, it is easy to understand that why studies of craniofacial and neural tube development have attracted so many researchers over a long period of time.

Here, multiple roles of *Noggin*, a BMP antagonist in development of the neural tube and craniofacial skeletal elements are studied. During midbrain neural tube

closure, *Nog*'s BMP antagonism is likely to prevent ectopic expression of Hh signaling which inhibits DLHP formation. Regulation of adhesion molecules by *Nog* may be also a crucial step for proper neural tube development. *Nog* in axial domain is critical for proper development of PA1 since loss of *Nog* in axial domain resulted in hypoplastic PA1 derivatives including micrognathia. This suggests that axial midline domain of *Nog* is a key BMP antagonism for early craniofacial development. On the other hand, loss of *Nog* from NCCs caused hyperplastic Meckel's cartilage formation due to increased cell proliferation in chondrocytes. In addition, *Nog* in NCCs plays an important role in regulating size and shape of skeletal elements of the skull base, which in turn could indirectly influence palatogenesis. Although this study revealed many answers in relation to the roles of *Nog* in development of craniofacial skeleton and neural tube closure, new interesting questions were also discovered. It is desirable that this dissertation will contribute to future researches, prevention, and treatments associated with developmental mechanisms and problems.

References

Anderson, R.M., Lawrence, A.R., Stottmann, R.W., Bachiller, D., Klingensmith, J., 2002. Chordin and noggin promote organizing centers of forebrain development in the mouse. Development 129, 4975-4987.

Anderson, R.M., Stottmann, R.W., Choi, M., Klingensmith, J., 2006. Endogenous bone morphogenetic protein antagonists regulate mammalian neural crest generation and survival. Developmental dynamics : an official publication of the American Association of Anatomists 235, 2507-2520.

Aquilina-Beck, A., Ilagan, K., Liu, Q., Liang, J.O., 2007. Nodal signaling is required for closure of the anterior neural tube in zebrafish. BMC developmental biology 7, 126.

Bachiller, D., Klingensmith, J., Kemp, C., Belo, J.A., Anderson, R.M., May, S.R., McMahon, J.A., McMahon, A.P., Harland, R.M., Rossant, J., De Robertis, E.M., 2000. The organizer factors Chordin and Noggin are required for mouse forebrain development. Nature 403, 658-661.

Baek, J.A., Lan, Y., Liu, H., Maltby, K.M., Mishina, Y., Jiang, R.L., 2011. Bmpr1a signaling plays critical roles in palatal shelf growth and palatal bone formation. Developmental Biology 350, 520-531.

Bastir, M., Rosas, A., Stringer, C., Cuetara, J.M., Kruszynski, R., Weber, G.W., Ross, C.F., Ravosa, M.J., 2010. Effects of brain and facial size on basicranial form in human and primate evolution. Journal of Human Evolution 58, 424-431.

Belo, J.A., Bouwmeester, T., Leyns, L., Kertesz, N., Gallo, M., Follettie, M., De Robertis, E.M., 1997. Cerberus-like is a secreted factor with neutralizing activity expressed in the anterior primitive endoderm of the mouse gastrula. Mech Dev 68, 45-57.

Bonilla-Claudio, M., Wang, J., Bai, Y., Klysik, E., Selever, J., Martin, J.F., 2012. Bmp signaling regulates a dose-dependent transcriptional program to control facial skeletal development. Development 139, 709-719.

Braybrook, C., Doudney, K., Marcano, A.C., Arnason, A., Bjornsson, A., Patton, M.A., Goodfellow, P.J., Moore, G.E., Stanier, P., 2001. The T-box transcription factor gene TBX22 is mutated in X-linked cleft palate and ankyloglossia. Nat Genet 29, 179-183.

Brewer, S., Feng, W., Huang, J., Sullivan, S., Williams, T., 2004. Wnt1-Cre-mediated deletion of AP-2alpha causes multiple neural crest-related defects. Dev Biol 267, 135-152.

Brunet, C.L., Sharpe, P.M., Ferguson, M.W., 1995. Inhibition of TGF-beta 3 (but not TGF-beta 1 or TGF-beta 2) activity prevents normal mouse embryonic palate fusion. Int J Dev Biol 39, 345-355.

Brunet, L.J., McMahon, J.A., McMahon, A.P., Harland, R.M., 1998. Noggin, cartilage morphogenesis, and joint formation in the mammalian skeleton. Science 280, 1455-1457.

Burstyn-Cohen, T., Kalcheim, C., 2002. Association between the cell cycle and neural crest delamination through specific regulation of G1/S transition. Dev Cell 3, 383-395.

Busch, C., Drews, U., Garbe, C., Eisele, S.R., Oppitz, M., 2007. Neural crest cell migration of mouse B16-F1 melanoma cells transplanted into the chick embryo is inhibited by the BMP-antagonist noggin. International journal of oncology 31, 1367-1378.

Chai, Y., Jiang, X., Ito, Y., Bringas, P., Jr., Han, J., Rowitch, D.H., Soriano, P., McMahon, A.P., Sucov, H.M., 2000a. Fate of the mammalian cranial neural crest during tooth and mandibular morphogenesis. Development 127, 1671-1679.

Chai, Y., Jiang, X.B., Ito, Y., Bringas, P., Han, J., Rowitch, D.H., Soriano, P., McMahon, A.P., Sucov, H.M., 2000b. Fate of the mammalian cranial neural crest during tooth and mandibular morphogenesis. Development 127, 1671-1679.

Chiang, C., Litingtung, Y., Lee, E., Young, K.E., Corden, J.L., Westphal, H., Beachy, P.A., 1996. Cyclopia and defective axial patterning in mice lacking Sonic hedgehog gene function. Nature 383, 407-413.

Choi, M., Klingensmith, J., 2009. Chordin is a modifier of tbx1 for the craniofacial malformations of 22q11 deletion syndrome phenotypes in mouse. PLoS genetics 5, e1000395.

Cohen, M.M., MacLean, R.E., 2000. Craniosynostosis : diagnosis, evaluation, and management, 2nd ed. Oxford University Press, New York.

Cooper, A.F., Yu, K.P., Brueckner, M., Brailey, L.L., Johnson, L., McGrath, J.M., Bale, A.E., 2005. Cardiac and CNS defects in a mouse with targeted disruption of suppressor of fused. Development 132, 4407-4417.

Copp, A.J., Greene, N.D., Murdoch, J.N., 2003. The genetic basis of mammalian neurulation. Nature reviews. Genetics 4, 784-793.

Couly, G., Creuzet, S., Bennaceur, S., Vincent, C., Le Douarin, N.M., 2002. Interactions between Hox-negative cephalic neural crest cells and the foregut endoderm in patterning the facial skeleton in the vertebrate head. Development 129, 1061-1073.

Couly, G.F., Coltey, P.M., Ledouarin, N.M., 1993. The Triple Origin of Skull in Higher Vertebrates - a Study in Quail-Chick Chimeras. Development 117, 409-429.

d'Amaro, R., Scheidegger, R., Blumer, S., Pazera, P., Katsaros, C., Graf, D., Chiquet, M., 2012. Putative functions of extracellular matrix glycoproteins in secondary palate morphogenesis. Frontiers in physiology 3, 377.

Danielian, P.S., Muccino, D., Rowitch, D.H., Michael, S.K., McMahon, A.P., 1998. Modification of gene activity in mouse embryos in utero by a tamoxifen-inducible form of Cre recombinase. Current biology : CB 8, 1323-1326.

Daskalogiannakis, J., Ross, R.B., Tompson, B.D., 2001. The mandibular catch-up growth controversy in Pierre Robin sequence. Am J Orthod Dentofacial Orthop 120, 280-285.

De Coster, P.J., Mortier, G., Marks, L.A., Martens, L.C., 2007. Cranial suture biology and dental development: genetic and clinical perspectives. J Oral Pathol Med 36, 447-455.

Dudas, M., Sridurongrit, S., Nagy, A., Okazaki, K., Kaartinen, V., 2004. Craniofacial defects in mice lacking BMP type I receptor Alk2 in neural crest cells. Mech Dev 121, 173-182.

Eom, D.S., Amarnath, S., Agarwala, S., 2013. Apicobasal polarity and neural tube closure. Development, growth & differentiation 55, 164-172.

Eom, D.S., Amarnath, S., Fogel, J.L., Agarwala, S., 2011. Bone morphogenetic proteins regulate neural tube closure by interacting with the apicobasal polarity pathway. Development 138, 3179-3188.

Eom, D.S., Amarnath, S., Fogel, J.L., Agarwala, S., 2012. Bone morphogenetic proteins regulate hinge point formation during neural tube closure by dynamic modulation of apicobasal polarity. Birth defects research. Part A, Clinical and molecular teratology 94, 804-816.

Figueroa, A.A., 2002. Long-term outcome study of bilateral mandibular distraction: A comparison of Treacher Collins and Nager syndromes to other types of micrognathia - Discussion. Plast Reconstr Surg 109, 1826-1827.

Fleming, A., Copp, A.J., 2000. A genetic risk factor for mouse neural tube defects: defining the embryonic basis. Human molecular genetics 9, 575-581.

Frommer, J., Margolie.Mr, 1971. Contribution of Meckels Cartilage to Ossification of Mandible in Mice. Journal of Dental Research 50, 1260-&.

Fuchs, A., Inthal, A., Herrmann, D., Cheng, S., Nakatomi, M., Peters, H., Neubuser, A., 2010. Regulation of Tbx22 during facial and palatal development. Dev Dyn 239, 2860-2874.

Gato, A., Martinez, M.L., Tudela, C., Alonso, I., Moro, J.A., Formoso, M.A., Ferguson, M.W., Martinez-Alvarez, C., 2002. TGF-beta(3)-induced chondroitin sulphate proteoglycan mediates palatal shelf adhesion. Dev Biol 250, 393-405.

Goldstein, A.M., Brewer, K.C., Doyle, A.M., Nagy, N., Roberts, D.J., 2005. BMP signaling is necessary for neural crest cell migration and ganglion formation in the enteric nervous system. Mech Dev 122, 821-833.

Goodrich, J.T., 2005. Skull base growth in craniosynostosis. Childs Nerv Syst 21, 871-879.

Goodrich, L.V., Jung, D., Higgins, K.M., Scott, M.P., 1999. Overexpression of ptc1 inhibits induction of Shh target genes and prevents normal patterning in the neural tube. Developmental biology 211, 323-334.

Goodrich, L.V., Milenkovic, L., Higgins, K.M., Scott, M.P., 1997. Altered neural cell fates and medulloblastoma in mouse patched mutants. Science 277, 1109-1113.

Grewal, J., Carmichael, S.L., Ma, C., Lammer, E.J., Shaw, G.M., 2008. Maternal periconceptional smoking and alcohol consumption and risk for select congenital anomalies. Birth defects research. Part A, Clinical and molecular teratology 82, 519-526.

Hall, R.J., Erickson, C.A., 2003. ADAM 10: an active metalloprotease expressed during avian epithelial morphogenesis. Dev Biol 256, 146-159.

Harfe, B.D., Scherz, P.J., Nissim, S., Tian, H., McMahon, A.P., Tabin, C.J., 2004. Evidence for an expansion-based temporal Shh gradient in specifying vertebrate digit identities. Cell 118, 517-528.

Harris, E.F., 1993. Size and form of the cranial base in isolated cleft lip and palate. Cleft Palate Craniofac J 30, 170-174.

He, F., Xiong, W., Wang, Y., Li, L., Liu, C., Yamagami, T., Taketo, M.M., Zhou, C., Chen, Y., 2011. Epithelial Wnt/beta-catenin signaling regulates palatal shelf fusion through regulation of Tgfbeta3 expression. Dev Biol 350, 511-519.

He, F., Xiong, W., Wang, Y., Matsui, M., Yu, X., Chai, Y., Klingensmith, J., Chen, Y., 2010. Modulation of BMP signaling by Noggin is required for the maintenance of palatal epithelial integrity during palatogenesis. Developmental biology 347, 109-121.

Hennekam, R.C., Van den Boogaard, M.J., 1990. Autosomal dominant craniosynostosis of the sutura metopica. Clin Genet 38, 374-377.

Higashihori, N., Buchtova, M., Richman, J.M., 2010. The function and regulation of TBX22 in avian frontonasal morphogenesis. Dev Dyn 239, 458-473.

Hogan, B., 1994. Manipulating the mouse embryo : a laboratory manual, 2nd ed. Cold Spring Harbor Laboratory Press, Plainview, N.Y.

Holder-Espinasse, M., Abadie, V., Cormier-Daire, V., Beyler, C., Manach, Y., Munnich, A., Lyonnet, S., Couly, G., Amiel, J., 2001. Pierre Robin sequence: a series of 117 consecutive cases. The Journal of pediatrics 139, 588-590.

Honein, M.A., Rasmussen, S.A., Reefhuis, J., Romitti, P.A., Lammer, E.J., Sun, L.X., Correa, A., 2007. Maternal smoking and environmental tobacco smoke exposure and the risk of orofacial clefts. Epidemiology 18, 226-233.

Hsu, D.R., Economides, A.N., Wang, X., Eimon, P.M., Harland, R.M., 1998. The Xenopus dorsalizing factor Gremlin identifies a novel family of secreted proteins that antagonize BMP activities. Molecular cell 1, 673-683.

Hu, D., Colnot, C., Marcucio, R.S., 2008. Effect of bone morphogenetic protein signaling on development of the jaw skeleton. Developmental dynamics : an official publication of the American Association of Anatomists 237, 3727-3737.

Huang, X., Yokota, T., Iwata, J., Chai, Y., 2011. Tgf-beta-mediated FasL-Fas-Caspase pathway is crucial during palatogenesis. J Dent Res 90, 981-987.

Iida, A., Ohashi, Y., Ono, K., Imai, N., Kannari, Y., 1995. Craniosynostosis with joint contractures, ear deformity, cleft palate, scoliosis, and other features. The Cleft palate-craniofacial journal : official publication of the American Cleft Palate-Craniofacial Association 32, 489-493.

Ikeda, A., Ikeda, S., Gridley, T., Nishina, P.M., Naggert, J.K., 2001. Neural tube defects and neuroepithelial cell death in Tulp3 knockout mice. Human molecular genetics 10, 1325-1334.

Jeong, J., Mao, J., Tenzen, T., Kottmann, A.H., McMahon, A.P., 2004. Hedgehog signaling in the neural crest cells regulates the patterning and growth of facial primordia. Genes & development 18, 937-951.

Jeong, J., Tenzen, T., McMahon, A.P., 2003. Direct hedgehog signaling in the neural crest cells is essential for the normal craniofacial development. Developmental Biology 259, 551-551.

Jiang, X., Rowitch, D.H., Soriano, P., McMahon, A.P., Sucov, H.M., 2000. Fate of the mammalian cardiac neural crest. Development 127, 1607-1616.

Jin, J.Z., Ding, J., 2006. Analysis of cell migration, transdifferentiation and apoptosis during mouse secondary palate fusion. Development 133, 3341-3347.

Johnson, C.P., Fujimoto, I., Rutishauser, U., Leckband, D.E., 2005. Direct evidence that neural cell adhesion molecule (NCAM) polysialylation increases intermembrane repulsion and abrogates adhesion. The Journal of biological chemistry 280, 137-145.

Kaartinen, V., Voncken, J.W., Shuler, C., Warburton, D., Bu, D., Heisterkamp, N., Groffen, J., 1995. Abnormal Lung Development and Cleft-Palate in Mice Lacking Tgf-Beta-3 Indicates Defects of Epithelial-Mesenchymal Interaction. Nature Genetics 11, 415-421.

Kanzler, B., Foreman, R.K., Labosky, P.A., Mallo, M., 2000. BMP signaling is essential for development of skeletogenic and neurogenic cranial neural crest. Development 127, 1095-1104.

Kawakami, T., Kawcak, T., Li, Y.J., Zhang, W., Hu, Y., Chuang, P.T., 2002. Mouse dispatched mutants fail to distribute hedgehog proteins and are defective in hedgehog signaling. Development 129, 5753-5765.

Kimonis, V., Gold, J.A., Hoffman, T.L., Panchal, J., Boyadjiev, S.A., 2007. Genetics of craniosynostosis. Semin Pediatr Neurol 14, 150-161.

Klingensmith, J., Matsui, M., Yang, Y.P., Anderson, R.M., 2010. Roles of bone morphogenetic protein signaling and its antagonism in holoprosencephaly. American journal of medical genetics. Part C, Seminars in medical genetics 154C, 43-51.

Koressaar, T., Remm, M., 2007. Enhancements and modifications of primer design program Primer3. Bioinformatics 23, 1289-1291.

Lammer, E.J., Shaw, G.M., Iovannisci, D.M., Van Waes, J., Finnell, R.H., 2004. Maternal smoking and the risk of orofacial clefts - Susceptibility with NAT1 and NAT2 polymorphisms. Epidemiology 15, 150-156.

Lana-Elola, E., Tylzanowski, P., Takatalo, M., Alakurtti, K., Veistinen, L., Mitsiadis, T.A., Graf, D., Rice, R., Luyten, F.P., Rice, D.P., 2011. Noggin null allele mice exhibit a microform of holoprosencephaly. Human molecular genetics 20, 4005-4015.

Lewis, J.E., Wahl, J.K., 3rd, Sass, K.M., Jensen, P.J., Johnson, K.R., Wheelock, M.J., 1997. Cross-talk between adherens junctions and desmosomes depends on plakoglobin. The Journal of cell biology 136, 919-934.

Li, L., Lin, M.K., Wang, Y., Cserjesi, P., Chen, Z., Chen, Y.P., 2011. BmprIa is required in mesenchymal tissue and has limited redundant function with BmprIb in tooth and palate development. Developmental Biology 349, 451-461.

Li, L., Wang, Y., Lin, M., Yuan, G., Yang, G., Zheng, Y., Chen, Y., 2013. Augmented BMPRIA-mediated BMP signaling in cranial neural crest lineage leads to cleft palate formation and delayed tooth differentiation. PloS one 8, e66107.

Lieberman, D.E., Pearson, O.M., Mowbray, K.M., 2000. Basicranial influence on overall cranial shape. Journal of Human Evolution 38, 291-315.

Lotz, M.M., Burdsal, C.A., Erickson, H.P., McClay, D.R., 1989. Cell adhesion to fibronectin and tenascin: quantitative measurements of initial binding and subsequent strengthening response. The Journal of cell biology 109, 1795-1805.

Lozanoff, S., Jureczek, S., Feng, T., Padwal, R., 1994. Anterior cranial base morphology in mice with midfacial retrusion. Cleft Palate Craniofac J 31, 417-428.

Luo, Y., High, F.A., Epstein, J.A., Radice, G.L., 2006. N-cadherin is required for neural crest remodeling of the cardiac outflow tract. Developmental biology 299, 517-528.

Matsui, M., Klingensmith, J., 2013. Development of the Craniofacial Skeleton, Primer on the Metabolic Bone Diseases and Disorders of Mineral Metabolism. John Wiley & Sons, Inc., pp. 893-903.

McBratney-Owen, B., Iseki, S., Bamforth, S.D., Olsen, B.R., Morriss-Kay, G.M., 2008. Development and tissue origins of the mammalian cranial base. Developmental biology 322, 121-132.

McMahon, J.A., Takada, S., Zimmerman, L.B., Fan, C.M., Harland, R.M., McMahon, A.P., 1998. Noggin-mediated antagonism of BMP signaling is required for growth and patterning of the neural tube and somite. Genes & development 12, 1438-1452.

Meigs, T.E., Fedor-Chaiken, M., Kaplan, D.D., Brackenbury, R., Casey, P.J., 2002. Galpha12 and Galpha13 negatively regulate the adhesive functions of cadherin. The Journal of biological chemistry 277, 24594-24600.

Melnick, M., Witcher, D., Bringas, P., Jr., Carlsson, P., Jaskoll, T., 2005. Meckel's cartilage differentiation is dependent on hedgehog signaling. Cells Tissues Organs 179, 146-157.

Menegaz, R.A., Sublett, S.V., Figueroa, S.D., Hoffman, T.J., Ravosa, M.J., 2009. Phenotypic plasticity and function of the hard palate in growing rabbits. Anatomical record 292, 277-284.

Mina, M., Havens, B., Velonis, D.A., 2007. FGF signaling in mandibular skeletogenesis. Orthod Craniofac Res 10, 59-66.

Mina, M., Wang, Y.H., Ivanisevic, A.M., Upholt, W.B., Rodgers, B., 2002. Region- and stage-specific effects of FGFs and BMPs in chick mandibular morphogenesis. Dev Dynam 223, 333-352.

Minina, E., Kreschel, C., Naski, M.C., Ornitz, D.M., Vortkamp, A., 2002. Interaction of FGF, Ihh/Pthlh, and BMP signaling integrates chondrocyte proliferation and hypertrophic differentiation. Developmental cell 3, 439-449.

Minina, E., Wenzel, H.M., Kreschel, C., Karp, S., Gaffield, W., McMahon, A.P., Vortkamp, A., 2001. BMP and Ihh/PTHrP signaling interact to coordinate chondrocyte proliferation and differentiation. Development 128, 4523-4534.

Molsted, K., Dahl, E., Skovgaard, L.T., Asher-McDade, C., Brattstrom, V., McCance, A., Prahl-Andersen, B., Semb, G., Shaw, B., The, R., 1993. A multicentre comparison of treatment regimens for unilateral cleft lip and palate using a multiple regression model. Scandinavian journal of plastic and reconstructive surgery and hand surgery / Nordisk plastikkirurgisk forening [and] Nordisk klubb for handkirurgi 27, 277-284.

Molsted, K., Kjaer, I., Dahl, E., 1995. Cranial base in newborns with complete cleft lip and palate: radiographic study. Cleft Palate Craniofac J 32, 199-205.

Mori-Akiyama, Y., Akiyama, H., Rowitch, D.H., de Crombrugghe, B., 2003. Sox9 is required for determination of the chondrogenic cell lineage in the cranial neural crest. Proc Natl Acad Sci U S A 100, 9360-9365.

Morris-Wiman, J., Brinkley, L., 1992. An extracellular matrix infrastructure provides support for murine secondary palatal shelf remodelling. The Anatomical record 234, 575-586.

Mossey PA, L.J., 2002. Epidemiology of oral cleft: an internationa perspective. Oxford University Press, New York, NY.

Moury, J.D., Schoenwolf, G.C., 1995. Cooperative model of epithelial shaping and bending during avian neurulation: autonomous movements of the neural plate, autonomous movements of the epidermis, and interactions in the neural plate/epidermis transition zone. Developmental dynamics : an official publication of the American Association of Anatomists 204, 323-337.

Murdoch, J.N., Copp, A.J., 2010. The relationship between sonic Hedgehog signaling, cilia, and neural tube defects. Birth defects research. Part A, Clinical and molecular teratology 88, 633-652.

Nawshad, A., Medici, D., Liu, C.C., Hay, E.D., 2007. TGFbeta3 inhibits E-cadherin gene expression in palate medial-edge epithelial cells through a Smad2-Smad4-LEF1 transcription complex. J Cell Sci 120, 1646-1653.

Nie, X.G., 2005. Cranial base in craniofacial development: Developmental features, influence on facial growth, anomaly, and molecular basis. Acta Odontol Scand 63, 127-135.

Nifuji, A., Noda, M., 1999. Coordinated expression of noggin and bone morphogenetic proteins (BMPs) during early skeletogenesis and induction of noggin expression by BMP-7. Journal of bone and mineral research : the official journal of the American Society for Bone and Mineral Research 14, 2057-2066.

Norman, R.X., Ko, H.W., Huang, V., Eun, C.M., Abler, L.L., Zhang, Z., Sun, X., Eggenschwiler, J.T., 2009. Tubby-like protein 3 (TULP3) regulates patterning in the mouse embryo through inhibition of Hedgehog signaling. Human molecular genetics 18, 1740-1754.

Ogle, R.C., Tholpady, S.S., McGlynn, K.A., Ogle, R.A., 2004. Regulation of cranial suture morphogenesis. Cells Tissues Organs 176, 54-66.

Patterson, V.L., Damrau, C., Paudyal, A., Reeve, B., Grimes, D.T., Stewart, M.E., Williams, D.J., Siggers, P., Greenfield, A., Murdoch, J.N., 2009. Mouse hitchhiker mutants have spina bifida, dorso-ventral patterning defects and polydactyly: identification of Tulp3 as a novel negative regulator of the Sonic hedgehog pathway. Human molecular genetics 18, 1719-1739.

Pauws, E., Moore, G.E., Stanier, P., 2009. A functional haplotype variant in the TBX22 promoter is associated with cleft palate and ankyloglossia. Journal of medical genetics 46, 555-561.

Potti, T.A., Petty, E.M., Lesperance, M.M., 2011. A comprehensive review of reported heritable noggin-associated syndromes and proposed clinical utility of one broadly inclusive diagnostic term: NOG-related-symphalangism spectrum disorder (NOG-SSD). Human mutation 32, 877-886.

Proetzel, G., Pawlowski, S.A., Wiles, M.V., Yin, M.Y., Boivin, G.P., Howles, P.N., Ding, J.X., Ferguson, M.W.J., Doetschman, T., 1995. Transforming Growth Factor-Beta-3 Is Required for Secondary Palate Fusion. Nature Genetics 11, 409-414.

Pruzinsky, T., 1992. Social and psychological effects of major craniofacial deformity. Cleft Palate Craniofac J 29, 578-584; discussion 570.

Pyrgaki, C., Liu, A., Niswander, L., 2011. Grainyhead-like 2 regulates neural tube closure and adhesion molecule expression during neural fold fusion. Developmental biology 353, 38-49.

Ramaesh, T., Bard, J.B., 2003. The growth and morphogenesis of the early mouse mandible: a quantitative analysis. Journal of anatomy 203, 213-222.

Reshef, R., Maroto, M., Lassar, A.B., 1998. Regulation of dorsal somitic cell fates: BMPs and Noggin control the timing and pattern of myogenic regulator expression. Genes & development 12, 290-303.

Rice, R., Spencer-Dene, B., Connor, E.C., Gritli-Linde, A., McMahon, A.P., Dickson, C., Thesleff, I., Rice, D.P., 2004. Disruption of Fgf10/Fgfr2b-coordinated epithelial-mesenchymal interactions causes cleft palate. The Journal of clinical investigation 113, 1692-1700.

Richtsmeier, J.T., Aldridge, K., DeLeon, V.B., Panchal, J., Kane, A.A., Marsh, J.L., Yan, P., Cole, T.M., 3rd, 2006. Phenotypic integration of neurocranium and brain. J Exp Zool B Mol Dev Evol 306, 360-378.

Rifat, Y., Parekh, V., Wilanowski, T., Hislop, N.R., Auden, A., Ting, S.B., Cunningham, J.M., Jane, S.M., 2010. Regional neural tube closure defined by the Grainy head-like transcription factors. Developmental biology 345, 237-245.

Rodriguez, P., Da Silva, S., Oxburgh, L., Wang, F., Hogan, B.L., Que, J., 2010. BMP signaling in the development of the mouse esophagus and forestomach. Development 137, 4171-4176.

Sahar, D.E., Longaker, M.T., Quarto, N., 2005. Sox9 neural crest determinant gene controls patterning and closure of the posterior frontal cranial suture. Developmental biology 280, 344-361.

Satokata, I., Maas, R., 1994. Msx1 Deficient Mice Exhibit Cleft-Palate and Abnormalities of Craniofacial and Tooth Development. Nature Genetics 6, 348-356.

Scott, I.C., Blitz, I.L., Pappano, W.N., Maas, S.A., Cho, K.W., Greenspan, D.S., 2001. Homologues of Twisted gastrulation are extracellular cofactors in antagonism of BMP signalling. Nature 410, 475-478.

Shoval, I., Ludwig, A., Kalcheim, C., 2007. Antagonistic roles of full-length N-cadherin and its soluble BMP cleavage product in neural crest delamination. Development 134, 491-501.

St-Jacques, B., Hammerschmidt, M., McMahon, A.P., 1999. Indian hedgehog signaling regulates proliferation and differentiation of chondrocytes and is essential for bone formation. Genes Dev 13, 2072-2086.

Stafford, D.A., Brunet, L.J., Khokha, M.K., Economides, A.N., Harland, R.M., 2011. Cooperative activity of noggin and gremlin 1 in axial skeleton development. Development 138, 1005-1014.

Stanier, P., Moore, G.E., 2004. Genetics of cleft lip and palate: syndromic genes contribute to the incidence of non-syndromic clefts. Hum Mol Genet 13, R73-R81.

Stottmann, R.W., Anderson, R.M., Klingensmith, J., 2001. The BMP antagonists Chordin and Noggin have essential but redundant roles in mouse mandibular outgrowth. Developmental biology 240, 457-473.

Stottmann, R.W., Berrong, M., Matta, K., Choi, M., Klingensmith, J., 2006. The BMP antagonist Noggin promotes cranial and spinal neurulation by distinct mechanisms. Developmental biology 295, 647-663.

Stottmann, R.W., Klingensmith, J., 2011. Bone morphogenetic protein signaling is required in the dorsal neural folds before neurulation for the induction of spinal neural crest cells and dorsal neurons. Dev Dyn 240, 755-765.

Suri, S., Ross, R.B., Tompson, B.D., 2010. Craniofacial morphology and adolescent facial growth in Pierre Robin sequence. Am J Orthod Dentofac 137, 763-774.

Tao, J., Kuliyev, E., Wang, X., Li, X., Wilanowski, T., Jane, S.M., Mead, P.E., Cunningham, J.M., 2005. BMP4-dependent expression of Xenopus Grainyhead-like 1 is essential for epidermal differentiation. Development 132, 1021-1034.

Taya, Y., O'Kane, S., Ferguson, M.W., 1999a. Pathogenesis of cleft palate in TGF-beta3 knockout mice. Development 126, 3869-3879.

Taya, Y., O'Kane, S., Ferguson, M.W.J., 1999b. Pathogenesis of cleft palate in TGF-beta 3 knockout mice. Development 126, 3869-3879.

Trumpp, A., Depew, M.J., Rubenstein, J.L., Bishop, J.M., Martin, G.R., 1999. Cre-mediated gene inactivation demonstrates that FGF8 is required for cell survival and patterning of the first branchial arch. Genes & development 13, 3136-3148.

Tsuzurahara, F., Soeta, S., Kawawa, T., Baba, K., Nakamura, M., 2011. The role of macrophages in the disappearance of Meckel's cartilage during mandibular development in mice. Acta Histochem 113, 194-200.

Tucker, A.S., Yamada, G., Grigoriou, M., Pachnis, V., Sharpe, P.T., 1999. Fgf-8 determines rostral-caudal polarity in the first branchial arch. Development 126, 51-61.

Wallingford, J.B., Niswander, L.A., Shaw, G.M., Finnell, R.H., 2013. The continuing challenge of understanding, preventing, and treating neural tube defects. Science 339, 1222002.

Wang, Y., Zheng, Y., Chen, D., Chen, Y., 2013. Enhanced BMP signaling prevents degeneration and leads to endochondral ossification of Meckel's cartilage in mice. Developmental biology 381, 301-311.

Warren, S.M., Brunet, L.J., Harland, R.M., Economides, A.N., Longaker, M.T., 2003. The BMP antagonist noggin regulates cranial suture fusion. Nature 422, 625-629.

Werth, M., Walentin, K., Aue, A., Schonheit, J., Wuebken, A., Pode-Shakked, N., Vilianovitch, L., Erdmann, B., Dekel, B., Bader, M., Barasch, J., Rosenbauer, F., Luft, F.C., Schmidt-Ott, K.M., 2010. The transcription factor grainyhead-like 2 regulates the molecular composition of the epithelial apical junctional complex. Development 137, 3835-3845.

Weseman, C.M., 1959. Congenital Micrognathia. Archiv Otolaryngol 69, 31-44.
Wijgerde, M., Karp, S., McMahon, J., McMahon, A.P., 2005. Noggin antagonism of BMP4 signaling controls development of the axial skeleton in the mouse. Developmental biology 286, 149-157.

Wilke, T.A., Gubbels, S., Schwartz, J., Richman, J.M., 1997. Expression of fibroblast growth factor receptors (FGFR1, FGFR2, FGFR3) in the developing head and face. Dev Dynam 210, 41-52.

Xu, X., Han, J., Ito, Y., Bringas, P., Jr., Urata, M.M., Chai, Y., 2006. Cell autonomous requirement for Tgfbr2 in the disappearance of medial edge epithelium during palatal fusion. Dev Biol 297, 238-248.

Ybot-Gonzalez, P., Cogram, P., Gerrelli, D., Copp, A.J., 2002. Sonic hedgehog and the molecular regulation of mouse neural tube closure. Development 129, 2507-2517.

Ybot-Gonzalez, P., Gaston-Massuet, C., Girdler, G., Klingensmith, J., Arkell, R., Greene, N.D., Copp, A.J., 2007. Neural plate morphogenesis during mouse neurulation is regulated by antagonism of Bmp signalling. Development 134, 3203-3211.

Yu, L., Gu, S., Alappat, S., Song, Y., Yan, M., Zhang, X., Zhang, G., Jiang, Y., Zhang, Z., Zhang, Y., Chen, Y., 2005. Shox2-deficient mice exhibit a rare type of incomplete clefting of the secondary palate. Development 132, 4397-4406.

Zhang, X.M., Ramalho-Santos, M., McMahon, A.P., 2001. Smoothened mutants reveal redundant roles for Shh and Ihh signaling including regulation of L/R symmetry by the mouse node. Cell 106, 781-792.

Zhang, Z., Song, Y., Zhao, X., Zhang, X., Fermin, C., Chen, Y., 2002. Rescue of cleft palate in Msx1-deficient mice by transgenic Bmp4 reveals a network of BMP and Shh signaling in the regulation of mammalian palatogenesis. Development 129, 4135-4146.

Zucchero, T.M., Cooper, M.E., Maher, B.S., Daack-Hirsch, S., Nepomuceno, B., Ribeiro, L., Caprau, D., Christensen, K., Suzuki, Y., Machida, J., Natsume, N., Yoshiura, K.I., Vieira, A.R., Orioli, I.M., Castilla, E.E., Moreno, L., Arcos-Burgos, M., Lidral, A.C., Field, L.L., Liu, Y.E., Ray, A., Goldstein, T.H., Schultz, R.E., Shi, M., Johnson, M.K., Kondo, S., Schutte, B.C., Marazita, M.L., Murray, J.C., 2004. Interferon regulatory factor 6 (IRF6) gene variants and the risk of isolated cleft lip or palate. New Engl J Med 351, 769-780.

Biography

Maiko Matsui studies developmental biology and is interested in craniofacial development in mammals. In her current research, she tries to identify the mechanisms that lead to abnormal and normal development of craniofacial skeletal structures.

At Duke University, she holds a Graduate School fellowship. Prior to joining Duke, she attended University of North Carolina-Greensboro, where she earned a B.S. in Biology with honors in 2006. Maiko was born in Kyoto, Japan.

Her list of publications includes:

Matsui M, and Klingensmith J. (2013) Development of the Craniofacial Skeleton. in CJ Rosen, R Bouillon, JE Compston, and V Rosen (eds.) *Primer on the Metabolic Bone Diseases and Disorders of Mineral Metabolism* 893-903.

Matsui M, Sharma KC, Cooke C, Wakimoto BT, Rasool M, Hayworth M, Hylton CA, and Tomkiel JE. (2011) Nuclear structure and chromosome segregation in *Drosophila* male meiosis depend on the ubiquitin ligase *dTopors*. *Genetics.* 189(3): 779-93.

He F, Xiong W, Wang Y, **Matsui M**, Yu X, Chai Y, Klingensmith J, and Chen Y. (2010) Modulation of BMP signaling by Noggin is required for the maintenace of palatal epithelial integrity during palatogenesis. *Dev Biol*. 374(1): 109-21.

Klingensmith J, **Matsui M**, Yang YP, and Anderson RM. (2010) Roles of bone morphogenetic protein signaling and its antagonism in holoprosencephaly. *Am J Med Genet C Semin Med Genet*. 154C(1): 43-51